## **NOTE TO USERS**

This reproduction is the best copy available.



## POTASSIUM CHANNEL CONTROL OF NEURONAL FREQUENCY RESPONSE

Lee David Ellis Department of Biology McGill University, Montreal September, 2007

A thesis submitted to the Faculty of Graduate Studies and Research in partial fulfillment of the requirements of the degree of Doctor of Philosophy.

© Lee D. Ellis, 2007



Library and Archives Canada

Published Heritage Branch

395 Wellington Street Ottawa ON K1A 0N4 Canada Bibliothèque et Archives Canada

Direction du Patrimoine de l'édition

395, rue Wellington Ottawa ON K1A 0N4 Canada

> Your file Votre référence ISBN: 978-0-494-38584-5 Our file Notre référence ISBN: 978-0-494-38584-5

#### NOTICE:

The author has granted a non-exclusive license allowing Library and Archives Canada to reproduce, publish, archive, preserve, conserve, communicate to the public by telecommunication or on the Internet, loan, distribute and sell theses worldwide, for commercial or non-commercial purposes, in microform, paper, electronic and/or any other formats.

#### **AVIS:**

L'auteur a accordé une licence non exclusive permettant à la Bibliothèque et Archives Canada de reproduire, publier, archiver, sauvegarder, conserver, transmettre au public par télécommunication ou par l'Internet, prêter, distribuer et vendre des thèses partout dans le monde, à des fins commerciales ou autres, sur support microforme, papier, électronique et/ou autres formats.

The author retains copyright ownership and moral rights in this thesis. Neither the thesis nor substantial extracts from it may be printed or otherwise reproduced without the author's permission.

L'auteur conserve la propriété du droit d'auteur et des droits moraux qui protège cette thèse. Ni la thèse ni des extraits substantiels de celle-ci ne doivent être imprimés ou autrement reproduits sans son autorisation.

In compliance with the Canadian Privacy Act some supporting forms may have been removed from this thesis.

While these forms may be included in the document page count, their removal does not represent any loss of content from the thesis.

Conformément à la loi canadienne sur la protection de la vie privée, quelques formulaires secondaires ont été enlevés de cette thèse.

Bien que ces formulaires aient inclus dans la pagination, il n'y aura aucun contenu manquant.



#### Abstract

The processing of sensory signals is an important, yet complex task in which a system must extract behaviorally relevant stimulus patterns from a vast array of sensory cues. When a neuron within a major sensory area is presented with a stimulus, one of the important characteristics used to distinguish between types of input is frequency. Often sensory neurons are tuned to narrow stimulus frequency ranges and are thus charged with the processing of subtypes of sensory signals. The weakly electric fish *Apteronotus lepthorhynchus* senses it's environment through modulations of a self-generated electric field. Two main types of sensory signals can be distinguished based on their frequency patterns. Prey stimuli cause low frequency perturbations of the electric field, while communication signals often result in high frequency signals. Pyramidal neurons in the electrosensory lateral line lobe (ELL) encode the low frequency signals with bursts, while the high frequency signals are relayed with single spikes. This thesis describes how a pyramidal neuron's response patterns can be tuned to specific frequencies by the expression of distinct classes of potassium channels.

I have cloned 3 small conductance (SK) calcium activated potassium channels from cDNA libraries created from the brain of *Apteronotus*. I have subsequently localized the *Apt*SK channels throughout the brain using both *in situ* hybridization (*Apt*SK1, 2 &3) and immunohistochemical (*Apt*SK1 &2) techniques. The 3 channels showed distinct expression patterns, with the *Apt*SK1 & 2 channels showing a partially overlapping expression pattern, while *Apt*SK3 appears to be expressed in unique areas of the brain. In the ELL *Apt*SK1 & 2 show a partially overlapping expression pattern, appearing in similar pyramidal neurons. However, their distribution within individual cell is unique, with *Apt*SK1 showing a dendritic localization, while *Apt*SK2 is primarily somatic. We have demonstrated that the unique expression pattern of the somatic *Apt*SK2 channel in the ELL coincides with the functional SK currents evaluated through *in vitro* electrophysiology. Further we have shown that neurons that encode low frequencies do not possess functional SK channels. It thus appears that the presence of the *Apt*SK2 channel subtype can predispose a neuron to respond to specific types of sensory signals.

In an attempt to evaluate if second messengers could modify the AptSK control of frequency tuning I investigated the consequences of muscarinic acetylcholine receptor (mAChR) activation on a pyramidal neurons response patterns. While it had been shown in vivo that mAChR activation increased a pyramidal neuron's response to low frequencies, I have found that this was not due to a decrease in AptSK current, but rather appears to be the result of a down-regulation of an A-type potassium channel.

Taken together the studies that comprise this thesis show how the selective expression of a single potassium channel subtype can control a sensory neurons response to specific environmental cues. The secondary modulation of the A-type current highlights the potential for a second messenger to control a neuron's sensory response through the down-regulation of constitutively expressed potassium current.

#### Résumé

Le traitement de signaux sensoriels est une tâche importante, mais demeure cependant complexe dans laquelle un système doit extraire des stimuli comportementaux appropriés à partir d'une abondance de signaux. Quand un stimulus est présenté à un neurone dans un secteur sensoriel majeur, une des caractéristiques importantes utilisée pour distinguer entre les types messages est la fréquence. Souvent, les neurones sensoriels ne répondent qu'à une gamme de stimulus de fréquence étroite et sont ainsi chargés du traitement des sous-types de signaux sensoriels. Le poisson faiblement électrique Apteronotus lepthorhynchus sens son environnement par la modulation d'un champ électrique produit par celui-ci. Deux types principaux de signaux sensoriels peuvent être distingués basés sur leurs modèles de fréquence. La présence de proies cause des perturbations de basses fréquences dans le champ électrique, tandis que la communication donne souvent des signaux de haute fréquence. Des neurones pyramidaux dans le lobe de la ligne latéral electrosensorielle (ELL) codent les signaux de basse fréquence avec des rafales de potentiels d'action, tandis que les signaux haute fréquence sont relayés avec un seul potentiel d'action. Cette thèse décrit comment les modèles de réponse d'un neurone pyramidal peuvent être accordés aux fréquences spécifiques par l'expression des classes distinctes de canaux potassiques.

J'ai cloné 3 canaux potassiques activés par le calcium à petites conductances (SK) à partir de bibliothèques cDNA créées du cerveau d'Apteronotus. J'ai par la suite localisé les canaux AptSK partout dans le cerveau en utilisant des techniques d'hybridization in situ (AptSK1, 2 & 3) et d'immunohistochimie (AptSK1 & 2). Les 3 canaux ont montré des modèles d'expression distincts, avec les canaux AptSK1 et 2 montrant une expression partiellement chevauchante, tandis qu'AptSK3 semble être exprimé dans d'autres régions du cerveau. Dans l'ELL, AptSK1 et 2 montrent un modèle d'expression qui se chevauche partiellement, apparaissant dans des neurones pyramidaux similaires. Toutefois, leur distribution dans chaque cellule est unique, avec AptSK1 montrant une localisation dendritique, tandis qu'AptSK2 est principalement somatique. Nous avons démontré que le modèle d'expression unique du canal AptSK2 somatique dans l'ELL coïncide avec les courants SK fonctionnels évalués par électrophysiologie in vitro. De plus, nous avons

montré que les neurones qui codent les fréquences basses ne possèdent pas de canaux SK fonctionnels. Il semble donc que la présence du sous-type de canal *Apt*SK2 peut prédisposer un neurone à répondre aux types spécifiques de signaux sensoriels.

Dans une tentative d'évaluer si de deuxièmes messagers pourraient modifier le contrôle d'AptSK sur l'accord de fréquence, j'ai examiné les conséquences de l'activation du récepteur muscarinique acetylcholine (mAChR) sur une réponse modèle de neurones pyramidaux. Puisqu'il avait été démontré *in vivo* que l'activation mAChR augmente la réponse d'un neurone pyramidal aux basses fréquences, j'ai constaté que ce n'était pas en raison d'une diminution du courant AptSK, mais semble plutôt être le résultat d'une réduction d'expression d'un canal potassique de type A.

En somme, les études comprises dans cette thèse démontrent comment l'expression sélective d'un seul sous-type de canal potassique peut contrôler une réponse de neurones sensorielle aux stimulus environnementaux spécifiques. La modulation secondaire du courant de type A met en évidence le potentiel d'un deuxième messager pour contrôler la réponse sensorielle d'un neurone par l'expression réduite d'un courant de potassium constitutivement exprimé.

#### **ACKNOWLEDGEMENTS**

There are a number of people to whom I am indebted for their help throughout my doctoral research. I would like to express my most sincere thanks to Rob Dunn, my supervisor, for his input on all aspects of my research, including not only the experimental component, but also for his advice on presenting research to a larger audience. I believe the Rob's advise has enabled me to critique my own work, which has strengthened all aspects of my research. I have also learned the importance of looking at research from all possible angles and not to settle for substandard work. I must also acknowledge Len Maler, his enthusiasm for research is contagious. I must thank both Rob and Len for their aid in the preparation of the manuscripts in this thesis. They were always available for input and have made an often, daunting task more manageable.

I would also like to thank the members of my committee Rudiger Krahe and Charles Bourque for their input and critique of my research. I am indebted to Charles Bourque for aiding me in setting up the sharp electrode physiology experiments. Without his input and accessibility, the work would have been much difficult. I must also thank my collaborators, Hamish Mehaffey and Ray Turner from the University of Calgary. They were both gracious hosts and teachers.

Also, it is important that I thank a number of people for their constant assistance, including Mathieu Lachance who was always willing to help out in anyway he could, Bill Ellis, for introducing me to the more subtle aspects of the electric fish system, and to Erik Harvey-Girard, who refined and taught me the *in situ* hybridization technique.

Finally I would like to thank my friends and family who provided constant support and relief from the stressful periods, in particular to my Mother who was always there to encourage me to persevere.

## **TABLE OF CONTENTS**

ABSTRACT	<del> </del>
RESUME	
ACKNOWLEDGEMENTS	
LIST OF FIGURES	<del> </del>
INTRODUCTION	·
LITERATURE REVIEW I. APTERONOTUS LEPTHORHYNCHUSTUDYING SENSORY PROCESSING IN THE WEAKLY ELECTISH_	
Overview	
Dendritic control of a pyramidal neurons response properties	
Bursting Potassium channels in <i>Apteronotus</i>	·
LITERATURE REVIEW II. SMALL CONDUCTANCE CALCIUM ACTIVATED POTASSIUM CHANNELS  SK channels control the mAHP	
Linking currents to channels	<u> </u>
SK channel gating mechanism	
SK channel contributions to cellular physiology	<u> </u>
LITERATURE REVIEW III. A-TYPE POTASSIUM CHANNELS_	· · · · · · · · · · · · · · · · · · ·
A-type potassium currents	
I <sub>A</sub> controls neuronal firing patterns	
I <sub>A</sub> control of higher order functions	
LITERATURE REVIEW IV. REGULATION OF POTASSIUM CONDUCTANCES	· · · · · · · · · · · · · · · · · · ·
Cholinergic pathways in the CNS	·
Feedback regulation by ACh  Muscarinic receptors	
Muscarinic receptors	

CHAPTER I. DIFFERENTIAL DISTRIBUTION OF THE SK	CHANNEL
SUBTYPES IN THE BRAIN OF THE WEAKLY ELECTRIC	
FISH	
INTRODUCTION	
INTRODUCTION	
RESULTS	
RESULTS	
CHAPTER II. SK CHANNELS PROVIDE A NOVEL MECHA	
THE CONTROL OF FREQUENCY TUNING IN ELECTROSI	
NEURONS	ENSURI
INTRODUCTION MATERIALS AND METHODS	
MATERIALS AND METHODS	
RESULTSDISCUSSION	<del> </del>
DISCUSSION	
CHAPTER III. MUSCARINIC RECEPTORS CONTROL FRE FUNING THROUGH THE DOWNREGULATION OF AN A-T	QEUNCY YPE
CHAPTER III. MUSCARINIC RECEPTORS CONTROL FRE FUNING THROUGH THE DOWNREGULATION OF AN A-TPOTASSIUM CURRENT	QEUNCY YPE
CHAPTER III. MUSCARINIC RECEPTORS CONTROL FRE FUNING THROUGH THE DOWNREGULATION OF AN A-T POTASSIUM CURRENT	QEUNCY YPE
CHAPTER III. MUSCARINIC RECEPTORS CONTROL FRE FUNING THROUGH THE DOWNREGULATION OF AN A-T POTASSIUM CURRENT  INTRODUCTION MATERIALS AND METHODS	QEUNCY YPE
CHAPTER III. MUSCARINIC RECEPTORS CONTROL FRE FUNING THROUGH THE DOWNREGULATION OF AN A-T POTASSIUM CURRENT	QEUNCY YPE
CHAPTER III. MUSCARINIC RECEPTORS CONTROL FRE FUNING THROUGH THE DOWNREGULATION OF AN A-T POTASSIUM CURRENT  INTRODUCTION  MATERIALS AND METHODS  RESULTS  DISCUSSION	QEUNCY YPE
CHAPTER III. MUSCARINIC RECEPTORS CONTROL FRE FUNING THROUGH THE DOWNREGULATION OF AN A-T POTASSIUM CURRENT  INTRODUCTION  MATERIALS AND METHODS  RESULTS  DISCUSSION  DISCUSSION	QEUNCY YPE
CHAPTER III. MUSCARINIC RECEPTORS CONTROL FRE TUNING THROUGH THE DOWNREGULATION OF AN A-T POTASSIUM CURRENT  INTRODUCTION  MATERIALS AND METHODS  RESULTS  DISCUSSION  DISCUSSION  AptSK channel distribution patterns suggest multiple roles in electrons.	QEUNCY YPE
CHAPTER III. MUSCARINIC RECEPTORS CONTROL FRE TUNING THROUGH THE DOWNREGULATION OF AN A-T POTASSIUM CURRENT  INTRODUCTION  MATERIALS AND METHODS  RESULTS  DISCUSSION  DISCUSSION  AptSK channel distribution patterns suggest multiple roles in electrocessing	QEUNCY YPE
CHAPTER III. MUSCARINIC RECEPTORS CONTROL FRE FUNING THROUGH THE DOWNREGULATION OF AN A-T POTASSIUM CURRENT  INTRODUCTION  MATERIALS AND METHODS  RESULTS  DISCUSSION  DISCUSSION  AptSK channel distribution patterns suggest multiple roles in electorocessing  Functional role of A-type currents	QEUNCY YPE
CHAPTER III. MUSCARINIC RECEPTORS CONTROL FRE TUNING THROUGH THE DOWNREGULATION OF AN A-T POTASSIUM CURRENT  INTRODUCTION  MATERIALS AND METHODS  RESULTS  DISCUSSION  OISCUSSION  AptSK channel distribution patterns suggest multiple roles in electrocessing  Functional role of A-type currents  Future Work I: AptSK channels	QEUNCY YPE
CHAPTER III. MUSCARINIC RECEPTORS CONTROL FRE FUNING THROUGH THE DOWNREGULATION OF AN A-T POTASSIUM CURRENT  INTRODUCTION  MATERIALS AND METHODS  RESULTS  DISCUSSION  OISCUSSION  AptSK channel distribution patterns suggest multiple roles in electrocessing  Functional role of A-type currents  Future Work I: AptSK channels  Dendritic distribution of AptSK1 channels	QEUNCY YPE
CHAPTER III. MUSCARINIC RECEPTORS CONTROL FRE TUNING THROUGH THE DOWNREGULATION OF AN A-T POTASSIUM CURRENT  INTRODUCTION  MATERIALS AND METHODS  RESULTS  DISCUSSION  DISCUSSION  AptSK channel distribution patterns suggest multiple roles in electorocessing  Functional role of A-type currents  Future Work I: AptSK channels	QEUNCY YPE
CHAPTER III. MUSCARINIC RECEPTORS CONTROL FRE FUNING THROUGH THE DOWNREGULATION OF AN A-T POTASSIUM CURRENT  INTRODUCTION  MATERIALS AND METHODS  RESULTS  DISCUSSION  OISCUSSION  AptSK channel distribution patterns suggest multiple roles in electrocessing  Functional role of A-type currents  Future Work I: AptSK channels  Dendritic distribution of AptSK1 channels  Secondary modulation of AptSK channels	QEUNCY YPE

## LIST OF FIGURES

## **CHAPTER I**

	comparisons between the Apteronotus SK channels reveals
significant amino aci	
<b>Figure 2</b> . <i>In situ</i> hytmRNA within the fo	oridization reveals a differential distribution for <i>Apt</i> SK1 & 2 rebrain
Figure 3. AptSK2 is	s expressed in electrosensory brain areas of the
diencephalon	
	oridization demonstrates the presence of low levels of AptSK2
	nin the optic tectum (TeO) and torus semicircularis (TS)
Figure 5. Cell speci	fic expression of AptSK1 and 2 in the cerebellum
F <b>igure 6</b> . AptSK1 ai	nd 2 show differential expression patterns in the brainstem
Figure 7. AptSK1 is	expressed in a map specific manner in the ELL
F <b>igure 8</b> . Immunohi	stochemistry reveals differential subcellular localization of
AptSK1 and 2 channe	els in the ELL
F <b>igure 9. Apt</b> SK1 la	beling of distal pyramidal cell dendrites in the ELL reveals a
distinct punctate stair	ning pattern
CHAPTER II	
Figure 1. Sequence	evaluation of SK2
Figure 2. Compartm	nental expression pattern of AptSK2 in the ELL
Figure 3. I-cells do	not respond to SK channel modulation
Figure 4. E-cell resp	onses to apamin match the AptSK2 distribution
atterning	
Figure 5. SK channe	els control the firing mode of a CLS cell
	response to low frequency stimuli follow SK channel block
CHAPTER III	
igure 1. The electro	osensory system
Figure 2. Carbachol	leads to increased cellular excitability in vivo
igure 3. Muscarinio	c receptor activation leads to an increase in burst firing in
ivo	
igure 4. Muscarinio	receptor activation increases the response to low frequency
ensory stimuli in vive	o
igure 5. Carbachol	activates muscarinic receptors in vitro
	n channel blocker can mirror the effects of carbachol
	and 4-AP lead to a decreased first spike latency
-	he effects of blocking A-type channels
-	ne effects of A-type channels on signal processing

## APPENDIX

Figure 1. Sense controls for in situ hybridization	160
Figure 2. Evaluation of AptSK1 and 2 antibodies	161
Figure 3. The short splice variant (SSV) of the AptSK1 channel is not expressed	
on the cell surface	162

## **INTRODUCTION**

It has long been known that K<sup>+</sup> currents are responsible for the repolarization of action potentials (Hodgkin and Huxley, 1953; Hodgkin and Huxley, 1952). As advances in molecular biology grew a number of K<sup>+</sup> channels were subsequently cloned, revealing a number of distinct subtypes that displayed diverse molecular structures (for a review see (Coetzee et al., 1999). The variations in channel sequence and structure can lead to distinct activation-inactivation properties between subtypes. The K<sup>+</sup> channels that were first described were activated by large depolarizations of the membrane, as would occur during an action potential (reviewed by Hille, 2001). As the diversity of known channels increased channel subtypes were found that could be active at more hyperpolarized membrane potentials and by various strengths of depolarization (A-type, H-type, M-type; Coetzee et al., 1999). Others were found to be partially sensitive to voltage but required an increase in intracellular calcium to become active (BK). In fact, some channels can be activated soley by elevations in calcium (SK). Structurally diverse groups of K<sup>+</sup> channels also exist that include inwardly rectifying (Kir) and "leak" channels that are open at the resting membrane potential. Each functional group of channels is further subdivided into a multitude of individual subtypes that often have similar sequence homologies and Closely related classes of K<sup>+</sup> channels may display similar kinetics. functions. Differences in the protein sequence of genetically similar channels may be necessary to control expression patterns or cellular compartmentalization, as will be highlighted later in this thesis. The contributions to neuronal membrane dynamics that different subtypes can make are as diverse as their individual structures.

This thesis describes an analysis of the contributions that subtypes of potassium channels can make to the frequency response properties of pyramidal neurons in the primary signal processing area of the weakly electric fish *Apteronotus leptorhynchus*. The brown ghost knife fish (*A. leptorhynchus*) senses its environment through a selfgenerated electric field. Perturbations of the field are created when the fish encounters external stimuli and are sensed by cutaneous electroreceptors that encode these signals through changes in firing rate (Bastian, 1981). The primary processing of these signals occurs in an area of the hindbrain known as the electrosensory lateral line lobe (ELL; for a review of the electrosensory system Turner and Maler, 1999). Processing of the electrosensory signals in the ELL has been found to display many similarities to the

processing of visual and auditory stimuli in mammalian systems (Carr et al., 1986) and the ELL has been suggested to be homologus to the dorsal cochlear nucleus. The ELL has a detailed neuroanatomy (Maler et al., 1991), well characterized physiology both *in vivo* and *in vitro* and distinct response patterns to natural sensory input (Bastian et al., 2002;Chacron et al., 2005;Chacron, 2006;Berman and Maler, 1998a;Berman and Maler, 1998c;Berman and Maler, 1998b). The advantages of studying the electrosensory system lie not only in the well described anatomy and physiology, but also in the fact that the system is much more simplistic than higher order mammalian sensory systems, allowing direct links between sensory stimuli and the response properties of individual sensory neurons to be made. When studying signal processing this knowledge can give more detailed information not only at the system level but also at the level of an individual neuron. The main focus of this thesis is on small-conductance calcium activated potassium channels (SK), with a subsequent analysis of the muscarinic receptor control of a low threshold potassium current that is likely produced by an A-type channel.

Three SK channel subtypes (AptSK1, 2 &3) were cloned from the brain of Apteronotus and the distribution pattern of each subunit was mapped throughout the entire brain. I have shown that the AptSK channels show a high degree of sequence homology and a partially overlapping distribution pattern. The AptSK1 & 2 channels were localized to similar brain areas, while the AptSK3 subunits were localized to distinct brain areas. Since the ELL is the major signal processing area and much of the topology and cellular responses both in vivo and in vitro are known, it was the main focus of the physiological studies described in this thesis. Within the ELL the AptSK1 and 2 channels showed an overlapping distribution pattern. While, it appears both channels may be expressed in the same cell types, the AptSK1 channels are primarily dendritic and the AptSK2 channels show a somatic compartmentalization.

In vitro electrophysiological characterization of ELL pyramidal neurons revealed a neuron specific response pattern to the pharmacological modulation of AptSK channels. It was shown that only a subset of pyramidal neurons expressed functional AptSK channels. Moreover, the response patterns of the pyramidal neurons to AptSK modulation matched well with the distribution pattern of the AptSK2 channels in the ELL. The relevance of the neuron specific expression pattern was revealed during the

evaluation of a pyramidal neurons response to noise stimuli meant to mimic natural sensory signals. Some neurons have baseline properties that make them more responsive to the high frequency components of the presented stimuli while others respond strongly to low frequencies (Oswald et al., 2004). We found that neurons that lacked functional *Apt*SK2 channels were the strongest encoders of low frequency signals, while the presence of *Apt*SK2 predisposed a neuron to be more responsive to the high frequency stimuli. These differences are relevant since low frequency stimuli are produced by signals from prey, while high frequency signals are generated by specific communication signals (male-female interactions and Chirps).

An *in vivo* electrophysiological study by Dr. Maurice Chacron and Dr. Rudiger Krahe (McGill University) revealed that activation of muscarinic acetylcholine receptors could alter a neuron's frequency response in a manner similar to that seen when *Apt*SK channels were blocked. Since it had previously been shown that activation of muscarinic receptors could modulate SK currents (Akins et al., 1990), I set out to determine if this mechanism was responsible for the changes in the filtering properties of ELL pyramidal neurons following muscarinic receptor activation. It was found that muscarinic input onto the apical dendrites of ELL pyramidal neurons did not appear to affect the function of *Apt*SK channels, however, it was revealed that secondary modulation of a potassium conductance, namely that produced by a low threshold A-type channel, could also regulate the signal processing properties of a pyramidal neuron.

This thesis shows how an intrinsic  $K^+$  conductance can regulate the response properties of neurons in a sensory processing area. The localization and physiological evaluation of the AptSK channels describes how a  $K^+$  conductance can control the baseline response properties of a sensory neuron. The reduction of  $I_A$  by the activation of mAChRs reveals how modulation of such a conductance can subsequently alter neuronal response properties. Taken together these studies show that control of the sensory responsiveness of a primary processing neuron can not only be accomplished through synaptic input, but the initial control of such response properties are mediated by a number of different  $K^+$  channels. This may help to explain the need for the vast number of  $K^+$  channel subtypes with different kinetics and localization properties.

#### **REFERENCES**

Akins PT, Surmeier DJ, Kitai ST (1990) Muscarinic modulation of a transient K+conductance in rat neostriatal neurons. Nature 344: 240-242.

Bastian, J. Electrolocation I. How the electroreceptors of Apteronotus albifrons code for moving objects and other electrical stimuli. 144, 465-479. 1981. Ref Type: Generic

Bastian J, Chacron MJ, Maler L (2002) Receptive field organization determines pyramidal cell stimulus-encoding capability and spatial stimulus selectivity. J Neurosci 22: 4577-4590.

Berman NJ, Maler L (1998a) Distal versus proximal inhibitory shaping of feedback excitation in the electrosensory lateral line lobe: implications for sensory filtering. J Neurophysiol 80: 3214-3232.

Berman NJ, Maler L (1998b) Inhibition evoked from primary afferents in the electrosensory lateral line lobe of the weakly electric fish (Apteronotus leptorhynchus). J Neurophysiol 80: 3173-3196.

Berman NJ, Maler L (1998c) Interaction of GABAB-mediated inhibition with voltage-gated currents of pyramidal cells: computational mechanism of a sensory searchlight. J Neurophysiol 80: 3197-3213.

Carr CE, Maler L, Taylor B (1986) A time-comparison circuit in the electric fish midbrain. II. Functional morphology. J Neurosci 6: 1372-1383.

Chacron MJ (2006) Nonlinear information processing in a model sensory system. J Neurophysiol 95: 2933-2946.

Chacron MJ, Maler L, Bastian J (2005) Feedback and feedforward control of frequency tuning to naturalistic stimuli. J Neurosci 25: 5521-5532.

Coetzee WA, Amarillo Y, Chiu J, Chow A, Lau D, McCormack T, Moreno H, Nadal MS, Ozaita A, Pountney D, Saganich M, Vega-Saenz dM,

Rudy B (1999) Molecular diversity of K+channels. Ann N Y Acad Sci 868: 233-285.

Hille B (2001) Ion Channels of Excitable Membranes. Sinauer Associates.

Hodgkin AL, Huxley AF (1952) Currents carried by sodium and potassium ions through the membrane of the giant axon of Loligo. J Physiol 116: 449-472.

Hodgkin AL, Huxley AF (1953) Movement of radioactive potassium and membrane current in a giant axon. J Physiol 121: 403-414.

Maler L, Sas E, Johnston S, Ellis W (1991) An atlas of the brain of the electric fish Apteronotus leptorhynchus. J Chem Neuroanat 4: 1-38.

Oswald AM, Chacron MJ, Doiron B, Bastian J, Maler L (2004) Parallel processing of sensory input by bursts and isolated spikes. J Neurosci 24: 4351-4362.

Turner RW, Maler L (1999) Oscillatory and burst discharge in the apteronotid electrosensory lateral line lobe. J Exp Biol 202: 1255-1265.

## LITERATURE REVIEW I

## APTERONOTUS LEPTHORHYNCHUS: STUDYING SENSORY PROCESSING IN THE WEAKLY ELECTRIC FISH

#### Overview

The Brown Ghost Knifefish Apteronotus leptorhynchus is a weakly electric fish, in that it makes use of a self-generated electric field to locate objects (electrolocation) and to communicate with other electric fish (electrocommunication). The electric field pulse is generated by an electric organ in the tail of the fish and sensed by electroreceptors on the skin. The skin electroreceptors encode perturbations in the electric field through changes in firing rate (Bastian, 1981). Two subtypes of electroreceptors (tuberous and ampullary) send their outputs directly to a specialized hindbrain region known as the Electrosensory Lateral Line Lobe (ELL: for a review of the ELL see Berman and Maler, 1999; Turner and Maler, 1999). Briefly, the ELL is subdivided into 4 segments: the segment closest to the midline (medial segment-MS) receives input from the ampullary receptors, while the lateral (LS), centrolateral (CLS) and centromedial (CMS) segments receive identical inputs from tuberous electroreceptors. The input from the primary sensory afferents is somatotopically organized within each segment (Carr et al., 1982; Heiligenberg and Dye, 1982). The main processing units within the ELL are pyramidal neurons, which receive the sensory input from the electroreceptors and relay the important signal characteristics onto higher brain centers. The physiological and molecular makeup of the different ELL maps suggests that pyramidal neurons in the most lateral map are specialized to encode high frequency communication signals while pyramidal neurons in the more medial maps encode low frequency prey signals (Shumway, 1989; Metzner and Juranek, 1997).

Two major subclasses of pyramidal neurons exist in the ELL: Basilar (E-type) pyramidal neurons, which receive direct input from electroreceptors onto their basilar dendrites and non-basilar (I-type) cells that do not possess basilar dendrites. Input onto I-type cells is relayed from the primary afferents by granule cells that synapse onto the I-cell soma. The E and I type cells are present in approximately equal numbers throughout the ELL (Maler, 1979). Moreover, E-type pyramidal neurons show a similar segment specific response to the frequency of the electroreceptor input (Oswald et al., 2004), with cells from the LS responding best to high-frequency signals (communication), while the CMS cells respond best to low-frequency signals (prey-type). I-type cells, on the other

hand, are tuned to low-frequency input independent of segmental location (Chacron et al., 2005;Oswald et al., 2004). While E and I cells are structurally different with respect to the presence of a basilar dendrite, they are similar in that they both have an apical dendrite that extends from the opposite side of the soma and terminates in the dorsal molecular layer (Reviewed in Turner & Maler, 1999). The size of the apical dendritic tree depends on the location of the pyramidal cell within the ELL. There are 3 subtypes of pyramidal neurons based on their location and the size of their apical dendritic arbors, namely, superficial, intermediate and deep. The dendrites show a decreasing size gradient from superficials to intermediates and deep pyramidal neurons, which have the smallest apical dendrites (Bastian et al., 2004).

#### Dendritic control of a pyramidal neurons response properties

The apical dendrites are important regulators of pyramidal neuron function in a number of ways. Firstly, inputs onto the apical dendrites are from higher brain areas and are controlled by both electrosensory and non-electrosensory signals (Bastian & Nguyenkim, 2001). This allows for feedback regulation of the firing properties of the pyramidal neurons (Chacron et al., 2005;Mehaffey et al., 2005). Input onto the apical dendrites may lead to plastic changes in neuronal firing. It has recently been shown that deep pyramidal neurons, which have small apical dendrites, are non-plastic, while the superficial pyramidal neurons can undergo plastic changes (Bastian et al., 2004). This may be important for the subtraction of redundant stimuli as the deep cells would faithfully relay sensory signals onto higher brain centers, which may then feedback onto the superficial neurons and cancel out the baseline stimuli. If this were in fact the role of deep pyramidal neurons then the plastic changes that are seen in the superficial neurons would be in response to "novel" sensory stimuli only.

Along with their feedback role the apical dendrites are also involved in the generation of burst events. In pyramidal neurons bursts are generated by the backpropagation of Na<sup>+</sup> spikes originating in the soma. The backpropagating spikes rebound to the soma leading to a depolarizing afterpotential (DAP)(Turner et al., 1994;Noonan et al., 2003). The delay in the rebound of the dendritic spike leads the DAP to appear after the cessation of the somatic spike. This leads to a smaller AHP following

a somatic action potential (AP), which decreases the interspike interval (ISI) between successive spikes, leading to the high frequency firing within the burst. The dendritic spike is broader, showing a slower repolarization, than the somatic spike. This causes the DAP to accumulate until it becomes of sufficient magnitude on it's own to cause a somatic AP. The resulting spike doublet does not back-propagate as the second spike falls within the dendritic refractory period, leading to the end of the burst. Control over the dynamics of the apical dendrites can then have profound effects on a pyramidal neurons ability to produce burst events.

#### **Bursting**

Bursts are important for the processing of electrosensory signals as it has been found that they can selectively encode the low frequency components of the sensory stimuli (Lemon and Turner, 2000;Fernandez et al., 2005b;Oswald et al., 2004;Oswald et al., 2007;Doiron et al., 2007). Burst regulation has already been established at the network level, as frequency tuning *in vivo* is controlled by feedback input onto ELL pyramidal cells (Chacron et al., 2005). Further support for feedback regulation of bursting comes from *in vitro* studies that show the DAP amplitude and bursting can be regulated by these feedback pathways (Mehaffey et al., 2005). It then appears the dendritic control of the DAP can affect the ability of a pyramidal neuron to burst, subsequently leading to the regulation of the frequency encoding properties of the cell.

#### Potassium Channels in Apteronotus

During the development of an *in vitro* brain-slice preparation of the ELL it became apparent that the firing properties of pyramidal neurons could be attributed to various potassium currents (Mathieson and Maler, 1988;Turner et al., 1994). The currents that have been studied in the most detail are those created by the Kv3 subfamily of potassium channels. Kv3 channels are high threshold voltage activated potassium channels and they have been localized to many brain areas important for the processing of electrosensory signals (Rashid et al., 2001a;Deng et al., 2005). Two subtypes of Kv3 channels are expressed in the ELL, namely Kv3.1 and Kv3.3. The Kv3.3 channel has a uniform distribution across the sensory maps of the ELL and can be localized to both the

pyramidal cell soma and dendrites (Rashid et al., 2001a). It has been found that this TEA sensitive current is the major repolarizing current following both somatic and dendritic spikes (Noonan et al., 2003;Rashid et al., 2001b). Moreover, a reduction in this current can increase the width of the AP and decrease the fAHP. In this way the discharge frequency and in particular the frequency of burst events can be regulated (Doiron et al., 2003;Fernandez et al., 2005a). The expression pattern of Kv3.1 channels varies from that of Kv3.3 in that it is expressed in a map specific pattern, showing an increasing gradient from the CMS to CLS and LS (Deng et al., 2005). Additionally, Kv3.1 appears to be restricted to the soma of pyramidal cells, while, as mentioned, Kv3.3 is expressed in both the soma and dendrites. Since Kv3.1 is expressed at high levels in the LS, which responds strongly to high frequency input (Shumway, 1989), it has been suggested that it may play a role in setting the baseline response properties of LS pyramidal neurons (Deng et al., 2005). It then appears that the map specific and subcellular localization of the Kv3 channels may impart unique roles for the two subtypes in the ELL.

The Kv3 currents are not the only potassium currents found in ELL pyramidal neurons. Additionally, the existence of a low-threshold A-type current (I<sub>A</sub>) has been suggested (Mathieson and Maler, 1988; Fernandez et al., 2005a). The presence of I<sub>A</sub> was first apparent when it was shown that following a step current injection there was a significant lag period before the generation of an action potential. This latent period could be shortened by applying a depolarized pre-pulse or alternatively lengthened with a hyperpolarizing pre-pulse. Control of the first spike latency is an attribute of low threshold hyperpolarization activated I<sub>A</sub> (Connor and Stevens, 1971; Neher, 1971). Furthermore, the drug sensitivities of the current controlling the latent period were consistent with those found for I<sub>A</sub> in other systems (Coetzee et al., 1999). The low threshold A-type current is insensitive to TEA, which potently blocks the Apteronotus Kv3 current, allowing the low-threshold current to be separated from the high-threshold Kv3 current (Fernandez et al., 2005a). The first spike latency could, however, be reduced by application of the potassium channel blocker 4-aminopyridine (4-AP; Mathieson and Maler, 1988). It then appears that there are both high and low threshold Kv channels present in ELL pyramidal neurons.

Voltage gate channels are not the only potassium conductance present in ELL pyramidal neurons, there also appears to be a Ca<sup>2+</sup> activated K<sup>+</sup> current. It has been shown that the presence of a large conductance (BK) Ca<sup>2+</sup> activated K<sup>+</sup> current in pyramidal neurons is unlikely (Noonan et al., 2003), however evidence does exist that there is a small conductance (SK) Ca<sup>2+</sup> activated K<sup>+</sup> current (Mathieson and Maler, 1988). The SK channel specific bee-venom toxin apamin (Burgess et al., 1981) was found to increase the firing rate in approximately 1/3 of the pyramidal cells in the ELL (From a random cell population across maps; Mathieson and Maler, 1988).

While the presence of K<sup>+</sup> currents other than those generate by Kv3 channels has been demonstrated in ELL pyramidal neurons, less is known of their individual roles in a pyramidal neurons input response. If the contributions of the Kv3 channel family to pyramidal neuron function are of any indication, their effects should be significant.

The electrosensory system of *Apteronotus* is well characterized both *in vivo* and *in vitro* (Bastian, 1999;Berman and Maler, 1999;Turner and Maler, 1999;Bastian et al., 2002;Chacron et al., 2005;Chacron, 2006;Berman and Maler, 1998a;Berman and Maler, 1998c;Berman and Maler, 1998b). Hence, much is known of the response properties of the skin electroreceptors and the neuronal circuitry involved in the processing of the electrosensory signals. This allows for links to be made between the characteristics of an individual neuron and behaviourally relevant responses to subsets of sensory input, something that is not always possible in more complex mammalian systems.

#### **REFERENCES**

Bastian, J. Electrolocation I. How the electroreceptors of Apteronotus albifrons code for moving objects and other electrical stimuli. 144, 465-479. 1981. Ref Type: Generic

Bastian J (1999) Plasticity of feedback inputs in the apteronotid electrosensory system. J Exp Biol 202: 1327-1337.

Bastian J, Chacron MJ, Maler L (2002) Receptive field organization determines pyramidal cell stimulus-encoding capability and spatial stimulus selectivity. J Neurosci 22: 4577-4590

Berman NJ, Maler L (1998a) Distal versus proximal inhibitory shaping of feedback excitation in the electrosensory lateral line lobe: implications for sensory filtering. J Neurophysiol 80: 3214-3232.

Berman NJ, Maler L (1998b) Inhibition evoked from primary afferents in the electrosensory lateral line lobe of the weakly electric fish (Apteronotus leptorhynchus). J Neurophysiol 80: 3173-3196.

Berman NJ, Maler L (1998c) Interaction of GABAB-mediated inhibition with voltage-gated currents of pyramidal cells: computational mechanism of a sensory searchlight. J Neurophysiol 80: 3197-3213.

Berman NJ, Maler L (1999) Neural architecture of the electrosensory lateral line lobe: adaptations for coincidence detection, a sensory searchlight and frequency-dependent adaptive filtering. J Exp Biol 202: 1243-1253.

Burgess GM, Claret M, Jenkinson DH (1981) Effects of quinine and apamin on the calciumdependent potassium permeability of mammalian hepatocytes and red cells. J Physiol 317: 67-90.

Carr CE, Maler L, Sas E (1982) Peripheral organization and central projections of the electrosensory nerves in gymnotiform fish. J Comp Neurol 211: 139-153.

Chacron MJ (2006) Nonlinear information processing in a model sensory system. J Neurophysiol 95: 2933-2946.

Chacron MJ, Maler L, Bastian J (2005) Feedback and feedforward control of frequency tuning to naturalistic stimuli. J Neurosci 25: 5521-5532.

Coetzee WA, Amarillo Y, Chiu J, Chow A, Lau D, McCormack T, Moreno H, Nadal MS, Ozaita A, Pountney D, Saganich M, Vega-Saenz dM, Rudy B (1999) Molecular diversity of K+channels. Ann N Y Acad Sci 868: 233-285.

Connor JA, Stevens CF (1971) Voltage clamp studies of a transient outward membrane current in gastropod neural somata. J Physiol 213: 21-30.

Deng Q, Rashid AJ, Fernandez FR, Turner RW, Maler L, Dunn RJ (2005) A C-terminal domain directs Kv3.3 channels to dendrites. J Neurosci 25: 11531-11541.

Doiron B, Oswald AM, Maler L (2007) Interval Coding II: Dendrite Dependent Mechanisms. J Neurophysiol.

Doiron B, Noonan L, Lemon N, Turner RW (2003) Persistent Na+ current modifies burst discharge by regulating conditional backpropagation of dendritic spikes. J Neurophysiol 89: 324-337.

Fernandez FR, Mehaffey WH, Molineux ML, Turner RW (2005a) High-threshold K+ current increases gain by offsetting a frequency-dependent increase in low-threshold K+ current. J Neurosci 25: 363-371.

Fernandez FR, Mehaffey WH, Turner RW (2005b) Dendritic Na+ current inactivation can increase cell excitability by delaying a somatic depolarizing afterpotential. J Neurophysiol 94: 3836-3848.

Heiligenberg W, Dye J (1982) Labelling of electroreceptive afferents in a gymnotoid fish by intracellular injection of HRP: The mystery of multiple maps. J Comp Physiol [A] 148: 287-296.

Lemon N, Turner RW (2000) Conditional spike backpropagation generates burst discharge in a sensory neuron. J Neurophysiol 84: 1519-1530.

Maler L (1979) The posterior lateral line lobe of certain gymnotoid fish: quantitative light microscopy. J Comp Neurol 183: 323-363.

Mathieson WB, Maler L (1988) Morphological and electrophysiological properties of a novel in vitro preparation: the electrosensory lateral line lobe brain slice. J Comp Physiol [A] 163: 489-506.

Mehaffey WH, Doiron B, Maler L, Turner RW (2005) Deterministic multiplicative gain control with active dendrites. J Neurosci 25: 9968-9977.

Metzner W, Juranek J (1997) A sensory brain map for each behavior? Proc Natl Acad Sci U S A 94: 14798-14803.

Neher E (1971) Two fast transient current components during voltage clamp on snail neurons. J Gen Physiol 58: 36-53.

Noonan L, Doiron B, Laing C, Longtin A, Turner RW (2003) A dynamic dendritic refractory period regulates burst discharge in the electrosensory lobe of weakly electric fish. J Neurosci 23: 1524-1534.

Oswald AM, Chacron MJ, Doiron B, Bastian J, Maler L (2004) Parallel processing of sensory input by bursts and isolated spikes. J Neurosci 24: 4351-4362.

Oswald AM, Doiron B, Maler L (2007) Interval Coding I: Burst Inter-spike Intervals as indicators of Stimulus Intensity. J Neurophysiol.

Rashid AJ, Dunn RJ, Turner RW (2001a) A prominent soma-dendritic distribution of Kv3.3 K+ channels in electrosensory and cerebellar neurons. J Comp Neurol 441: 234-247.

Rashid AJ, Morales E, Turner RW, Dunn RJ (2001b) The contribution of dendritic Kv3 K+ channels to burst threshold in a sensory neuron. J Neurosci 21: 125-135.

Shumway CA (1989) Multiple electrosensory maps in the medulla of weakly electric

gymnotiform fish. I. Physiological differences. J Neurosci 9: 4388-4399.

Turner RW, Maler L (1999) Oscillatory and burst discharge in the apteronotid electrosensory lateral line lobe. J Exp Biol 202: 1255-1265.

Turner RW, Maler L, Deerinck T, Levinson SR, Ellisman MH (1994) TTX-sensitive dendritic sodium channels underlie oscillatory discharge in a vertebrate sensory neuron. J Neurosci 14: 6453-6471.

## **LITERATURE REVIEW II**

### SMALL CONDUCTANCE CALCIUM ACTIVATED POTASSIUM CHANNELS

#### SK channels control the mAHP

It is now known that an AHP can be subdivided into a number of components, however, early studies initially viewed the AHP as a single phenomenon that was rapidly activated following an action potential and decayed with a time constant of hundreds of milliseconds. It was shown that cumulative summation of the AHP increased the spacing between successive action potentials, thus decreasing the frequency of firing in a process known as spike frequency adaptation (Baldissera and Gustafsson, 1971). This then would allow the AHP to directly control the firing patterns of neurons in which it was present. It appeared that the summation of the AHP was directly attributable to an increased K<sup>+</sup> conductance mediated by a rise in intracellular Ca<sup>2+</sup> (Barrett and Barret, 1976;Krnjevic et al., 1978). As research continued into AHPs in different systems it became apparent that the characteristics of the AHP varied from neuron to neuron (Krnjevic et al., 1978; Hotson and Prince, 1980). Studies of CA1 hippocampal neurons (Guinea pig) suggested that the AHP was composed of two separate phases (Gustafsson and Wigstrom, 1981), an initial phase and a second phase that followed the depolarizing after potential (DAP). It was found that the slower component of the AHP became evident following multiple spikes, while the initial or fast AHP (fAHP) was obvious following a single spike. The slower AHP was found to summate becoming more prominent following multiple spikes. This began to suggest two separate mechanisms for generation of the fAHP and the slower phase. A study in frog ganglion cells (Pennefather et al., 1985) along with a rat CA1 study (Lancaster and Adams, 1986) used an approach, that at the time was quite novel, to evaluate the AHP current, termed the "hybrid clamp". The hybrid clamp involved a switch from current to voltage clamp at the peak of the AHP allowing direct measurement of the currents underlying the AHP. This allowed for the separation of the rapidly occurring current (I<sub>c</sub>) that was thought to be responsible for the fAHP (Hotson and Prince, 1980), from the slower AHP (I<sub>AHP</sub>), suggesting the presence of two separate channels (Pennefather et al., 1985).

In the frog ganglia both the  $I_c$  and the  $I_{AHP}$  are  $Ca^{2+}$  activated currents. The  $I_c$  is rapidly activated, has a large conductance and inactivates upon membrane repolarization, despite the likelihood of a continued elevation in  $Ca^{2+}$ . It is gated not only by  $Ca^{2+}$  but also shows voltage dependence. The  $I_{AHP}$  on the other hand is apparent following  $I_c$ 

elevation and inactivates slowly. The  $I_c$  and  $I_{AHP}$  showed alternative drug sensitivities, with  $I_c$  responsive to low levels of TEA, while,  $I_{AHP}$  is insensitive to TEA, but could be blocked by apamin (Pennefather et al., 1985;Lancaster and Adams, 1986: note: it has now been found that the mAHP can be blocked by high levels of TEA). These findings suggested that distinct currents were responsible for the two phases of the AHP and may have been due to separate  $Ca^{2+}$  activated  $K^+$  channels. While here I only focus on the  $Ca^{2+}$  activated  $K^+$  contribution to the fAHP it should be noted that voltage gated potassium channels (Kv) are the classic mediators of the fAHP and are present in this respect in most neurons.

#### **Linking Currents to Channels**

In the early 1980's advances in the use of the patch clamp technique, specifically the use of inside-out and outside-out patches, allowed for access to and control over the intracellular environment. This enabled evaluation of the large conductance (BK) Ca<sup>2+</sup> activated K<sup>+</sup> channel at the single channel level (reviewed by Marty, 1983). These channels were found to have a large conductance compared to channels previously studied, in the order of 180-240 pS. The voltage dependency and rate of inactivation was found to vary with increasing Ca2+ concentration. The rapid kinetics and large conductance rates of the BK channels lent well to a role in the generation of the I<sub>c</sub> current. Later definitions of the pharmacological properties of BK channels (reviewed in Sah and Davies, 2000) further implicate them as underlying the I<sub>c</sub> current. BK channels along with voltage gate potassium channels (Kv) are now thought to comprise the major components of the fAHP. The fAHP repolarizes the membrane following an AP (controlling spike width) and plays a role in setting firing frequency. While it does overlap to a small degree with the later AHP components the rapid inactivation of the BK and Kv channels prevents the fAHP from contributing to processes such as spike frequency adaptation that require a more prolonged hyperpolarizing current.

Whole cell physiology allowed the slower component of the AHP to be further characterized. It was found that it was comprised of two separate currents with distinct kinetics: the medium and slow AHP (mAHP, sAHP: Storm, 1989;Lancaster and Nicoll, 1987). However, it was more difficult to discern the channels responsible for these later

AHP components. In membrane patch studies of GH3 pituitary cells (Lang and Ritchie, 1987) and rat hippocampal pyramidal neurons (Lancaster et al., 1991) a Ca<sup>2+</sup> activated K<sup>+</sup> channel with a small conductance rate (SK channels; 10-20 pS) was found, in addition to the BK channel. This current could be separated from the I<sub>C</sub> (BK) due to its lack of voltage sensitivity. Application of 1 µM Ca<sup>2+</sup> to the intracellular membrane of inside out patches at a holding potential of -70 mV (below BK channel threshold) revealed the presence of the SK current (Lancaster et al., 1991). Ionic substitutions revealed that the current was indeed a K<sup>+</sup> current that required the presence of Ca<sup>2+</sup> to become activated. Along with the lack of voltage dependence, characterization of the channel properties revealed a linear current-voltage (I-V) relationship with a slope conductance of 20 pS and a reversal potential of -4 mV in equimolar K<sup>+</sup>. The bee venom toxin apamin was first found to block Ca<sup>2+</sup> activated K<sup>+</sup> currents in hepatocytes of the guinea pig (Burgess et al., 1981). It was revealed that apamin was specific for the SK channel mediated mAHP (Romey et al., 1984; Lang and Ritchie, 1990), thus providing a valuable tool to evaluate the functional role of the SK channels. While, SK channels were held responsible for the mAHP and sAHP, apamin did not block these currents in all cell lines tested (see Sah, 1996 for review). This suggested the possibility of multiple SK channel subtypes. The cloning of the SK channels was required to further define their anatomical/molecular and physiological characteristics. It was revealed that SK channels are tetrameric complexes with each individual subunit being composed of 6 transmembrane segments as well as intracellular amino and carboxy termini (Kohler et al., 1996). In mammals 3 distinct SK subtypes (SK1-3) are evident that show high homology in their transmembrane regions. Very little homology with other cloned K<sup>+</sup> channels is evident, with the exception of a 12 amino acid segment lying in the putative pore region that imparts K<sup>+</sup> selectivity. The cloning of the SK channels allowed for their expression and characterization in exogenous systems. Excised patches of Xenopus laevis oocyte membrane allowed the application of Ca<sup>2+</sup> directly to the intracellular membrane surface (Kohler et al., 1996). Varying the level of Ca<sup>2+</sup> in the bath solution revealed channel activation kinetics that produced Hill coefficients in a range suggesting the requirement of 4 Ca<sup>2+</sup> molecules to open channels. By applying a constant Ca<sup>2+</sup> concentration (5µM) and subjecting the membrane to a voltage ramp from -100 mV to 100 mV an I-V curve with a reversal

potential of 0 mV (in ND96 solution) was revealed. Evaluation of the I-V curve in the presence of apamin and d-tubocurare (dTC) revealed that the rSK2 channel could be blocked by apamin and dTC, while the hSK1 channel was insensitive to 100nM apamin and 30x less sensitive to dTC. This evaluation of the individual SK channels matched well with the previous data looking at SK channels in neurons (Lang and Ritchie, 1987;Lancaster et al., 1991). Based on these findings it was suspected that the apamin insensitive sAHP was the result of SK1 activation (Kohler et al., 1996). However, when SK1 channels were expressed in HEK and COS-7 cells, they were found to be blocked by apamin (Shah and Haylett, 2000;Strobaek et al., 2000), although at a level 4x that of SK2 channels. It was later found that in neurons SK1 channels were indeed sensitive to apamin but at levels higher than those originally used (Shah and Haylett, 2000;Strobaek et al., 2000).

#### SK channel gating mechanism

Evaluation of the molecular structure of SK channels revealed a novel gating mechanism involving the association of calmodulin (CaM; Xia et al., 1998). It was noted that unlike other calcium-binding proteins, SK channels had no characteristic Ca2+ binding motif, such as an E-F hand or Ca2+ bowl. A number of negatively charged residues (potential Ca<sup>2+</sup> binding sites) in the putative transmembrane regions were eliminated, however, this did not alter channel activation. Further mutational analysis of various channel segments revealed that normal channel function relied on a region of the C-terminal tail proximal to the 6<sup>th</sup> transmembrane segment (T6). Yeast two-hybrid studies revealed that this region would bind calmodulin (CaM; thus termed the calmodulin binding domain-CaMBD). It was found that the initial segment of the CaMBD could bind CaM in the absence of Ca<sup>2+</sup>. Immunohistochemical studies and attempts to dissociate CaM from the channels made it apparent that CaM was constitutively bound to the channel. A second region that was closer to the C-terminus was found to also bind CaM, but only when Ca<sup>2+</sup> was present. Crystallographic studies revealed that upon the binding of Ca2+ the CaM molecule attached to one of the 3 adjacent channel subunits (Schumacher et al., 2001). The SK channels essentially become a dimer of dimers in the presence of Ca<sup>2+</sup>. While CaM has 4 potential Ca<sup>2+</sup>

binding domains, 2 are occluded by the constitutive association with the SK channel C-terminus (Keen et al., 1999). This gives each subunit of the tetramer 2 potential Ca<sup>2+</sup> binding sites, however, each CaM only needs to bind one Ca<sup>2+</sup> molecule in order for the channels to open.

#### SK channel contributions to cellular physiology

It has been demonstrated in different systems that through their regulatory role SK channels can be involved in a number of processes such as, the regulation of neuronal firing rates and frequencies (Wolfart et al., 2001; Cloues and Sather, 2003), setting thresholds for the induction of synaptic plasticity (Lancaster et al., 2001; Stackman et al., 2002; Kramar et al., 2004; Hammond et al., 2006) the electic coupling between dendrites and soma (Womack and Khodakhah, 2003). SK channels are expressed in all areas of the CNS and PNS, with the expression level of each specific subtype depending on the area being evaluated (Rebecca Rimini et al., 2000). Expression of individual subunits overlaps throughout different systems, although it has been shown that individual subunits can be segregated in specific cellular regions (Sailer et al., 2002), perhaps suggestive of differential co-localization with specific Ca<sup>2+</sup> sources. While SK channels have been shown to play a role in a number of different systems and processes, their roles in larger neurological processes, such as information processing remains vague. Altered SK channel function has been weakly linked to schizophrenia (Tomita et al., 2003) and regulation of learning in mice (Stackman et al., 2002). Both of the above examples show a down regulation of SK channels, the first leading to a disease state of hyperexcitability, with the second showing an increase in the ability of mice to learn. It then appears that SK channels have a role in the maintenance of a fine balance in neuronal processing.

#### REFERENCES

Baldissera F, Gustafsson B (1971) Regulation of repetitive firing in motoneurones by the afterhyperpolarization conductance. Brain Res 30: 431-434.

Barrett EF, Barret JN (1976) Separation of two voltage-sensitive potassium currents, and demonstration of a tetrodotoxin-resistant calcium current in frog motoneurones. J Physiol 255: 737-774.

Burgess GM, Claret M, Jenkinson DH (1981) Effects of quinine and apamin on the calcium-dependent potassium permeability of mammalian hepatocytes and red cells. J Physiol 317: 67-90.

Cloues RK, Sather WA (2003) Afterhyperpolarization regulates firing rate in neurons of the suprachiasmatic nucleus. J Neurosci 23: 1593-1604.

Gustafsson B, Wigstrom H (1981) Evidence for two types of afterhyperpolarization in CA1 pyramidal cells in the hippocampus. Brain Res 206: 462-468.

Hammond RS, Bond CT, Strassmaier T, Ngo-Anh TJ, Adelman JP, Maylie J, Stackman RW (2006) Small-conductance Ca2+-activated K+channel type 2 (SK2) modulates hippocampal learning, memory, and synaptic plasticity. J Neurosci 26: 1844-1853.

Hotson JR, Prince DA (1980) A calcium-activated hyperpolarization follows repetitive firing in hippocampal neurons. J Neurophysiol 43: 409-419.

Keen JE, Khawaled R, Farrens DL, Neelands T, Rivard A, Bond CT, Janowsky A, Fakler B, Adelman JP, Maylie J (1999) Domains responsible for constitutive and Ca(2+)-dependent interactions between calmodulin and small conductance Ca(2+)-activated potassium channels. J Neurosci 19: 8830-8838.

Kohler M, Hirschberg B, Bond CT, Kinzie JM, Marrion NV, Maylie J, Adelman JP (1996) Small-conductance, calcium-activated potassium channels from mammalian brain. Science 273: 1709-1714.

Kramar EA, Lin B, Lin CY, Arai AC, Gall CM, Lynch G (2004) A novel mechanism for the facilitation of theta-induced long-term potentiation by brain-derived neurotrophic factor. J Neurosci 24: 5151-5161.

Krnjevic K, Puil E, Werman R (1978) EGTA and motoneuronal after-potentials. J Physiol 275: 199-223.

Lancaster B, Adams PR (1986) Calcium-dependent current generating the afterhyperpolarization of hippocampal neurons. J Neurophysiol 55: 1268-1282.

Lancaster B, Hu H, Ramakers GM, Storm JF (2001) Interaction between synaptic excitation and slow afterhyperpolarization current in rat hippocampal pyramidal cells. J Physiol 536: 809-823.

Lancaster B, Nicoll RA (1987) Properties of two calcium-activated hyperpolarizations in rat hippocampal neurones. J Physiol 389: 187-203.

Lancaster B, Nicoll RA, Perkel DJ (1991) Calcium activates two types of potassium channels in rat hippocampal neurons in culture. J Neurosci 11: 23-30.

Lang DG, Ritchie AK (1987) Large and small conductance calcium-activated potassium channels in the GH3 anterior pituitary cell line. Pflugers Arch 410: 614-622.

Lang DG, Ritchie AK (1990) Tetraethylammonium blockade of apaminsensitive and insensitive Ca2(+)-activated K+channels in a pituitary cell line. J Physiol 425: 117-132.

Marty A (1983) Blocking of large unitary calcium-dependent potassium currents by internal sodium ions. Pflugers Arch 396: 179-181.

Pennefather P, Lancaster B, Adams PR, Nicoll RA (1985) Two distinct Ca-dependent K currents in bullfrog sympathetic ganglion cells. Proc Natl Acad Sci U S A 82: 3040-3044.

Rebecca Rimini, Joseph M.Rimland, and Georg C.Terstappen. Quantitative Expression analysis of the small conductance calcium-activated potassium channels, SK1, SK2 and SK3, in human brain. 85, 218-220. 2000. Ref Type: Generic

Romey G, Hugues M, Schmid-Antomarchi H, Lazdunski M (1984) Apamin: a specific toxin to study a class of Ca2+-dependent K+ channels. J Physiol (Paris) 79: 259-264.

Sah P (1996) Ca(2+)-activated K+ currents in neurones: types, physiological roles and modulation. Trends Neurosci 19: 150-154.

Sah P, Davies P (2000) Calcium-activated potassium currents in mammalian neurons. Clin Exp Pharmacol Physiol 27: 657-663.

Sailer CA, Hu H, Kaufmann WA, Trieb M, Schwarzer C, Storm JF, Knaus HG (2002) Regional differences in distribution and functional expression of small-conductance Ca2+-activated K+ channels in rat brain. J Neurosci 22: 9698-9707.

Schumacher MA, Rivard AF, Bachinger HP, Adelman JP (2001) Structure of the gating domain of a Ca2+-activated K+ channel complexed with Ca2+/calmodulin. Nature 410: 1120-1124.

Shah M, Haylett DG (2000) The pharmacology of hSK1 Ca2+-activated K+ channels expressed in mammalian cell lines. Br J Pharmacol 129: 627-630.

Stackman RW, Hammond RS, Linardatos E, Gerlach A, Maylie J, Adelman JP, Tzounopoulos T (2002) Small conductance Ca2+-activated K+ channels modulate synaptic plasticity and memory encoding. J Neurosci 22: 10163-10171.

Storm JF (1989) An after-hyperpolarization of medium duration in rat hippocampal pyramidal cells. J Physiol 409: 171-190.

Stroback D, Jorgensen TD, Christophersen P, Ahring PK, Olesen SP (2000) Pharmacological characterization of small-conductance Ca(2+)-activated K(+) channels stably expressed in HEK 293 cells. Br J Pharmacol 129: 991-999.

Tomita H, Shakkottai VG, Gutman GA, Sun G, Bunney WE, Cahalan MD, Chandy KG, Gargus JJ (2003) Novel truncated isoform of SK3 potassium channel is a potent dominant-negative regulator of SK currents: implications in schizophrenia. Mol Psychiatry 8: 524-35, 460.

Wolfart J, Neuhoff H, Franz O, Roeper J (2001) Differential expression of the small-conductance, calcium-activated potassium channel SK3 is critical for pacemaker control in dopaminergic midbrain neurons. J Neurosci 21: 3443-3456.

Womack MD, Khodakhah K (2003) Somatic and dendritic small-conductance calcium-activated potassium channels regulate the output of cerebellar purkinje neurons. J Neurosci 23: 2600-2607.

Xia XM, Fakler B, Rivard A, Wayman G, Johnson-Pais T, Keen JE, Ishii T, Hirschberg B, Bond CT, Lutsenko S, Maylie J, Adelman JP (1998) Mechanism of calcium gating in small-conductance calcium-activated potassium channels. Nature 395: 503-507.

# LITERATURE REVIEW III A-TYPE POTASSIUM CHANNELS

#### A-type potassium currents

The fast transient A-type potassium current ( $I_A$ ) has both rapid inactivation and subthreshold activation kinetics allowing it to dampen membrane excitability. Originally described in the molluscan ganglion cells the outwardly rectifying  $I_A$  was found to be distinct from high-threshold potassium currents ( $I_K$ ; Connor and Stevens, 1971;Neher, 1971). It was shown that, in the mollusk,  $I_A$  was activated at potentials below –40 mV and was completely inactivated at –40 mV, whereas  $I_K$  was not activated until above –30 mV. These characteristics were separated in large part by the different drug sensitivities of the two currents.  $I_K$  was blocked by TEA, while  $I_A$  showed little response to TEA, but could be blocked by 4-AP. The unique kinetics and drug sensitivities suggested the presence of two distinct  $K^+$  currents having high ( $I_K$ ) and low ( $I_A$ ) activation thresholds.

Since that time I<sub>A</sub> has been found in a multitude of neuronal cell types (Rudy, 1988) and displays a rapid subthreshold activation, bimodal inactivation and rapid recovery from inactivation (I<sub>A</sub> kinetics reviewed by Jerng et al., 2004). The kinetics of I<sub>A</sub> shows a high amount of variability depending on cell type. The  $V_{1/2}$  of activation can lie between -47 and 0 mV, with a slope factor  $(k_A)$  between 5 and 27 mV. This allows for a large range of subthreshold voltages in which IA can become activated, and it does so with an activation time constant  $(\tau_A)$  between 1 and 5 ms. Inactivation has both a rapid  $(\tau$ = 7 to 95 ms) and slow component (20 to 50%,  $\tau$  = 60 to 300 ms) and also shows a large variation in its steady state inactivation curve ( $V_{1/2} = -56$  to -94 mV;  $k_i = 6$  to 10 mV). While this does mean that much of IA becomes inactivated at voltages below the activation threshold, the overlap of the steady state activation and inactivation curves produces a "window current" in which a fraction of IA is active. The large variability in both the activation and inactivation properties between cell types means that the size of the window current and the voltage at which it peaks can also vary significantly. The window current has the potential to be present at voltages well below the action potential threshold and at a neurons normal resting potential, giving IA the ability to regulate the resting membrane potential and firing rate (Kim et al., 2005).

#### I<sub>A</sub> controls neuronal firing patterns

The properties of I<sub>A</sub> allow it to control a number of important aspects of neuronal firing. One of the first descriptions of such control was based on the rapid subthreshold recovery from inactivation, which allows I<sub>A</sub> to become de-inactivated during an AHP and then activated as the membrane recovers from the AHP. This delays the membrane repolarization following an action potential and can help set the interspike interval (Connor and Stevens, 1971, see also, Hille, 2001). A number of the firing properties of a neuron can be controlled by I<sub>A</sub>, including: the action potential waveform and duration (Bardoni and Belluzzi, 1993), firing threshold (Kim et al., 2005), adapting spike behavior (Malin and Nerbonne, 2000), first spike latency (Schoppa and Westbrook, 1999;Shibata et al., 2000), action potential back propagation (Hoffman et al., 1997), the timing and integration of synaptic inputs (Salkoff et al., 1992;Schoppa and Westbrook, 1999), LTP and LTD (Frick et al., 2004) along with a role in setting neuronal gain (Burdakov et al., 2004).

#### IA control of higher order functions

The importance and diversity of the controls I<sub>A</sub> can have on a neuron's firing properties becomes apparent when one looks at the regulation of learning and memory. It has been suggested that I<sub>A</sub> can contribute to learning and memory in a several ways. Dendritic I<sub>A</sub> can control short-term excitability (Johnston et al., 2000) and induction of synaptic plasticity (Ramakers and Storm, 2002;Schreurs et al., 1997). I<sub>A</sub> can also contribute to learning and memory through its control of neuronal firing patterns (Andreasen and Lambert, 1995;Flores-Hernandez et al., 1994), membrane excitability (Alkon, 1983;Farley and Alkon, 1985;Schreurs et al., 1998) and subsequent release of neurotransmitters (Pena and Tapia, 2000;Cassel et al., 2005;Schweizer et al., 2003). While there are a multitude of variables involved in learning and memory formation that are not linked to I<sub>A</sub> this highlights the idea that through different controls on a neurons firing properties, one type of current can contribute to higher order processes.

The question then becomes: how exactly can I<sub>A</sub> control different properties in various neurons? The neuron specific kinetics may be the result of subtype specific expression patterns, as a number of potassium channels can produce A-type currents,

including the Kv4, Kv1.4 and Kv1.5 channels (Coetzee et al., 1999). The effect of having a number of channels that can contribute to I<sub>A</sub> may reflect the need for different channel kinetics in order to manufacture different neuronal firing properties. Alternatively, it has also been shown that different subtypes show compartment specific distribution patterns in a number of neuronal cells types. For example, in the CA1 region of the hippocampus Kv4 subunits have been found in the soma and dendrites of pyramidal neurons, while the Kv1.4 subunits can be localized to axonal projections (Sheng et al., 1992;Coetzee et al., 1999). The distribution patterns are cell type specific as Kv1.4, for example, can be found in the dendrites and soma of neurons in the dorsal cochlear nucleus (Juiz et al., 2000). The fact that multiple channel subtypes can produce an A-type current may be required for any combination of the above ideas: it may be due to the need for slightly different channel kinetics, to control the distribution properties of specific subunits, or a combination of the two. Any of these differences could then result in different roles for I<sub>A</sub> in each neuron.

#### REFERENCES

Alkon DL (1983) Learning in a marine snail. Sci Am 249: 70-8, 80.

Andreasen M, Lambert JD (1995) Regenerative properties of pyramidal cell dendrites in area CA1 of the rat hippocampus. J Physiol 483 ( Pt 2): 421-441.

Bardoni R, Belluzzi O (1993) Kinetic study and numerical reconstruction of A-type current in granule cells of rat cerebellar slices. J Neurophysiol 69: 2222-2231.

Burdakov D, Alexopoulos H, Vincent A, Ashcroft FM (2004) Low-voltage-activated Acurrent controls the firing dynamics of mouse hypothalamic orexin neurons. Eur J Neurosci 20: 3281-3285.

Cassel JC, Schweizer T, Lazaris A, Knorle R, Birthelmer A, Godtel-Armbrust U, Forstermann U, Jackisch R (2005) Cognitive deficits in aged rats correlate with levels of L-arginine, not with nNOS expression or 3,4-DAP-evoked transmitter release in the frontoparietal cortex. Eur Neuropsychopharmacol 15: 163-175.

Coetzee WA, Amarillo Y, Chiu J, Chow A, Lau D, McCormack T, Moreno H, Nadal MS, Ozaita A, Pountney D, Saganich M, Vega-Saenz dM, Rudy B (1999) Molecular diversity of K+channels. Ann N Y Acad Sci 868: 233-285.

Connor JA, Stevens CF (1971) Voltage clamp studies of a transient outward membrane current in gastropod neural somata. J Physiol 213: 21-30

Farley J, Alkon DL (1985) Cellular mechanisms of learning, memory, and information storage. Annu Rev Psychol 36: 419-494.

Flores-Hernandez J, Galarraga E, Pineda JC, Bargas J (1994) Patterns of excitatory and inhibitory synaptic transmission in the rat neostriatum as revealed by 4-AP. J Neurophysiol 72: 2246-2256.

Frick A, Magee J, Johnston D (2004) LTP is accompanied by an enhanced local excitability of

pyramidal neuron dendrites. Nat Neurosci 7: 126-135.

Hille B (2001) Ion Channels of Excitable Membranes. Sinauer Associates.

Hoffman DA, Magee JC, Colbert CM, Johnston D (1997) K+ channel regulation of signal propagation in dendrites of hippocampal pyramidal neurons. Nature 387: 869-875.

Jerng HH, Pfaffinger PJ, Covarrubias M (2004) Molecular physiology and modulation of somatodendritic A-type potassium channels. Mol Cell Neurosci 27: 343-369.

Johnston D, Hoffman DA, Magee JC, Poolos NP, Watanabe S, Colbert CM, Migliore M (2000) Dendritic potassium channels in hippocampal pyramidal neurons. J Physiol 525 Pt 1: 75-81.

Juiz JM, Lujan R, Dominguez dT, Fuentes V, Ballesta JJ, Criado M (2000) Subcellular compartmentalization of a potassium channel (Kv1.4): preferential distribution in dendrites and dendritic spines of neurons in the dorsal cochlear nucleus. Eur J Neurosci 12: 4345-4356.

Kim J, Wei DS, Hoffman DA (2005) Kv4 potassium channel subunits control action potential repolarization and frequency-dependent broadening in rat hippocampal CA1 pyramidal neurones. J Physiol 569: 41-57.

Malin SA, Nerbonne JM (2000) Elimination of the fast transient in superior cervical ganglion neurons with expression of KV4.2W362F: molecular dissection of IA. J Neurosci 20: 5191-5199.

Neher E (1971) Two fast transient current components during voltage clamp on snail neurons. J Gen Physiol 58: 36-53.

Pena F, Tapia R (2000) Seizures and neurodegeneration induced by 4-aminopyridine in rat hippocampus in vivo: role of glutamate-and GABA-mediated neurotransmission and of ion channels. Neuroscience 101: 547-561.

Ramakers GM, Storm JF (2002) A postsynaptic transient K(+) current modulated by arachidonic acid regulates synaptic integration and threshold for LTP induction in hippocampal pyramidal cells. Proc Natl Acad Sci U S A 99: 10144-10149.

Rudy B (1988) Diversity and ubiquity of K channels. Neuroscience 25: 729-749.

Salkoff L, Baker K, Butler A, Covarrubias M, Pak MD, Wei A (1992) An essential 'set' of K+channels conserved in flies, mice and humans. Trends Neurosci 15: 161-166.

Schoppa NE, Westbrook GL (1999) Regulation of synaptic timing in the olfactory bulb by an Atype potassium current. Nat Neurosci 2: 1106-1113.

Schreurs BG, Gusev PA, Tomsic D, Alkon DL, Shi T (1998) Intracellular correlates of acquisition and long-term memory of classical conditioning in Purkinje cell dendrites in slices of rabbit cerebellar lobule HVI. J Neurosci 18: 5498-5507.

Schreurs BG, Tomsic D, Gusev PA, Alkon DL (1997) Dendritic excitability microzones and occluded long-term depression after classical conditioning of the rabbit's nictitating membrane response. J Neurophysiol 77: 86-92.

Schweizer T, Birthelmer A, Lazaris A, Cassel JC, Jackisch R (2003) 3,4-DAP-evoked transmitter release in hippocampal slices of aged rats with impaired memory. Brain Res Bull 62: 129-136.

Sheng M, Tsaur ML, Jan YN, Jan LY (1992) Subcellular segregation of two A-type K+channel proteins in rat central neurons. Neuron 9: 271-284.

Shibata R, Nakahira K, Shibasaki K, Wakazono Y, Imoto K, Ikenaka K (2000) A-type K+ current mediated by the Kv4 channel regulates the generation of action potential in developing

cerebellar granule cells. J Neurosci 20: 4145-4155.

# <u>LITERATURE REVIEW IV</u> REGULATION OF POTASSIUM CONDUCTANCES

As outlined, two different K<sup>+</sup> channels (SK & A-type) with distinct kinetics are responsible for a number of the baseline properties of a large diversity of neurons. As such, increasing or decreasing the contribution of either conductance to a cell's firing properties has the potential to regulate a number of neuronal functions. It has been shown that both of these currents can undergo secondary modulation that can alter their response properties.

A number of neurotransmitters and second messengers can regulate both SK and A-type channels. SK channels can be phosphorylated by PKA (Ren et al., 2006) or constitutively associated serine-threonine protein kinase CK2 (Bildl et al., 2004;Allen et al., 2007). Moreover, SK channel function can be modulated by neurotransmitters including, norepinephrine (Nicoll, 1988) and serotonin (Grunnet et al., 2004). A-type channels can also be phosphorylated by PKA along with PKC (Hoffman and Johnston, 1998), cAMP kinase (Anderson et al., 2000) and MAP kinase (Yuan et al., 2002) leading to a downregulation of I<sub>A</sub>. Neurotransmitters that can regulate I<sub>A</sub> include glutamate (Schoppa, 2006), acetylcholine (Akins et al., 1990;Nakajima et al., 1986), serotonin (Sakurai et al., 2006), dopamine (Perez et al., 2006), anandamide (Tang et al., 2005) and histamine (Starodub and Wood, 2000). It has also been shown that I<sub>A</sub> can be controlled by intracellular calcium levels (Chen and Wong, 1991;An et al., 2000;Beck et al., 2002).

The modulation of  $I_A$  can alter a number of neuronal and network properties in many of the ways previously discussed. The complexities involved in the downstream consequences of  $I_A$  regulation and the pathways involved are beyond the scope of this thesis. I will however focus on the muscarinic regulation of  $I_A$  at the neuron, network and systems levels.

#### Cholinergic pathways in the CNS

There are two major cholinergic pathways in the mammalian CNS, one that originates from the forebrain and the other coming from the brainstem (Mesulam et al., 1983b;Mesulam et al., 1983a;Hallanger et al., 1987;Rye et al., 1987). The brainstem cholinergic system mainly projects to the thalamus, while, the forebrain pathways, originating from 6 different nuclei, can synapse on the cortex, hippocampus, basolateral amygdala, thalamus and the olfactory bulb (reviewed by Everitt and Robbins,

1997;Lucas-Meunier et al., 2003). The projections and pathways are much more complex than can be described here, however, this does highlight the fact that a large number of neurons in the CNS use acetylcholine as a neurotransmitter and the inputs of these neurons can reach a vast number of cells throughout the brain. Through these pathways acetyl-choline (ACh) can regulate information processing in several brain areas (Everitt and Robbins, 1997;Sarter et al., 2005), which will be the focus of the rest of this review.

#### Feedback regulation by ACh

Since many of the major cholinergic pathways originate from the forebrain, their input can often be considered as cognitive control over the major sensory processing areas. Some of the higher order functions that can be controlled by cholinergic input include: attention (Bucci et al., 1998; Voytko et al., 1994), learning (Miranda and Bermudez-Rattoni, 1999; Fine et al., 1997) & memory (Hasselmo et al., 1992; Sarter et al., 2005), stress responses (Newman et al., 2001), and sleep (Jasper and Tessier, 1971; Jimenez-Capdeville and Dykes, 1996). Many of these processes are modulated when a cholinergic pathway is activated in conjunction with an external sensory stimulus. Pairing of this kind often results in a heightened stimulus response and can lead to longterm changes in not only the properties of individual neurons but also the system in general. An example of such control occurs following stimulation of the primary somatosensory cortex, which when paired with an external stimuli, can enhance the animal's response to the stimuli (Donoghue and Carroll, 1987; Rasmusson and Dykes, 1988). The cholinergic pathways can act in a feedback manner that can translate into increased attentional performance at the behavioral level (Metherate, 2004; Sarter et al., 2005), which may be accomplished through an enhancement of the signal to noise ratio at the cellular level.

Acetylcholine can activate two types of receptors the nicotinic (nAChR), and muscarinic (mAChR) receptors. The nicotinic receptors are ionotropic and can conduct a number of ions. Muscarinic receptors on the other hand are metabotropic receptors coupled to a number of signaling cascades that can have a multitude of cellular effects. The activation of the two different receptors can then act on alternate time scales, with

the nAChR's controlling rapid responses and the mAChR pathways producing more sustained responses. This thesis deals with the contribution of potassium channels to neuronal firing properties, and as such, their possible modulation of mAChR cascades will be emphasized.

#### Muscarinic receptors

Muscarinic acetylcholine receptors (mAChR) are metabotropic G-protein coupled They can be formed by 5 different subunits (M<sub>1</sub> to M<sub>5</sub>) which can be subdivided into two separate groups, the M1 family (M<sub>1</sub>, M<sub>3</sub>, M<sub>5</sub>) and the M2 family (M<sub>2</sub>,  $M_4$ ). The M1 family is more common in the CNS and is coupled (through  $G_{q/11}$ ) to the phospholipase C (PLC) pathway. Alternatively, the M2 family (though G<sub>i/o</sub>) can inhibit adenylate cyclase (AC) or activate G-protein coupled K<sup>+</sup> channels. In general this makes the M1 pathway excitatory and the M2 pathway inhibitory (reviews: Matsui et al., 2004; Hille, 2001). For the purposes of this review I will mainly focus on the M1 receptors. As mentioned, the activation of M1 stimulates the PLC pathways. The two major PLC pathways are activated when PLC hydrolyzes phosphatidylinositol (PIP<sub>2</sub>) leading to the formation of inositoltriphosphate (IP<sub>3</sub>) and diacylglycerol (DAG). This subsequently leads to increases in phosphokinase C (PKC) and can cause the release of Ca<sup>2+</sup> from the endoplasmic reticulum. The downstream effects of the activation of these pathways are complex and extensive and will not be outlined in detail here. The diversity of actions that these pathways can have is highlighted when one looks at individual ion channels. The modulation of a number of ion channels including calcium (Delgado-Lezama et al., 1997; Svirskis and Hounsgaard, 1998; Tai et al., 2006) and sodium channels (Mittmann and Alzheimer, 1998) along with calcium activated (SK) (Stocker et al., 1999), hyperpolarization activated (A and H-type)(Nakajima et al., 1986; Akins et al., 1990) and muscarine sensitive potassium channels (M-type)(Chen and Johnston, 2004) can lead to increases in cell excitability.

Links between the control of an individual conductance and the resulting effects at the systems level have not been definitively made for mAChR activation. Evidence does exist that this may occur. For example, it has long been known that the activation of muscarinic ACh receptors (mAChR) in mammalian cortical neurons can depolarize the

membrane, which can enhance the neurons responsiveness to other excitatory input (Krnjevic et al., 1971). It was speculated at the time that this was the result of a decrease in an outwardly rectifying conductance, likely through the regulation a K<sup>+</sup> channel. It then becomes plausible that some of the aforementioned cholinergic pathways have the potential to control sensory responses through the regulation of any number of intrinsic ionic conductances.

#### REFERENCES

Akins PT, Surmeier DJ, Kitai ST (1990) Muscarinic modulation of a transient K+conductance in rat neostriatal neurons. Nature 344: 240-242.

Allen D, Fakler B, Maylie J, Adelman JP (2007) Organization and regulation of small conductance Ca2+-activated K+ channel multiprotein complexes. J Neurosci 27: 2369-2376.

An WF, Bowlby MR, Betty M, Cao J, Ling HP, Mendoza G, Hinson JW, Mattsson KI, Strassle BW, Trimmer JS, Rhodes KJ (2000) Modulation of A-type potassium channels by a family of calcium sensors. Nature 403: 553-556.

Anderson AE, Adams JP, Qian Y, Cook RG, Pfaffinger PJ, Sweatt JD (2000) Kv4.2 phosphorylation by cyclic AMP-dependent protein kinase. J Biol Chem 275: 5337-5346.

Beck EJ, Bowlby M, An WF, Rhodes KJ, Covarrubias M (2002) Remodelling inactivation gating of Kv4 channels by KChIP1, a small-molecular-weight calcium-binding protein. J Physiol 538: 691-706.

Bildl W, Strassmaier T, Thurm H, Andersen J, Eble S, Oliver D, Knipper M, Mann M, Schulte U, Adelman JP, Fakler B (2004) Protein kinase CK2 is coassembled with small conductance Ca(2+)-activated K+ channels and regulates channel gating. Neuron 43: 847-858.

Bucci DJ, Holland PC, Gallagher M (1998) Removal of cholinergic input to rat posterior parietal cortex disrupts incremental processing of conditioned stimuli. J Neurosci 18: 8038-8046.

Chen QX, Wong RK (1991) Intracellular Ca2+ suppressed a transient potassium current in hippocampal neurons. J Neurosci 11: 337-343.

Chen X, Johnston D (2004) Properties of single voltage-dependent K+ channels in dendrites of CA1 pyramidal neurones of rat hippocampus. J Physiol 559: 187-203.

Delgado-Lezama R, Perrier JF, Nedergaard S, Svirskis G, Hounsgaard J (1997) Metabotropic synaptic regulation of intrinsic response properties of turtle spinal motoneurones. J Physiol 504 (Pt 1): 97-102.

Donoghue JP, Carroll KL (1987) Cholinergic modulation of sensory responses in rat primary somatic sensory cortex. Brain Res 408: 367-371.

Everitt BJ, Robbins TW (1997) Central cholinergic systems and cognition. Annu Rev Psychol 48: 649-684.

Fine A, Hoyle C, Maclean CJ, Levatte TL, Baker HF, Ridley RM (1997) Learning impairments following injection of a selective cholinergic immunotoxin, ME20.4 IgG-saporin, into the basal nucleus of Meynert in monkeys. Neuroscience 81: 331-343.

Grunnet M, Jespersen T, Perrier JF (2004) 5-HT1A receptors modulate small-conductance Ca2+-activated K+ channels. J Neurosci Res 78: 845-854.

Hallanger AE, Levey AI, Lee HJ, Rye DB, Wainer BH (1987) The origins of cholinergic and other subcortical afferents to the thalamus in the rat. J Comp Neurol 262: 105-124.

Hasselmo ME, Anderson BP, Bower JM (1992) Cholinergic modulation of cortical associative memory function. J Neurophysiol 67: 1230-1246.

Hille B (2001) Ion Channels of Excitable Membranes. Sinauer Associates.

Hoffman DA, Johnston D (1998) Downregulation of transient K+ channels in dendrites of hippocampal CA1 pyramidal neurons by activation of PKA and PKC. J Neurosci 18: 3521-3528.

Jasper HH, Tessier J (1971) Acetylcholine liberation from cerebral cortex during paradoxical (REM) sleep. Science 172: 601-602.

Jimenez-Capdeville ME, Dykes RW (1996) Changes in cortical acetylcholine release in the rat during day and night: differences between motor and sensory areas. Neuroscience 71: 567-579.

Krnjevic K, Pumain R, Renaud L (1971) The mechanism of excitation by acetylcholine in the cerebral cortex. J Physiol 215: 247-268.

Lucas-Meunier E, Fossier P, Baux G, Amar M (2003) Cholinergic modulation of the cortical neuronal network. Pflugers Arch 446: 17-29.

Matsui M, Yamada S, Oki T, Manabe T, Taketo MM, Ehlert FJ (2004) Functional analysis of muscarinic acetylcholine receptors using knockout mice. Life Sci 75: 2971-2981.

Mesulam MM, Mufson EJ, Levey AI, Wainer BH (1983a) Cholinergic innervation of cortex by the basal forebrain: cytochemistry and cortical connections of the septal area, diagonal band nuclei, nucleus basalis (substantia innominata), and hypothalamus in the rhesus monkey. J Comp Neurol 214: 170-197.

Mesulam MM, Mufson EJ, Wainer BH, Levey AI (1983b) Central cholinergic pathways in the rat: an overview based on an alternative nomenclature (Ch1-Ch6). Neuroscience 10: 1185-1201.

Metherate R (2004) Nicotinic acetylcholine receptors in sensory cortex. Learn Mem 11: 50-59.

Miranda MI, Bermudez-Rattoni F (1999) Reversible inactivation of the nucleus basalis magnocellularis induces disruption of cortical acetylcholine release and acquisition, but not retrieval, of aversive memories. Proc Natl Acad Sci U S A 96: 6478-6482.

Mittmann T, Alzheimer C (1998) Muscarinic inhibition of persistent Na+ current in rat neocortical pyramidal neurons. J Neurophysiol 79: 1579-1582.

Nakajima Y, Nakajima S, Leonard RJ, Yamaguchi K (1986) Acetylcholine raises excitability by inhibiting the fast transient potassium current in cultured hippocampal neurons. Proc Natl Acad Sci U S A 83: 3022-3026.

Newman MB, Nazian SJ, Sanberg PR, Diamond DM, Shytle RD (2001) Corticosterone-attenuating and anxiolytic properties of mecamylamine in the rat. Prog

Neuropsychopharmacol Biol Psychiatry 25: 609-620.

Nicoll RA (1988) The coupling of neurotransmitter receptors to ion channels in the brain. Science 241: 545-551.

Perez MF, White FJ, Hu XT (2006) Dopamine D(2) receptor modulation of K(+) channel activity regulates excitability of nucleus accumbens neurons at different membrane potentials. J Neurophysiol 96: 2217-2228.

Rasmusson DD, Dykes RW (1988) Long-term enhancement of evoked potentials in cat somatosensory cortex produced by co-activation of the basal forebrain and cutaneous receptors. Exp Brain Res 70: 276-286.

Ren Y, Barnwell LF, Alexander JC, Lubin FD, Adelman JP, Pfaffinger PJ, Schrader LA, Anderson AE (2006) Regulation of surface localization of the small conductance Ca2+activated potassium channel, Sk2, through direct phosphorylation by cAMP-dependent protein kinase. J Biol Chem 281: 11769-11779.

Rye DB, Saper CB, Lee HJ, Wainer BH (1987) Pedunculopontine tegmental nucleus of the rat: cytoarchitecture, cytochemistry, and some extrapyramidal connections of the mesopontine tegmentum. J Comp Neurol 259: 483-528.

Sakurai A, Darghouth NR, Butera RJ, Katz PS (2006) Serotonergic enhancement of a 4-AP-sensitive current mediates the synaptic depression phase of spike timing-dependent neuromodulation. J Neurosci 26: 2010-2021.

Sarter M, Hasselmo ME, Bruno JP, Givens B (2005) Unraveling the attentional functions of cortical cholinergic inputs: interactions between signal-driven and cognitive modulation of signal detection. Brain Res Brain Res Rev 48: 98-111.

Schoppa NE (2006) AMPA/kainate receptors drive rapid output and precise synchrony in olfactory bulb granule cells. J Neurosci 26: 12996-13006.

Starodub AM, Wood JD (2000) Histamine suppresses A-type potassium current in myenteric neurons from guinea pig small intestine. J Pharmacol Exp Ther 294: 555-561.

Stocker M, Krause M, Pedarzani P (1999) An apamin-sensitive Ca2+-activated K+ current in hippocampal pyramidal neurons. Proc Natl Acad Sci U S A 96: 4662-4667.

Svirskis G, Hounsgaard J (1998) Transmitter regulation of plateau properties in turtle motoneurons. J Neurophysiol 79: 45-50.

Tai C, Kuzmiski JB, MacVicar BA (2006) Muscarinic enhancement of R-type calcium currents in hippocampal CA1 pyramidal neurons. J Neurosci 26: 6249-6258.

Tang SL, Tran V, Wagner EJ (2005) Sex differences in the cannabinoid modulation of an A-type K+ current in neurons of the mammalian hypothalamus. J Neurophysiol 94: 2983-2986.

Voytko ML, Olton DS, Richardson RT, Gorman LK, Tobin JR, Price DL (1994) Basal forebrain lesions in monkeys disrupt attention but not learning and memory. J Neurosci 14: 167-186.

Yuan LL, Adams JP, Swank M, Sweatt JD, Johnston D (2002) Protein kinase modulation of dendritic K+ channels in hippocampus involves a mitogen-activated protein kinase pathway. J Neurosci 22: 4860-4868.

#### SUMMARY OF CHAPTERS

The 3 chapters of this thesis are comprised of individual manuscripts.

Chapter 1: This chapter describes the initial cloning and localization of 3 SK channels (AptSK1, 2 &3) throughout the entire brain of A. leptorhynchus. The 3 AptSK channels show high sequence homology to one another and sequence conservation with SK channels previously cloned from other species. It is shown through in situ hybridization that AptSK1 and 2 show a partially overlapping distribution pattern throughout the brain, while AptSK3 is expressed independently. Immunohistochemistry reveals distinct subcellular distributions for the AptSK1 & 2 channels in pyramidal neurons of the ELL. The main text of this chapter includes references to studies described in Chapter 2 since this manuscript was submitted for publication following the manuscript that comprises Chapter 2. Also, this manuscript is presented as Chapter 1 since the cloning and localization of the AptSK channels was accomplished before physiological characterization was attempted and thus follows the logical progression of the research.

Chapter 2: The AptSK2 channel was localized within the ELL showing a segment specific distribution pattern between the sensory maps of the ELL. Physiological characterization of the pyramidal neurons in the ELL supported the distribution patterns found through the in situ hybridization studies. Further, through neurobiotin labeling of cells following physiological characterization, it was revealed that the two subclasses (E and I) of neurons differentially express functional AptSK channels. E-type neurons (basilar) possess functional AptSK channels, while I-cells (non-basilar) do not. The presence of AptSK2 channels predisposed pyramidal neurons to respond to high frequencies by preventing strong responses to low frequency input.

Chapter 3: The final chapter evaluates the role that secondary modulation of a potassium conductance can have on the frequency response properties of pyramidal neurons. Activation of muscarinic acetylcholine receptors (mAChRs) *in vivo* was found to produce increases in a pyramidal neuron's response to low frequency input similar to that seen

following AptSK channel block. Interestingly, it was found that mAChR activation did not lead to a down-regulation of AptSK channels in vitro. Rather it was found to reduce a low threshold potassium current that is likely produced by an A-type channel. Mathematical modeling provided further support to this notion by demonstrating that an A-type current has the ability to regulate the frequency response properties of a pyramidal neuron.

# **CHAPTER I**

# DIFFERENTIAL DISTRIBUTION OF THE SK CHANNEL SUBTYPES IN THE BRAIN OF THE WEAKLY ELECTRIC FISH

Lee D. Ellis, Leonard Maler, and Robert J. Dunn

Journal of Comparative Neurology 2007, accepted for publication

## **CONTRIBUTIONS OF AUTHORS**

Lee Ellis performed all of the experiments in this study. This manuscript was written by Lee Ellis and Len Maler (University of Ottawa) with editing by Rob Dunn. Lee Ellis created all of the figures for the manuscript.

#### **Abstract**

Calcium signals in vertebrate neurons can induce hyperpolarizing membrane responses through the activation of Ca<sup>2+</sup>-activated potassium channels. Of these, small conductance (SK) channels regulate neuronal responses through the generation of the mAHP. We have previously shown that an SK channel (AptSK2) contributes to signal processing in the electrosensory system of Apteronotus lepthorhynchus. It was shown that for pyramidal neurons in the electrosensory lateral line lobe (ELL), AptSK2 expression selectively decreases responses to low frequency signals. The localization of all the SK subunits throughout the brain of Apteronotus then became of substantial interest. We have now cloned two additional SK channel subunits from Apteronotus and determined the expression patterns of all three AptSK subunits throughout the brain. In situ hybridization experiments have revealed that, as in mammalian systems, the AptSK1 and 2 channels showed a partially overlapping expression pattern while the AptSK3 channel was expressed in different brain areas. The AptSK1 and 2 channels were the primary subunits found in the major electrosensory processing areas. Immunohistochemistry further revealed distinct compartmentalization of the AptSK1 and 2 channels in the ELL. AptSK1 was localized to the apical dendrites of pyramidal neurons, while AptSK2 channels are primarily somatic. The distinct expression patterns of all 3 AptSK channels may reflect subtype specific contributions to neuronal function and the high homology between subtypes from a number of species suggests that the functional roles for each channel subtype are conserved from early vertebrate evolution.

#### Introduction

The electrosensory system of the brown ghost knifefish Apteronotus leptorhynchus has been thoroughly characterized with respect to the processing of naturalistic sensory inputs and control of electromotor output (Bell and Maler, 2005; Fortune, 2006; Krahe and Gabbiani, 2004; Sawtell et al., 2005). Much of the circuitry and cellular machinery have been evaluated and found to control specific aspects of sensory processing (Berman and Maler, 1999; Middleton et al., 2006). This allows the properties of individual cells to be linked directly to the processing of behaviorally relevant stimuli. Apteronotus makes use of an electric organ in its tail to produce a sinusoidal electric organ discharge (EOD) that generates a weak electric field around its body. The electric field provides Apteronotus with a means to locate objects (electrolocation) and to communicate with conspecifics (electrocommunication). The EOD is sensed by cutaneous tuberous electroreceptors that transmit these signals in a linear manner (Gussin et al., 2007; Benda et al., 2005; Nelson et al., 1997) to an area of the hindbrain the electrosensory lateral line lobe (ELL). The pyramidal neurons present in the ELL are responsible for the initial processing of the electrosensory signals and their relay to higher brain centers.

Previous studies of A. leptorynchus have shown evidence for the presence of small conductance calcium activated potassium channels (SK) in ELL pyramidal cells (Mathieson and Maler, 1988; Ellis et al., 2007). Activation of SK channels occurs solely in response to elevations in Ca<sup>2+</sup> and generates the medium after hyperpolarization (mAHP review (Sah, 1996)). The Apteronatus SK2 channels (AptSK2) have been cloned and localized in the ELL and show a cell-type specific expression pattern (Ellis et al., 2007). Physiological analysis revealed that the medium after-hyperpolarization (mAHP) generated by the AptSK2 channels controls the frequency tuning of ELL pyramidal neurons by regulating their propensity to produce spike bursts. The presence of the AptSK2 in a subset of ELL pyramidal cells predisposes them to respond to high frequency communication signals and filter out the low frequency signals due to prey. AptSK2 channels are therefore essential for appropriate processing of signals emanating from conspecifics versus prey.

In mammalian neurons, three separate classes of SK channels are present (SK1, SK2 & SK3) and these are differently distributed throughout the CNS (Kohler et al., 1996; Shmukler et al., 2001; Ro et al., 2001; Jager et al., 2000; Burnham et al., 2002). In a number of neuronal subtypes SK channels have been shown to control various cellular dynamics and stimulus responses. The role of SK channels depends on both the intrinsic properties of the specific cell type and the subcellular compartment to which they are localized. In the soma SK channels have been found to co-localize with voltage gated calcium channels (VGCC), allowing them to control spike frequency and patterning (Wolfart et al., 2001; Cloues and Sather, 2003). In dendrites, SK channels can be found in spines or along the shaft of the dendrite. Synaptic localization allows SK channels to set thresholds for plasticity, including the induction of long-term potentiation (LTP) (Lancaster et al., 2001). Specifically in the amygdala (Faber et al., 2005) and hippocampus (Ngo-Anh et al., 2005) SK channel activation in dendritic spines has been shown to shunt the induction of LTP by NMDAR activation. Alternatively, when localized to dendritic shafts, SK channels can limit plateau potentials, thus restricting the spread of the depolarization (Cai et al., 2004). They have also been found to be involved in the electric coupling between dendrites and somata (Womack and Khodakhah, 2003). The important role of SK channels in ELL pyramidal neurons and the many roles that SK channels play in other systems made the evaluation of the distribution patterns of all SK channel subtypes throughout the brain of Apteronotus of substantial interest. The electrosensory system of Apteronotus provides an excellent environment in which to analyze the contributions that the distinct SK channel subtypes can make to sensory processing.

In order to set the stage for functional studies involving the *Apt*SK channels we have now cloned the *Apt*SK1 and 3 channels in addition to the previously cloned *Apt*SK2 channel. Through the use of *in situ* hybridization and immunohistochemistry, we describe a partially overlapping expression pattern of *Apt*SK1 & 2 channels, with high levels found in the major electrosensory brain areas. Conversely, the *Apt*SK3 channel is found primarily in the brainstem and cerebellum, with little expression in brain areas important for electrosensory processing.

#### **Materials and Methods**

#### Isolation of Apteronotus SK channel cDNA

The AptSK1 channel sequence was initially isolated using degenerate PCR. Degenerate PCR primers were constructed with an inosine nucleotide (I) at every third residue of the primer sequence, allowing the primer to anneal to any possible codon for a given amino acid. The primers were based on comparisons of human and trout SK channel sequences that revealed high levels of sequence conservation between the putative (S1-S6) transmembrane segments. The degenerate primers used were: forward 5' ATCTTYGGIATGTTYGGIATIGT 3' and reverse 5' TSTAGATIAGCCAIGTYTCY 3'. Degenerate PCR was performed on reverse transcribed DNA created from Apteronotus whole brain tissue (Bottai et al., 1997) using the Invitrogen superscript first strand synthesis system. Following the identification of a sequence with high homology to known SK1 channels, the 5' and 3' tails were further isolated through rapid amplification of cDNA ends (RACE) using the Generacer kit (Invitrogen). Primers from the known channel sequence were matched with Generacer primers from the Invitrogen kit.

The AptSK3 channel sequence was also isolated through the use of degenerate PCR. A comparison of the cloned AptSK1 and AptSK2 (Ellis et al., 2007) sequences with the trout SK3 (tSK3;(Panofen et al., 2002)) channel again revealed high homology among the putative S1-S6 segments, with marked differences in the 5' and 3' intracellular sequences. Especially notable was an elongation of tSK3 5' sequence, which extended past the alignment with the known start sites of both AptSK1 and SK2. The 5' degenerate primer 5'-GCI TCI CTI CCC AAR YTG CCY CTG TC-3' was designed based on the tSK3 sequence just 5' to the start of the AptSK1 and SK2 channels and matched to the primer 5'-TTG GTG AGY TGT GTG TCC ATC ATG AAG TT-3' encoding a sequence in the CaMBD.

Once the sequences of the SK channels were assembled, primers to amplify the full- length channels were designed from the 5' and 3' untranslated (UTR) sequences. The channels were amplified by PCR using Pfu polymerase to decrease the likelihood of error introduction. The channels were sequenced by Genome Quebec (Montreal).

#### Apteronotus Brain Slice Preparation

Fish were anesthetized in tank water containing MS-222 (3-aminobenzoic acid ethyl ester) and respirated with O<sub>2</sub> bubbled MS-222 water during the perfusion procedure while surrounded in ice. Following surgical exposure of the heart, 20 mL cold phosphate buffered saline (PBS) was perfused via a needle inserted into the conus arteriosus. The fish were then perfused with 40 mL cold PBS containing 4% paraformaldehyde (PFA). Whole brains were surgically removed and placed in 4% PFA containing solutions. If the brains were subsequently to undergo cryostat sectioning for *in situ* hybridization, they were cryoprotected by placing them in a 4% PFA solution containing 10-15% sucrose overnight at 4°C. Brains used for vibratome sectioning were left in 4% PFA at 4°C until use. Cryostat sections (20μm) were cut and mounted on poly-L lysine coated slides and stored at -20°C until use. Vibratome sections (40μm) were cut fresh on the day they were to be used and placed immediately into PBS.

#### In situ Hybridization

Probe templates for the AptSK1, 2 & 3 channels were created from the 5' region of the channels and designed to be approximately the same size (400 nucleotides). Sense and anti-sense probes were created from the same cDNA plasmids. The RNA synthesis reaction involved the use of a digoxin labeled UTP in the NTP mix at a ratio of 1:3 with unlabeled UTP. In situ hybridization was preformed on cryostat sections prepared as outlined above. The hybridization procedure was based on a protocol previously designed for Apteronotus slices (Bottai et al., 1997), but modified for the use of DIG labeled probes (see (Ellis et al., 2007).

#### **Generation of Antibodies**

Antigenic protein was created to represent the initial 57 amino acids from the N-terminus of the AptSK1 channel sequence and 136 amino acids from the C-terminus of AptSK2, representing all the amino acids following the calcium independent portion of the calmodulin-binding domain (Xia et al., 1998). Histidine residues were added to the N-terminal region of the protein using the Gateway<sup>®</sup> (Invitrogen) system in order to allow for protein purification using the Histrap HP kit<sup>®</sup> (Amersham Biosciences). The

purified protein was injected subcutaneously into Rabbits after it was combined (500 mg in 500  $\mu$ L) with 500  $\mu$ L of Freund's adjuvant. Complete adjuvant was used for the first injection, while incomplete was used for the subsequent boosts. The first boost was given 3 weeks from the initial injection and the subsequent 2 boosts were given every 4 weeks. The entire serum was harvested 4 weeks after the final boost.

The AptSK1 antibody was affinity purified using GST tagged antigenic protein created with the Gateway<sup>©</sup> (Invitrogen) system. Following expression in E. coli cells, the GST-SK1 antigentic protein was purified using a glutathione column and the purified GST-SK1 protein linked to the Affi-Gel<sup>©</sup> beads from Bio-Rad Laboratories. Aliquots of whole serum were passed over the column to bind AptSK1 specific antibodies. Antibodies were liberated from the column with either an acidic (pH 2.5) or basic (pH 11.5) elution series. The pH was restored to neutral and the antibody solutions were diluted to 50% with glycerol for long-term storage at -20°C. The AptSK2 antibodies were purified from whole serum with a protein A column following standard procedures. Following elution samples were dialyzed against PBS, followed by PBS-50% glycerol and stored at -20°C until use.

#### **Measurement of Antibody Specificity**

The properties of the AptSK1 and 2 antibodies were evaluated in part through western blot analysis. Western blots using the AptSK1 and AptSK2 antibodies revealed staining patterns similar to those previously seen in mammalian systems. The AptSK1 blot of whole brain protein showed 3 prominent bands, one estimated to be 67.4 KDa, the second 57.6 KDa and the third 47.9 KDa. The largest and smallest bands correspond well to the predicted products of the two AptSK1 splice variants cloned from Apteronotus. The AptSK2 blot showed a single band of approximately 63.7 KDa.

In order to ensure that the antibodies generated were specific, the *Apt*SK1 and *Apt*SK2 channels were expressed in Chinese hamster ovary cells (CHO). Expression of the *Apt*SK1 channel in CHO cells allowed for the binding of the *Apt*SK1 Ab while the *Apt*SK2 Ab did not produce positive staining. Transfection of CHO cells with *Apt*SK2 channel plasmids alternatively resulted in a marked signal when the *Apt*SK2 Ab was

applied, which was not seen when the AptSK1 Ab was used. These results confirm that indeed both the antibodies generated were subunit specific.

## **Immunohistochemistry**

Transverse vibratome sections (40  $\mu$ M) were left free-floating in PBS at 4°C until use. Slices were blocked in 96 well plates containing 60  $\mu$ L blocking buffer for 1 hour at room temperature. At the concentration of primary antibody determined from CHO cells, slices were placed in 96 well plates, covered and left at 4°C for 24 hours. When colabeling experiments were to be performed anti MAP-2 (BD Pharmigen) was also added at a concentration of 1:300. Washing was preformed in 24 well plates, with 1 slice and 1 mL of PBS per well, for 1 hour at room temperature. Secondary antibodies were goat anti rabbit Alexa 488 and goat anti mouse 568, which were both used at 1:200 dilutions in blocking buffer. Slices were incubated in secondary for 12-15 hours followed by 1 hour of washing with PBS. Subsequently slices were mounted onto slides and allowed to dry for 1 hour before they were coverslipped with antifade media.

#### Results

#### Isolation of SK channel cDNA's in the Apteronotus Brain

The cloning and sequencing of the SK channel cDNA's from the brain of *Apteronotus* was accomplished through an analysis of the sequence similarities between SK channels previously cloned from the trout and human cDNA's (Kohler et al., 1996;Panofen et al., 2002). The three subtypes of SK channels (SK1, 2 & 3) are tetrameric with structures similar to that of voltage-gated potassium channels (Kohler et al., 1996). Areas of high homology between the 1<sup>st</sup> transmembrane segment (S1) and the CaM binding domain (CaMBD) exist between subtypes and species. This allowed for the design of degenerate primers to amplify the sequences between S1 and the CaMBD of all the SK channel mRNA's. Rapid amplification of cDNA ends (RACE) then allowed for the isolation of the 5' and 3' channel sequence.

The same technique had previously allowed for the cloning of the *Apt*SK2 channel (Ellis et al., 2007). Between species SK2 channels show the lowest amount of sequence variation, with the *Apt*SK2 channel showing a 96.0% identity to the trout ortholog and 86.8% to the hSK2. Through further sequence assembly and analysis we have revealed two additional SK channels that, based on homology and channel specific sequence patterns, were labeled *Apt*SK1 and *Apt*SK3.

Although sequence analysis revealed that SK1 channels show the greatest amino acid divergence between species, the highly conserved nature of the SK channels is demonstrated by the 73.4% sequence identity to the human SK1 channel protein, with the majority of that identity lying between the S1 and CaMBD regions (91.6% similarity). The 3' RACE PCR of the *Apt*SK1 channel produced 2 different splice variants, for the c-terminal segment of the channel protein. One of the splice variants produced a full length channel of 549 amino acids (shown in Fig 1), while the other was spliced just before a presumptive three amino acid exon comprised of an alanine-glutamine-lysine (AQK) sequence that is specific for SK1 channels (Fig 1; 415-417;(Kohler et al., 1996)). Analogous splice variants have been shown in other species, where a lack of the C-terminal tail prevented surface expression (Lee et al., 2003). Similarly, the short *Apt*SK1 splice variant was not expressed on the surface of HEK cells (data not shown). PCR primers designed for the 3' UTR of both isoforms have shown that they are both easily

amplified from whole brain tissue (data not shown). Isolation of further AptSK1 splicing was not pursued at this time.

The AptSK3 channel sequence has not been cloned in its entirety. The AptSK3 protein sequence has a large putative N-terminus beginning with a methionine residue that aligns well with the start of both the AptSK1 and SK2 (Fig. 1). The currently available sequence information is truncated shortly after the S6 transmembrane segment, and thus lacks the putative C-terminal intracellular tail region.

Comparison of the AptSK channel protein sequences (Fig 1) reveals an  $87 \pm 2.6$ % similarity between the putative S1-S6 transmembrane regions. While the N-terminal region that precedes S1 shows only a 39.5  $\pm$  8.5% identity. Interaction of the C-terminal tail of SK channels with CaM requires an arginine (R) and lysine (K) residues found to be conserved in all SK channels (Kohler et al., 1996;Lee et al., 2003). Both the AptSK1 (R427, K430) and AptSK2 (R422, K436) channels present these residues in the appropriate positions. A number of drugs have been found to specifically block SK channels, one of the most highly used and recognized being the bee venom toxin apamin. Two amino acids, namely an asparagine (Asn-N) and an aspartic acid (Asp-D), in the outer vestibule of the pore have previously been implicated in the distinct apamin block of each channel subtype (Ishii et al., 1997). Both of these amino acids appear on the SK2 channel (D307; N334), while only the aspartic acid (D354) is present on SK3 and neither residue is present in the SK1 channels. It has been suggested that the presence of these two residues strengthens the binding of apamin, thus making SK2 the most sensitive to apamin followed by SK3 and finally SK1. The occurrence of these two residues in the AptSK channels matches the previous findings for mammalian channels, and should then impart similar sensitivities to apamin. Recently a single amino acid on the extracellular loop between S3 and S4 has been found to be responsible for some of the apamin specificity for the SK1 and SK2 channels (Nolting et al., 2007). The AptSK1 channel shows homology to the hSK1 in this position, suggesting that, while it will have a lower sensitivity to apamin than AptSK2, it should still be blocked. The sequence patterns for the 3 AptSK channels would then seem to mirror the pattern seen for mouse, rat, human and trout channels and would be predicted to impart relative apamin sensitivities of SK1<SK3<SK2.

#### In situ Hybridization

The hybridization probes for the AptSK1 & 3 channels were created from the 5' sequence and were designed to be approximately the same size as the probes previously used to localize the AptSK2 channel to the ELL (approximately 400 nucleotides in length). In the case of the AptSK1 channel, due to the existence of splice variants, a 3' in situ probe was also created that was approximately the same length as the 5' probes. It should be noted that in the AptSK1 experiments shown below, the 5' probes were used, and that parallel studies with the 3' probes yielded similar results in all cases. Evaluation of the zebrafish genome revealed the potential existence of more than 3 sequences similar to the core of the SK channels (Ellis unpub. obs). While this may suggest duplication of the SK channels in teleosts, a blast search of the zebrafish genome with the AptSK1 and 2 probes used for the *in situ* hybridization studies did not reveal corresponding sequences. Since the genome of Apteronotus is not available for sequence comparisons, the fact that the cloned AptSK channels show little sequence similarity with each other in the region used to create the in situ probes, and there was little homology for the probes within the zebrafish genome, the specificity of the probes for the cloned AptSK channels can be considered high. The probes were labeled using a digoxin (DIG) modified UTP system (see materials and methods) and since all the probes were of similar lengths and had a similar percentage of UTP, they should produce relatively similar DIG labeling. Sense probes for all 3 channels revealed light, non-specific staining (data not shown). Expression of AptSK2 was the highest throughout the brain of Apteronotus, with some overlapping expression of AptSK1 in both forebrain and hindbrain regions. The major electrosensory brain areas showed the highest levels of AptSK expression (1+2) and were therefore analyzed in the greatest detail. AptSK3 was mainly expressed in the rhombencephalon (large reticular neurons) and cerebellum, at overall lower relative levels than AptSK2 and showed little overlap with AptSK1 (data not shown). AptSK3 channels were not detected in electrosensory brain areas, which are the primary focus of this study, and thus a detailed mapping is not reported here. Identification of the brain regions described below is based on an atlas of the brain of A. leptorhynchus (Maler et al., 1991).

#### Telencephalon

The telencephalon represents an example of partially overlapping expression levels of AptSK1 and 2. As previously mentioned, AptSK3 showed little overlap with AptSK1 or 2 and was not found in the forebrain. AptSK1 is expressed at low levels in the telencephalon and is restricted mainly to the central part of the dorsal telencephalon (DC) and the central part of the ventral telencephalon (Vc) (Fig 2A). It should be noted that both the 5' and 3' probes for the AptSK1 channel showed similar results. AptSK2 is abundantly expressed throughout the dorsal telencephalon: dorsolateral (Dld, Dlv), medial (DM) and central (DC) as well in the dorsal magnocellular cell group (DDmg); it is also highly expressed within all subdivisions of the ventral telencephalon (Fig. 2B,C,D). The olfactory bulb projects to two targets in dorsal telencephalon: the ventral division of the dorsolateral telencephalon (DLv) and the dorsal posterior (DP) telencephalon (Sas and Maler, 1987); SK2 is highly expressed in DLv but not DP (Fig. 2, B-D). The high expression levels of AptSK2 in the dorsolateral telencephalon is of note since it has been suggested that this region of the teleost forebrain might, in part, be similar to the mammalian medial pallium (hippocampus)(Northcutt, 2006; Yamamoto et al., 2007), which prominently expresses of AptSK2 channels (Sailer et al., 2002).

#### **Diencephalon and Brainstem**

Other areas of notable mRNA expression for *Apt*SK1 include the diencephalon where staining was found in the preglomerular nucleus (PG, data not shown). In the midbrain, *Apt*SK2 channels were expressed at high levels in the rostral (PGr, Fig. 2D) and lateral (not shown) PG. Cell groups in the preoptic area and rostral hypothalamus also displayed high levels of SK2 expression (Fig. 2C,D) while other hypothalamic areas had relatively lower levels (Fig. 3: tuberis anterior and the nucleus diffusus lateralis; data not shown for other hypothalamic regions).

Both *Apt*SK1 (data not shown) and SK2 (Fig 4A) were found at modest levels in torus semicircularis (TS) and optic tectum (TeO).

The cerebellum displayed a prominent expression of all 3 AptSK channels. AptSK1 channels were found at high levels in Purkinje cells (Fig. 5A), while AptSK2

channels were found in cerebellar projection neurons (eurydendroid cells, (Finger, 1978; Carr et al., 1981) and golgi cells as well as in Purkinje cells (Fig. 5B); *Apt*SK3 channels were expressed at high levels only in cerebellar granule cells (data not shown). The cerebellum of gymnotiform fish includes a caudal lobe associated with electrosensory processing (eminentia granularis posterior, EGp); a transitional zone (ZT) lies in between the corpus cerebellum and EGp (Sas and Maler, 1987). There was an interesting gradient in the expression of cerebellar *Apt*SK1; it was strongly expressed in Purkinje cells of the corpus cerebellum but its expression was lower in ZT (Fig. 5A) and further reduced in EGp Purkinje cells (data not shown). No such gradient was evident for *Apt*SK2 (Fig. 5B). Moderate levels of *Apt*SK2 were found in purkinje cells of the valvula cerebellum (data not shown).

AptSK1 is highly expressed in reticular formation as well as in auditory brainstem nuclei (Fig. 6A) while AptSK1 is strongly expressed in inferior olive and the lateral reticular nucleus (Sas and Maler, 1983). It is interesting to note that the cells of the nucleus medialis (nM), which is in receipt of lateral line input (Maler et al., 1974), do not express either AptSK1 or AptSK2 (Fig. 6A,B). This is similar to the immediately adjacent medial segment of the ELL (see below); it is possible that the lack of expression of AptSK channels in nM is associated with the frequency content of lateral line signals (Ellis et al., 2007), see below).

#### **Electrosensory Brain Regions.**

#### Diencephalon and Brainstem

Midbrain and diencephalic nuclei that are involved in electroreception, namely the torus semicircularis (TS), optic tectum (TeO) and nucleus electrosensorius (nE), had only low levels of expression of *Apt*SK1 (data not shown); cells in the TS and TeO also had only modest levels of expression of *Apt*SK2 (Fig. 4A). However, the nE, a nucleus involved in detecting electrocommunication signals (Heiligenberg et al., 1991;Keller et al., 1990), expressed high levels of *Apt*SK2 mRNA (Fig 3). The preparemaker nucleus (PPn-C; chirp subdivision) also showed high levels of *Apt*SK2 expression (Fig 3). We saw no evidence for *Apt*SK expression in the pacemaker nucleus.

#### Nucleus Praeminentialis

The nucleus praeminentialis (nP) is an electrosensory brain region involved in feedback regulation of electrosensory processing, different subsets of nP neurons project back to ELL via either direct or indirect pathways (Bell and Maler, 2005). Neurons throughout nP strongly express *Apt*SK2 (Fig 4 A,B). In contrast, *Apt*SK1 positive neurons were confined to the lateral aspect of nP (Fig 4C) and a small number of *Apt*SK3 positive neurons were scattered throughout the nucleus (data not shown). Based on cell size and location (Sas and Maler, 1983;Sas and Maler, 1987) it appears likely that *Apt*SK2 is expressed in neurons involved in both direct (stellate cells, (Sas and Maler, 1987;Bratton and Bastian, 1990) and indirect feedback (multipolar and boundary cells, (Sas and Maler, 1983;Sas and Maler, 1987;Bastian and Bratton, 1990) to ELL. *Apt*SK1 expression appears to be prominent mainly in the boundary cells that provide indirect feedback to ELL (Sas and Maler, 1983;Sas and Maler, 1987).

This data suggests that, while *Apt*SK channels may not play a prominent role in ascending electrosensory pathways (TS, TeO), they may be critically important for feedback regulation of electrosensory processing.

#### The Electrosensory Lateral Line Lobe (ELL)

The primary electrosensory area (ELL) showed an overlapping pattern of mRNA labeling between AptSK1 (Fig 7) and the previously localized AptSK2 (Ellis et al., 2007), with no noticeable staining for AptSK3 (data not shown). The ELL receives direct input from cutaneous electroreceptors and is responsible for the primary processing of electrosensory information, which is then relayed onto higher brain areas. The ELL is subdivided into 4 topographic maps of the fish body (Heiligenberg and Dye, 1982;Carr et al., 1986). The most medial segment (MS) receives input from ampullary receptors, with the three sequential lateral segments (centromedial- CMS; centrolateral-CLS, lateral-LS) receiving identical inputs from tuberous receptors (Maler et al., 1981). Each segment is organized in an identical laminar pattern. Electroreceptor afferents terminate in a deep neuropil layer on the basal dendrites of both pyramidal (output) cells and interneurons. There are several classes of pyramidal cells (superficial, intermediate and deep) defined on the basis of morphological, biochemical and physiological criteria (Bastian and

Courtright, 1991;Bastian et al., 2002;Bastian et al., 2004;Berman et al., 1995). Superficial and intermediate pyramidal cells are located in the pyramidal cell layer, along with polymorphic cells, a class of GABAergic interneuron (Maler et al., 1991). The ELL granular layer contains both deep pyramidal cells as well as numerous GABAergic granular interneurons. The largest area of the ELL is the molecular layer containing feedback afferent input. This area is primarily comprised of the apical dendrites from superficial and intermediate pyramidal cells along with various interneurons (stellate and vml cells) (Maler et al., 1991). The deep pyramidal cells have only small apical dendrites in comparison to the superficial and intermediate types (Bastian et al., 2004). The distribution of *Apt*SK1 mRNA varies strongly across not only the ELL segments but also across pyramidal cell classes within one segment, similar to what was previously reported for *Apt*SK2 (Ellis et al., 2007).

The AptSK1 antisense probe showed a distinct map-specific expression pattern, with prominent expression in the LS and CLS, when compared to the more lightly labeled CMS and MS (Fig 7). Superficial and intermediate pyramidal cells follow this pattern showing strong labeling in LS and CLS but are barely detectable in CMS and MS (Fig 7B). Deep pyramidal cells and polymorphic interneurons are also strongly labeled in LS while granular interneurons are only modestly labeled in this segment (Fig 7B); these cell types are minimally labeled in the other segments.

#### **Immunohistochemistry**

As previously mentioned, the highest sequence divergence amongst SK channels lies in the N and C-terminal intracellular regions. These areas of heterogeneity were taken advantage of for the purposes of creating subunit specific rabbit polyclonal antibodies. The *Apt*SK1 Ab was specific for the N-terminus, while the *Apt*SK2 Ab bound to the C-terminal region. Again, while duplication of either of the *Apt*SK channels within Teleosts cannot be assured, comparison of the protein sequence used to create the *Apt*SK1 Ab with the zebrafish protein database revealed a single protein in which 57 of 73 (78%) amino acids were conserved, while the zebrafish SK2 (31%) and SK3 (23%) channels showed little conservation in this region. The specificity of the Ab's was further assessed through a CHO cell expression system and western blot analysis (see

methods). The Abs created for the AptSK1 and 2 channels did not cross react with the full-length channel proteins expressed in CHO cells. Western blots using the AptSK1 and AptSK2 antibodies revealed different staining patterns for the AptSK1 and 2 Abs that were similar to those previously seen in mammalian systems (data not shown). These results along with the genetic analysis would strongly suggest that the Abs generated are specific for the cloned AptSK channels.

Immunohistochemical studies of *Apteronotus* brain showed similar staining patterns to those seen with the *in situ* hybridization in all brain regions (data not shown) and additionally revealed a number of unique features of *Apt*SK1 and 2 channel distribution in the ELL. Low power confocal microscopy revealed that, for both channel subtypes, cellular staining was strong in the LS and CLS, with much less staining in the CMS and MS as anticipated from the *in situ* hybridization results (Fig 8 A+C). Granule and VML interneurons in the LS were also labeled with the *Apt*SK2 probe, confirming the *in situ* hybridization results (Fig 8D). Previous work has suggested that *Apt*SK2 expression is confined to basilar pyramidal neurons (E-type cells)(Ellis et al., 2007), in contrast *Apt*SK1 appears to be expressed in both subtypes (basilar and non-basilar, I-type cells; Fig 8B) of pyramidal cells in the LS.

The subcellular distribution of *Apt*SK1 and *Apt*SK2 did however differ dramatically with *Apt*SK2 being confined to the somata of pyramidal cells (Fig 8C), while *Apt*SK1 was localized to pyramidal cell apical dendrites in the molecular layer (Fig 8A). In order to confirm the somatic localization co-labeling experiments were performed with an antibody to the dendrite-specific marker microtubule associated protein-2 (MAP-2)(Maler et al., 1981;Rashid et al., 2001). MAP-2 labeling was mainly found in the vertically oriented thick pyramidal cell apical dendrites of the ELL molecular layer, consistent with electron microscopic observations of the presence of numerous microtubules in these dendrites(Maler et al., 1981). *Apt*SK2 immunostaining has almost no overlap with the MAP-2 dendritic labeling, confirming a primarily somatic localization (Fig 8D). In contrast, *Apt*SK1 staining was evident in the apical and basal dendrites of pyramidal cells, as well as their somata, giving the cells and elongated appearance (Fig. 8B). Double labeling revealed that *Apt*SK1 immunoreactivity is indeed colocalized with MAP-2 in dendrites. Fig 8B shows a clear overlap exists (white)

between the two antibodies in both the basal and apical dendrites. The vast majority of MAP-2 positive profiles were also positive for AptSK1 suggesting that all pyramidal cell dendrites contain this channel (Fig 9A). This dendritic staining also displayed an interesting "punctate" pattern. Higher maginification revealed the existence of AptSK1 positive "mushroom" shaped protrusions from the shaft of the AptSK1/MAP-2 positive dendrites (Fig 9B-arrows). The lack of MAP-2 co-labeling of these protrusions makes it likely they represent dendritic spines that, in ELL pyramidal cells, do not contain microtubules (Maler et al., 1981). The distribution of AptSK1 "puncta" strongly suggests that the spines of pyramidal cell apical dendrites contain AptSK1 channels (Maler, 1979;Maler et al., 1981). Our confocal microscopic data cannot ascertain whether the AptSK1 label associated with MAP-2 labeling represents AptSK1 channels on the dendritic shaft or in transit within intracellular organelles.

#### **Discussion**

This study describes the cloning and distribution of two additional AptSK channels (AptSK1, AptSK3) from the weakly electric fish Apteronotus leptorhynchus, as well as the complete distribution of the previously cloned AptSK2 (Ellis et al., 2007). The AptSK1 channel was isolated in its entirety, with a partial cloning of the AptSK3 Sequence analysis revealed that the amino acids previously linked to the constitutive interaction with CaM are conserved in both AptSK1 and AptSK2 (Lee et al., 2003). Since it is the binding of Ca<sup>2+</sup> to CaM that induces the conformational changes required for SK channel gating (Schumacher et al., 2001), it can be inferred that the Apteronotus channels will be gated through a similar mechanism and possess similar activation kinetics to SK channels from other species. The sequences in the pore region of the channels that confer potassium selectivity are also highly conserved among AptSK subtypes hence their conductance properties can be predicted to remain constant (Kohler et al., 1996). The alterations of pyramidal cell dynamics previously seen upon the application of apamin to the ELL (Mathieson and Maler, 1988; Ellis et al., 2007) can be attributed to the drugs effects on the SK channels, since the amino acids found to impart specific apamin sensitivities onto SK channels (Ishii et al., 1997; Nolting et al., 2007) are conserved for AptSK1, 2 and 3. Overall the channel characteristics previously described for SK channels in other systems should be conserved in the Apteronotus SK channels.

In situ hybridization revealed only partially overlapping distributions for all three SK subtypes. AptSK1 channels were expressed at moderate levels, appearing at higher levels in the hindbrain (ELL and cerebellum), while AptSK2 channels were the most abundant of the SK's and were found throughout the brain, with the AptSK3 channels confined primarily to midbrain regions. Notably, very high levels of expression of AptSK2 were found in dorsal forebrain, a region hypothesized to be similar, at least in terms of connectivity and function, to the mammalian medial pallium (hippocampus) (Northcutt, 2006; Yamamoto et al., 2007). It has been suggested that SK channels can regulate plasticity and learning (Stackman et al., 2002) and it is possible that the AptSK2 channel will regulate dorsal forebrain dependent learning in teleosts (spatial learning and trace conditioning) (Rodriguez et al., 2001; Portavella et al., 2004).

SK channels were generally only present in low amounts in the ascending electrosensory system (TS, TeO) with the exception of the nucleus electrosensorius. They were however highly expressed in both the ELL and in nP, a brain region concerned with feedback regulation of ELL (Bastian and Bratton, 1990; Bratton and Bastian, 1990). AptSK2 was highly expressed in one subdivision of the preparemaker nucleus (PPnC). Activation of the PPnC evokes brief (approx 20ms) electrocommunication signals (chirps) (Kawasaki et al., 1988) that have been found to occur at a maximum rate of 1-3 Hz. We hypothesize that the SK channel mediated mAHP may help to set the inter-chirp interval, and thus control chirp frequency. Alternatively it has been found that, after injections of testosterone, chirps may last more than 20 ms (Dulka et al., 1995), making it possible that regulation of AptSK channels may control chirp duration. Chirp rate is sexually dimorphic, which corresponds with a sexual dimorphism of substance P (Weld and Maler, 1992; Dulka et al., 1995) and 5-HT (Telgkamp et al., 2007) expression in the PPnC, 5-HT in particular has been shown to regulate the mAHP in ELL (Ellis, unpub. obs.). It would be interesting to investigate whether this effect is due to a down-regulation of AptSK current by either 5-HT or substance P. Serotonin is not the only neurotransmitter that has been shown to down-regulate SK channel activity and since the PPnC receives innervation from multiple other neuropeptide systems (Zupanc and Maler, 1997), the potential for SK channel down-regulation is extensive.

#### SK channels and electrosensory processing

Below we focus on nP and ELL; both regions show partially overlapping patterns of staining for the *Apt*SK1 and 2 channels, with no appreciable levels of the *Apt*SK3 channel detected.

#### AptSK channels in the ELL

Detailed analysis revealed AptSK1 and 2 channels display a map specific expression pattern across the topographic maps of the ELL. While the localization of the AptSK2 mRNA has been previously published (Ellis et al., 2007), here we have used immunohistochemistry to demonstrate that the global pattern of AptSK2 protein expression matches the previous in situ hybridization results. This held true for the

AptSK1 channels with a close match between the map specific expression patterns of mRNA and protein. Overall AptSK2 channels showed the more robust expression pattern, appearing both at higher levels and in a larger number of cells/cell types than AptSK1. The global distribution of AptSK1 was similar to that of AptSK2 in that both had a gradient of expression across the ELL segments with pyramidal cells of LS having higher levels of expression than those of CLS, while CMS pyramidal cells had little or no expression. The main difference in expression patterns was seen with respect to Several classes of GABAergic interneurons showed robust AptSK2 interneurons. expression (granular and vml cells), while AptSK1 was prominent in only one class of interneuron-polymorphic cells. While there did exist a high degree of overlap with respect to expression patterns for the AptSK1 and 2 in pyramidal neurons, immunohistochemistry revealed striking subcellular compartmentalization. The AptSK2 channels appeared to be confined to pyramidal cell somata. The AptSK1 channels, in contrast, appeared to be primarily localized to the apical and basilar dendrites of pyramidal cells, with only occasional light somatic staining observed. These results indicate that while both channel subtypes are expressed in a similar manner with respect to the ELL segments, they quite likely have very different functions.

#### AptSK1 channels may control NMDA receptor activation in the ELL

We have previously proposed that *AptSK2* channels regulate the depolarizing after-potentials (DAPs) in the somata of pyramidal cells (Ellis et al., 2007). The confinement of *AptSK1* to pyramidal cell dendrites and perhaps even dendritic spines of apical dendrites indicates an entirely different role for this channel. The synaptic input to the spines of apical dendrites arises from direct and indirect feedback pathways, both of which are glutamatergic and utilize AMPA and NMDA receptors. The feedback evoked EPSPs have a large NMDA receptor component and immunohistochemical studies have localized NMDA receptors to the dendritic spines (Berman et al., 2001). Recent reports from mammalian amygdala (Faber et al., 2005) and hippocampus (Ngo-Anh et al., 2005) have demonstrated that hyperpolarizations generated by active SK channels can regulate Ca<sup>2+</sup> influx through NMDA receptors and thus synaptic plasticity. Feedback input to the ELL is highly plastic and this plasticity is dependent on both NMDA receptors (Lewis

and Maler, 2004), Bastian, pers. comm.) and Ca<sup>2+</sup> influx (Bastian, 1999). We propose that the *Apt*SK1 channel can regulate synaptic plasticity induced by feedback in a manner similar to that reported for the amygdala and hippocampus- by decreasing the NMDA receptor open time and thus Ca<sup>2+</sup> influx into dendritic spines. Feedback plasticity is involved in the cancellation of spatially extensive low frequency electrosensory input (Bastian et al., 2004;Chacron et al., 2003) but this effect has only been explored in the CLS and LS. The reduced levels of *Apt*SK1 in the CMS may suggest that feedback plasticity might be qualitatively different in this segment. The ELL therefore offers a natural preparation for the study of regulation of NMDA receptor mediated plasticity by SK1 channels.

It is interesting to note that the pattern of *Apt*SK1 channel expression is paralleled by that of the *Apteronotus* ryanodine receptors (RYR) since these are similarly expressed at a far higher density in pyramidal cell dendrites of the LS than CMS (Zupanc et al., 1992). RYR have been shown to mediate Ca<sup>2+</sup> induced Ca<sup>2+</sup> release (CICR) that amplifies Ca<sup>2+</sup> influx from NMDA receptors or voltage gated Ca channels (Emptage et al., 1999;Akita and Kuba, 2000). SK channels can be activated by RYR controlled CICR (Akita and Kuba, 2000), which suggests that the LS may have more abundant sources of Ca<sup>2+</sup> available to activate the high density of dendritic SK1 channels.

#### AptSK2 Channel Expression may control activity of GABAergic interneurons

We have previously shown that *Apt*SK2 channels are involved in map specific control of frequency tuning in the ELL (Ellis et al., 2007). The cells that showed *Apt*SK2 expression had a reduced low-frequency response, making the cells broadband to high pass in nature. Frequency tuning of pyramidal neurons may not be the only role of the *Apt*SK2 channels in the ELL. Granular interneurons of the LS and, to a lesser extent, CLS also express high levels of *Apt*SK2. The majority of these cells are GABAergic (Maler and Mugnaini, 1994) and their activation by P-unit stimulation evokes rapid GABA<sub>A</sub> mediated IPSPs (Berman and Maler, 1998). These IPSPs truncate P-unit evoked EPSPs in pyramidal cells, thus shortening them considerably, producing more precise excitation which may also contribute to high frequency tuning. The activation of *Apt*SK2 channels in these cells can be predicted to dampen their excitability, which may further

contribute to the frequency filtering properties of pyramidal neurons. Molecular layer interneurons (VML cells) also express high levels of *AptSK2*, however it is unclear at this time what role they may play.

## AptSK2 Channels in the nP

One of the highest levels of AptSK2 expression in the brain of A. leptorhynchus was found in nP, a nucleus devoted entirely to feedback to the ELL (Bell and Maler, 2005). The ELL projects to the nP in a topographic manner: the medial to lateral direction in ELL projects ventral to dorsal in nP(Bell and Maler, 2005). Thus LS is represented most dorsally in nP while MS is found most ventrally. The direct feedback pathway is reciprocal: each region of nP projects back to the segment that innervates it (Bell and Maler, 2005). In contrast, the indirect feedback pathway cuts across segmental boundaries. Therefore, unlike the situation in ELL where AptSK2 is highest in LS, feedback to all segments of the ELL will be regulated by AptSK1. Further, the indirect feedback pathway to all ELL segments will also be strongly controlled by AptSK2 in Pd neurons such as boundary cells. AptSK1 labeling in nP was far weaker and confined entirely to the lateral boundary cells.

The role of AptSK2 in nP is at present unknown. The work of Bastian and coworkers suggests two possibilities: Firstly, the stellate cells that provide a direct feedback projection to the ELL are highly phasic in their response to sustained electrosensory input (Bratton and Bastian, 1990) and AptSK2 channels might produce strong AHPs in response to the discharge of stellate cells, thus contributing to the termination of their discharge. Secondly, neurons conveying indirect feedback to the ELL (multipolar cells, (Bastian and Bratton, 1990; Middleton et al., 2006) are tuned to high frequencies. As found in pyramidal neurons, such tuning can be provided in part by AptSK2 channels. Given the importance of feedback to electrosensory function the role that AptSK2 channels play in the nP may be important for all ELL segments.

## Regulation of SK Channel Compartmentalization

Differential distributions of AptSK1 and 2 channels within the same neuronal cell type has been previously noted for both the rat and mouse channels (Bruening-Wright et

al., 2002; Sailer et al., 2004). In the ELL, as reported for a number of mammalian brain areas, including the cortex and hippocampus, the AptSK1 channels showed a primarily dendritic localization, while AptSK2 channels were restricted to the soma and proximal dendrites. The precise mechanisms through which SK channels are differentially distributed within individual neurons were not investigated. The carboxyl tail of the SK channels is a region we propose to be involved in regulating channel distribution. This region has been previously studied as a CaMBD and it was found that channel assembly and surface expression can be partially linked to an interaction with CaM (Schumacher et al., 2004; Schumacher et al., 2001). However, it has also been shown in HEK cells that transport of channels out of the golgi requires not only an association with CaM but also the amino acid sequence distal to the CaMBD (Roncarati et al., 2005), Ellis unpublished observations). The sequence following the constitutive portion of the CaMBD is highly divergent between the AptSK1 and 2 channels showing a 48.9 % identity. This area would then seem a prime target for regulation of channel distribution within neurons. The caboxyl tail region has been implicated in the dendritic regulation of other potassium channels in ELL pyramidal neurons. Differential distributions of the AptKv3 class of channels in pyramidal neurons has been linked to a PSIL sequence on the c-terminus of AptKv3.3, that possibly acts as a PDZ binding motif, allowing for selective transport of the channels to the apical dendrites (Deng et al., 2005). This sequence was not found on the AptKv3.1 channels that remained in the soma and proximal dendrites of the pyramidal neurons.

#### The ELL as an Ideal Setting to Study SK Channel Function

Natural differences in the expression patterns of AptSK channels across the maps of the ELL provide an excellent setting to study their contributions to the cellular bases of sensory processing. The various subsets of pyramidal neurons that exist across the maps display distinct arrays of ion channels that confer unique neuronal properties. Along with the intrinsic differences, feedback and input from interneurons varies both between pyramidal subtypes and across the maps of the ELL. This provides a unique setting in which to study the functional roles of SK channels. Many of the characteristics of ELL pyramidal neuron function both at the single neuron level and with respect to the overall

neural network have been elucidated. The electrophysiological and molecular biological approaches necessary to investigate properties of the ELL are well established and further studies of the *Apteronotus* SK channels may provide useful insights into the function of these widely expressed channels.

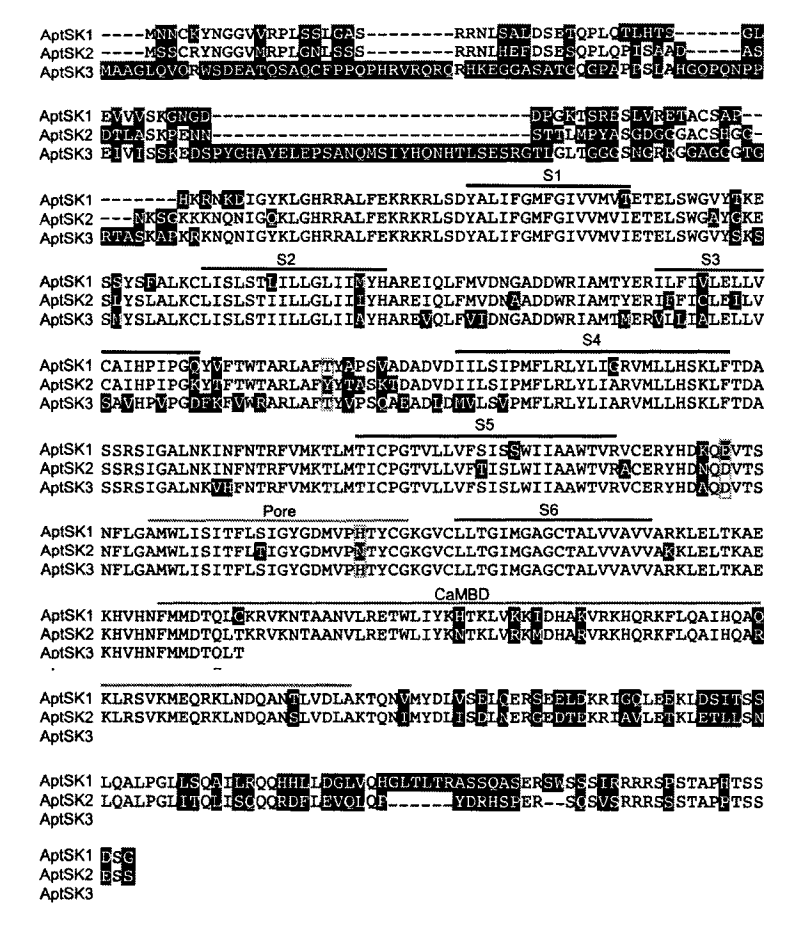


**Figure 1**. Sequence comparisons between the *Apteronotus* SK channels reveals significant amino acid conservation. Amino acid comparisons of the cloned *Apt*SK channel sequences. Predicted transmembrane sequences (S1-S6) are marked by black lines, with the putative pore and calmodulin binding domain (CaMBD) highlighted with grey lines. Black-boxed sequence represents areas of divergence. Grey outline: amino acids suggested to be responsible for apamin sensitivity.

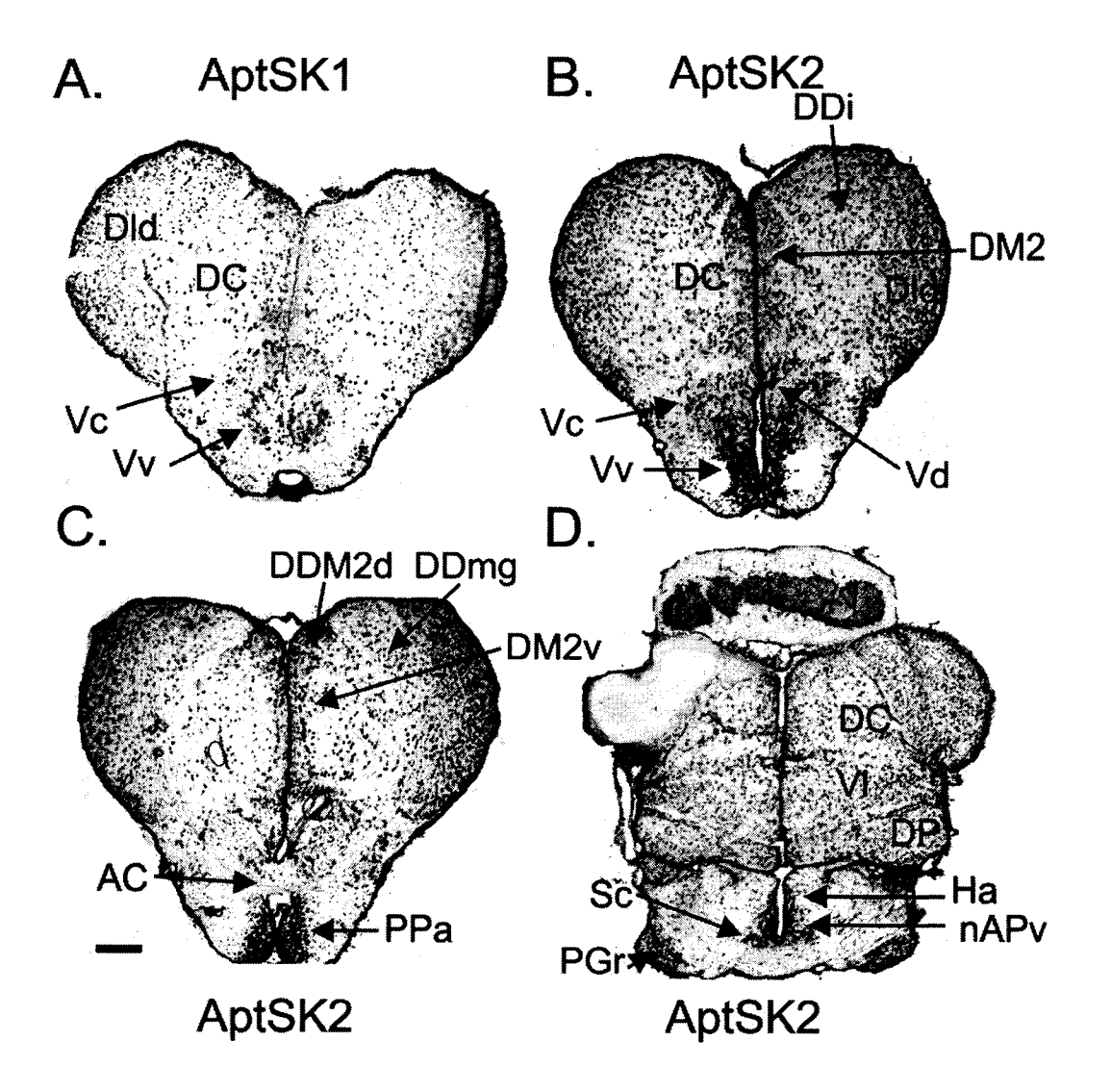
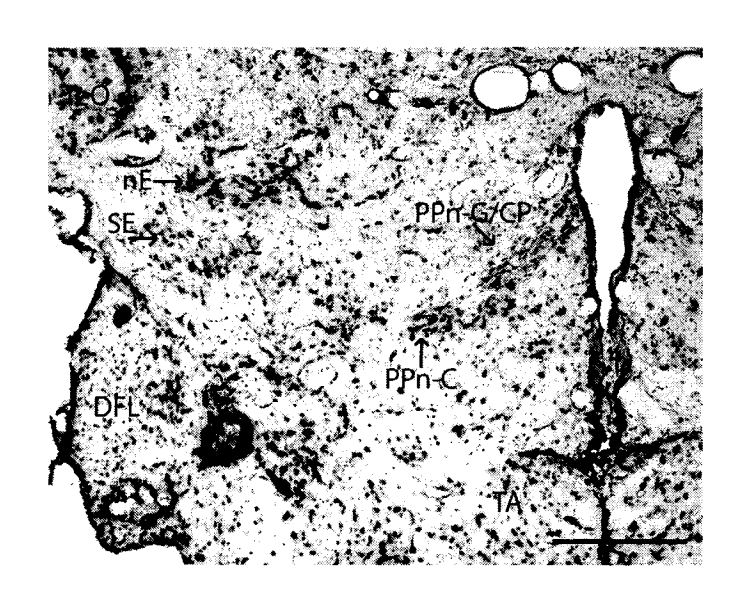


Figure 2. In situ hybridization reveals a differential distribution for AptSK1 & 2 mRNA within the forebrain. A. Digoxin (DIG) labeled probes reveled AptSK1 staining primarily in the central division of the dorsal forebrain (DC) along with both the central (Vc) and ventral (Vv) divisions of the ventral telencephalon. B, C, D. AptSK2 probes revealed strong staining in many regions of the dorsal telencephalon; most notably DC, the intermediate (DDi) and magnocellular (DDmg) subdivisions of the dorsal telencephalon, the dorsolateral telencephalon dorsal (DLd) and ventral (DLv) divisions, and the dorsomedial telencephalon (DM2d). In contrast the dorsal posterior telencephalon (DP, olfactory) was only lightly labeled. Preoptic (anterior subdivision of the preopticus periventricularis, PPa) and hypothalamic nuclei (anterior hypothalamus, HA, nucleus anterior periventricularis, nAPv) including the suprachiasmatic nucleus (Sc) were also strongly labeled as were the preglomerular nuclei (the rostral nucleus preglomerulus, PGr, is illustrated). Scalebar: 100μm.



**Figure 3**. AptSK2 is expressed in electrosensory brain areas of the diencephalon. Significant levels of AptSK2 mRNA are found in the nucleus electrosensorius (nE), prepacemaker nucleus (PPn-C, PPn-G/CP) and subelectrosensorius nucleus (SE) with moderate levels found in the nucleus tuberis anterior (TA) and nucleus diffusus lateralis (DFL). Scalebar:  $100 \, \mu M$ .

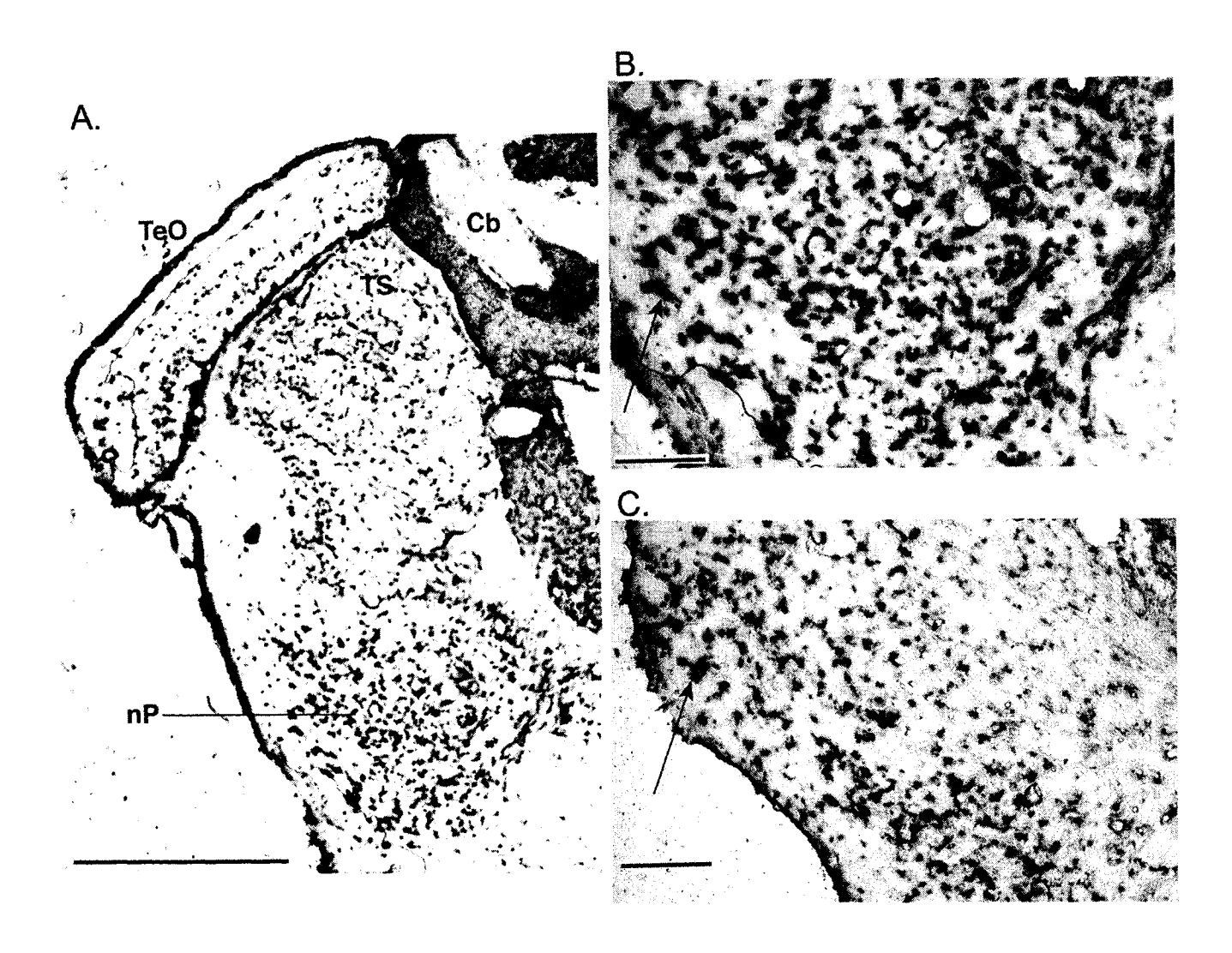
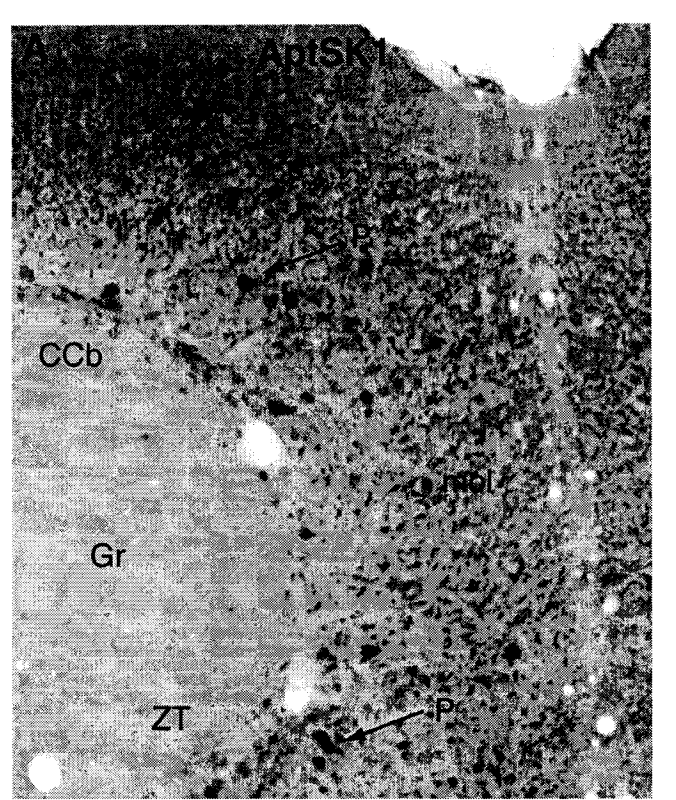


Figure 4. A. In situ hybridization demonstrates the presence of low levels of AptSK2 in some neurons within the optic tectum (TeO) and torus semicircularis (TS). In contrast, neurons throughout the nucleus praeminentialis (nP) appear labeled. B. Moderate levels of AptSK1 are found in the lateral aspect of nP; arrow points to a boundary cell. C. Strong labeling for AptSK2 is seen in nP neurons of all size classes including boundary cells (arrow). Cb- cerebellum. Scale bar: 500  $\mu$ m for A and 100  $\mu$ m for B, C.

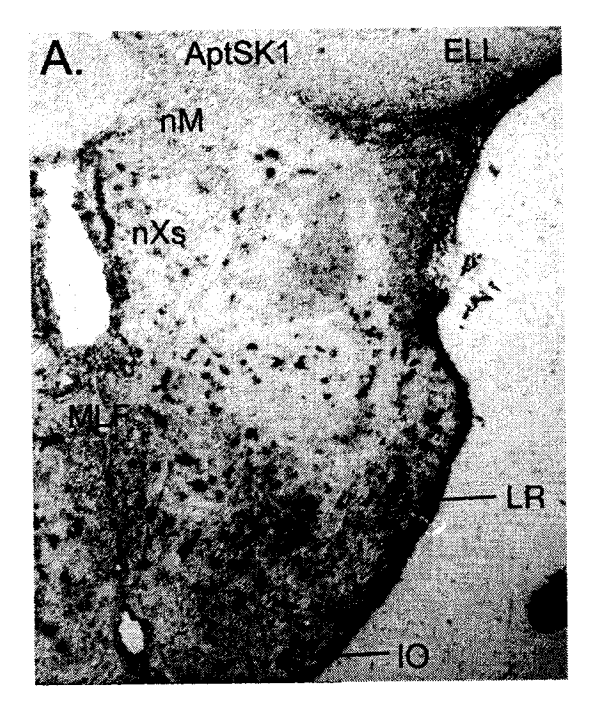




**Figure 5**. Cell specific expression of *Apt*SK1 and 2 in the cerebellum. A. Immunohistochemistry reveals the presence of *Apt*SK1 in the somata and dendrites of Purkinje cells (P) of the corpus cerebellum (CCb). Note that Purkinje cells of the transistional zone (ZT) of the cerebellum are not as densely labeled. B. *Apt*SK2 is present in eurydendroid (E) and golgi (G) cells as well as in Purkinje cells. Note that staining is more homogenous across CCb and ZT.

Abbreviations: Gr- granule cell layer of the cerebellum; mol- molecular layer of the cerebellum

Scale bar: 100 µm



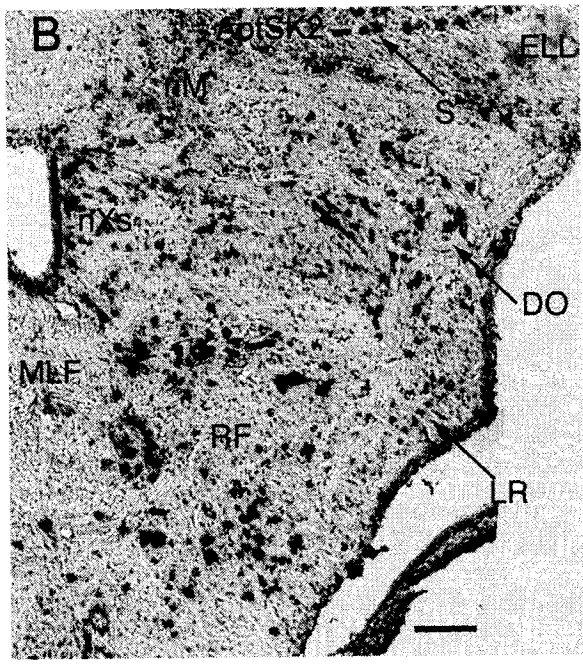


**Figure 6.** AptSK1 and 2 show differential expression patterns in the brainstem. A. AptSK1 is expressed in spherical cells (s) of the ELL and in neurons of the dorsal octavolateral nucleus (DO) and reticular formation (RF). Note lack of labeling of cells in the nucleus medialis (nM). B. AptSK2 mRNA is strongly expressed in neurons within the inferior olive (IO) and lateral reticular nucleus (LR). Neurons in nM are again not labeled. Abbreviations: ELL- electrosensory lateral line lobe; MLF- medial longitudinal fasciculus; nXs- sensory nucleus of the vagus.

Scale bar: 100 µm

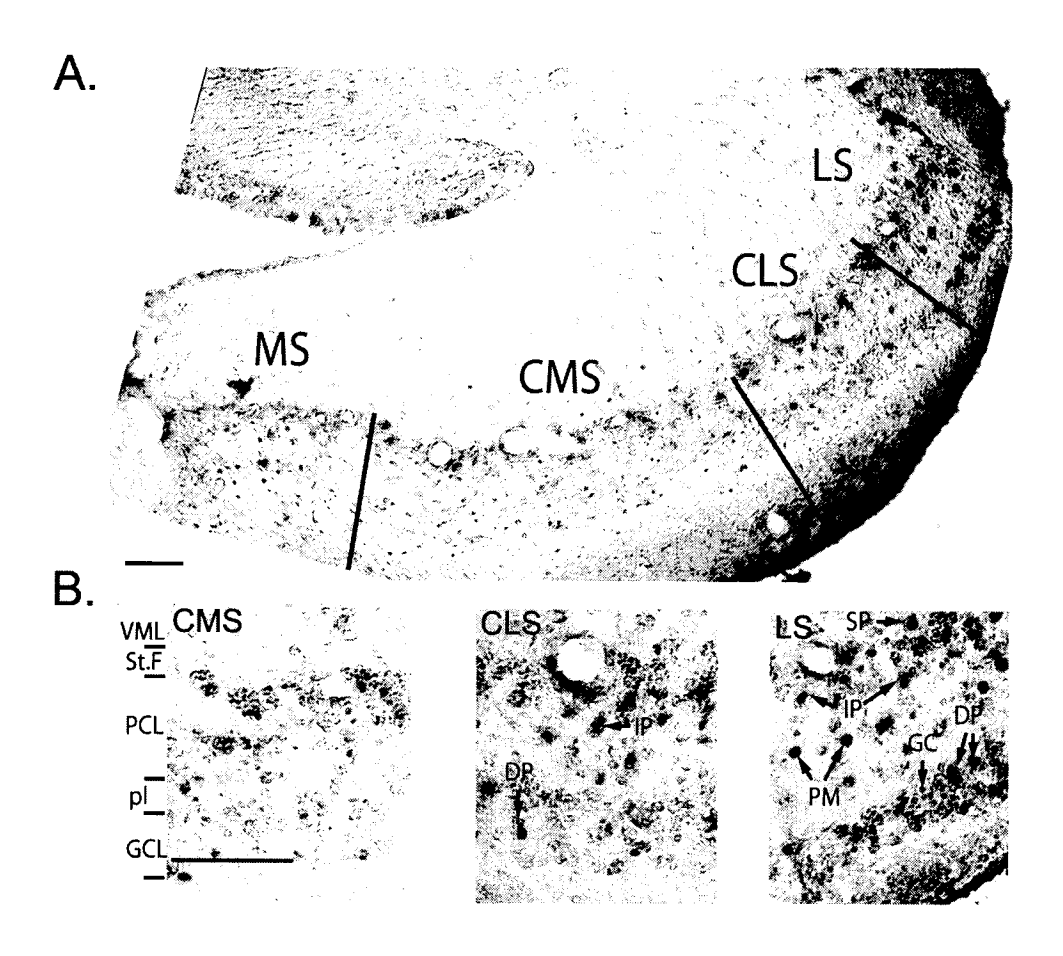


Figure 7. AptSK1 is expressed in a map specific manner in the ELL. A. High levels of AptSK1 labeling are found in the lateral (LS) and centrolateral (CLS) segments with a greatly diminished labeling in the centromedial segment (CMS) and barely detectable staining in the medial segment (MS). B. Inspection of the staining pattern at high magnification revealed staining of all 3 subsets of pyramidal neuron within the LS: deep (DP), intermediate (IP) and superficial (SP) pyramidal cells, along with strong labeling of granule (GC) and polymorphic (PM) cells. A map specific expression pattern was seen in the pyramidal cell layer (PCL), with diminished staining when moving from the LS to the CMS and near background levels of staining seen in the granule cell layer (GCL) of CMS and CLS. Scale bars, 100 μm.

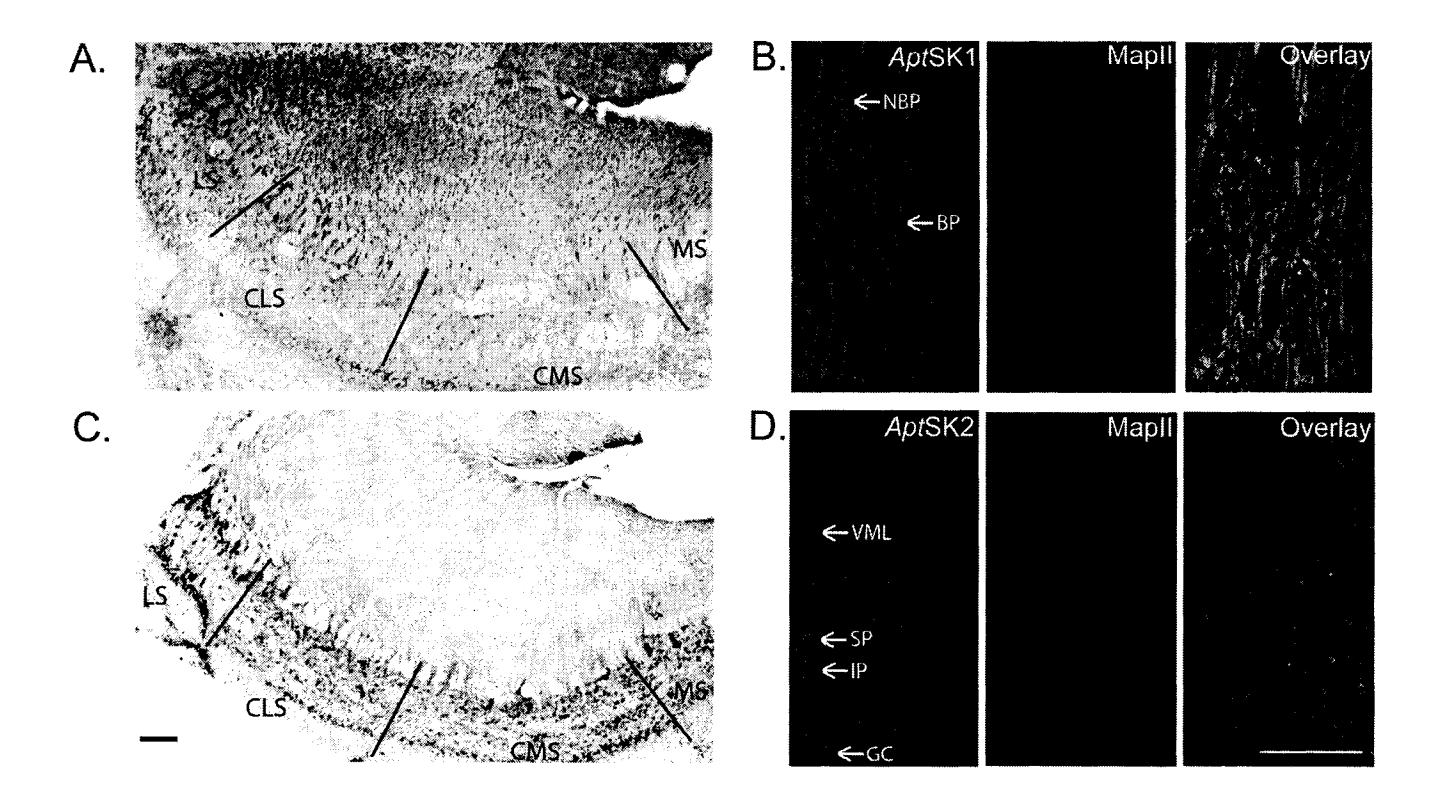
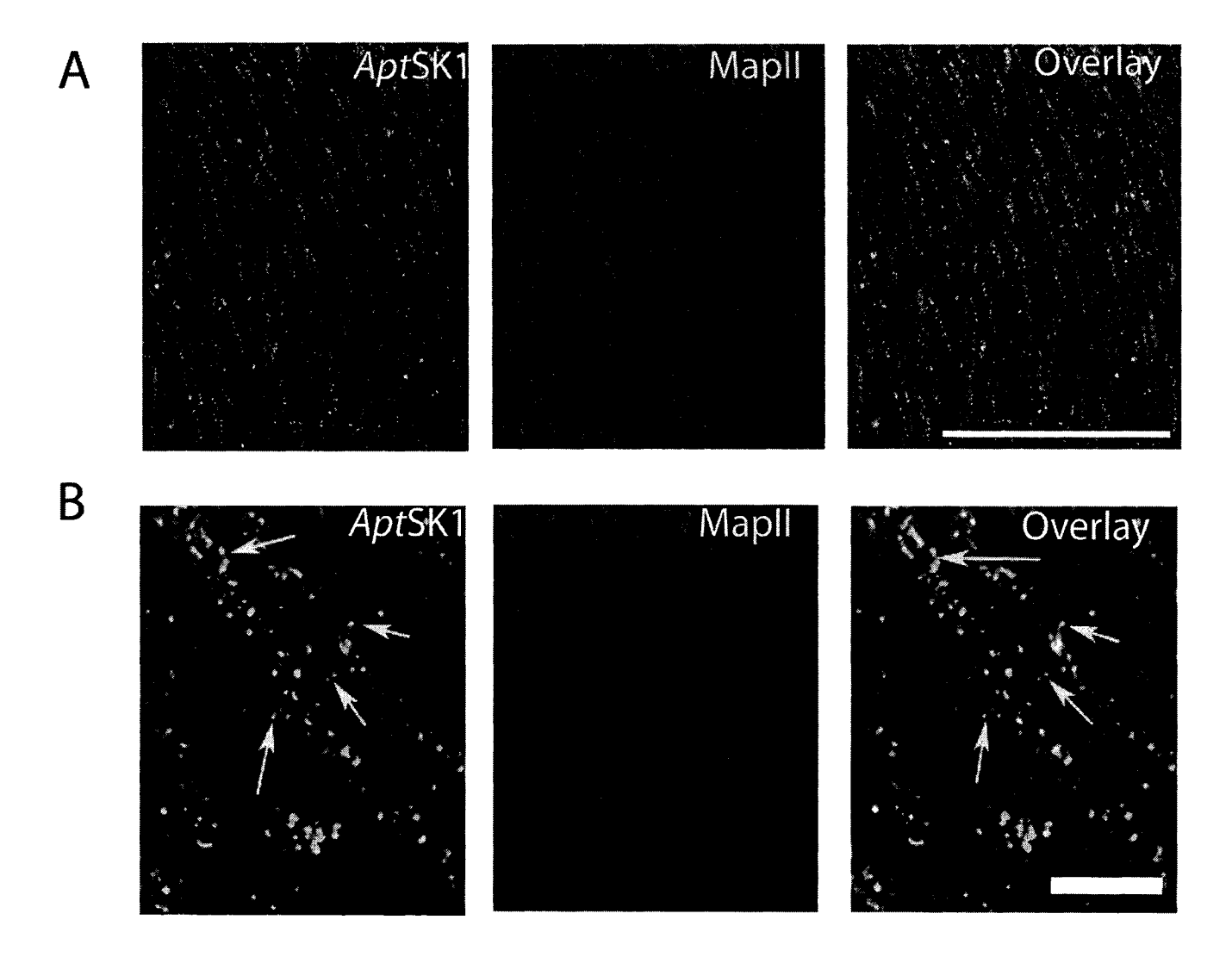


Figure 8. Immunohistochemistry reveals differential subcellular localization of AptSK1 and 2 channels in the ELL. A. AptSK1 antibodies confirm the map specific expression pattern of AptSK1 with higher levels found in the lateral segment (LS) than in the centromedial segment (CMS), with intermediate levels in the centrolateral segment (CLS). Additionally, AptSK1 shows a distinct subcellular localization pattern with prominent expression in the VML & DML, which contain the apical dendrites of pyramidal cells. B. AptSK2 antibodies confirm the map specific expression pattern previously demonstrated by in situ hybridization for AptSK2, showing high expression in LS and diminishing towards CMS. Also note the strong labeling of granular interneurons in LS as previously reported (Ellis et al., 2007). In contrast with AptSK1, no labeling in seen in the ELL molecular layer. C. Double labeling of ELL pyramidal neurons with AptSK1 (green) and Map2 (magenta) specific antibodies confirms the dendritic localization of AptSK1 (white). It also appears that AptSK1 is expressed in both nonbasilar (NBP) and basilar (BP) pyramidal neurons (arrows). D. Map2 co-labeling reveals a somatic localization for the AptSK2 channels (green). The previously noted expression in ventral molecular layer cells (VML), superficial (SP) and intermediate (IP) pyramidal neurons along with granule cells (GC) is confirmed. Scalebars: 100 µM.



**Figure 9.** AptSK1 labeling of distal pyramidal cell dendrites in the ELL reveals a distinct punctate staining pattern. A. Dendrites of the DML above the CLS show AptSK1 labeling (green) in the majority of the dendrites, as seen through co-labeling with Map2 (magenta). B. At higher magnification AptSK1positive dendritic protrusions are seen (arrows); these are not labeled with the Map2 antibody. Scalebars: A. 100  $\mu$ M, B. 10  $\mu$ M.

#### **Reference List**

Akita T, Kuba K (2000) Functional triads consisting of ryanodine receptors, Ca(2+) channels, and Ca(2+)-activated K(+) channels in bullfrog sympathetic neurons. Plastic modulation of action potential. J Gen Physiol 116: 697-720.

Bastian J (1999) Plasticity of feedback inputs in the apteronotid electrosensory system. J Exp Biol 202: 1327-1337.

Bastian J, Bratton B (1990) Descending control of electroreception. I. Properties of nucleus praeeminentialis neurons projecting indirectly to the electrosensory lateral line lobe. J Neurosci 10: 1226-1240.

Bastian J, Chacron MJ, Maler L (2002) Receptive field organization determines pyramidal cell stimulus-encoding capability and spatial stimulus selectivity. J Neurosci 22: 4577-4590.

Bastian J, Chacron MJ, Maler L (2004) Plastic and nonplastic pyramidal cells perform unique roles in a network capable of adaptive redundancy reduction. Neuron 41: 767-779.

Bastian J, Courtright J (1991) Morphological correlates of pyramidal cell adaptation rate in the electrosensory lateral line lobe of weakly electric fish. J Comp Physiol [A] 168: 393-407.

Bell and Maler (2005) Central neuroanatomy of electrosensory systems in fish. In: Springer Handbook of Auditory Research: Electroreception (Bullock TH, Hopkins C.D., Popper A.N., Fay R.R., eds), pp 68-111. New York.: Springer.

Benda J, Longtin A, Maler L (2005) Spike-frequency adaptation separates transient communication signals from background oscillations. J Neurosci 25: 2312-2321.

Berman N, Dunn RJ, Maler L (2001) Function of NMDA receptors and persistent sodium channels in a feedback pathway of the electrosensory system. J Neurophysiol 86: 1612-1621.

Berman NJ, Hincke MT, Maler L (1995) Inositol 1,4,5-trisphosphate receptor localization in the brain of a weakly electric fish (Apteronotus leptorhynchus) with emphasis on the electrosensory system. J Comp Neurol 361: 512-524.

Berman NJ, Maler L (1998) Interaction of GABAB-mediated inhibition with voltage-gated currents of pyramidal cells: computational mechanism of a sensory searchlight. J Neurophysiol 80: 3197-3213.

Berman NJ, Maler L (1999) Neural architecture of the electrosensory lateral line lobe: adaptations for coincidence detection, a sensory searchlight and frequency-dependent adaptive filtering. J Exp Biol 202: 1243-1253.

Bottai D, Dunn RJ, Ellis W, Maler L (1997) N-methyl-D-aspartate receptor 1 mRNA distribution in the central nervous system of the weakly electric fish Apteronotus leptorhynchus. J Comp Neurol 389: 65-80.

Bratton B, Bastian J (1990) Descending control of electroreception. II. Properties of nucleus praeeminentialis neurons projecting directly to the electrosensory lateral line lobe. J Neurosci 10: 1241-1253.

Bruening-Wright A, Schumacher MA, Adelman JP, Maylie J (2002) Localization of the activation gate for small conductance Ca2+-activated K+ channels. J Neurosci 22: 6499-6506.

Burnham MP, Bychkov R, Feletou M, Richards GR, Vanhoutte PM, Weston AH, Edwards G (2002) Characterization of an apamin-sensitive small-conductance Ca(2+)-activated K(+) channel in porcine coronary artery endothelium: relevance to EDHF. Br J Pharmacol 135: 1133-1143.

Cai X, Liang CW, Muralidharan S, Kao JP, Tang CM, Thompson SM (2004) Unique roles of SK and Kv4.2 potassium channels in dendritic integration. Neuron 44: 351-364.

Carr CE, Maler L, Heiligenberg W, Sas E (1981) Laminar organization of the afferent and efferent systems of the torus semicircularis of gymnotiform fish: morphological substrates for parallel processing in the electrosensory system. J Comp Neurol 203: 649-670.

Carr CE, Maler L, Taylor B (1986) A time-comparison circuit in the electric fish midbrain. II. Functional morphology. J Neurosci 6: 1372-1383.

Chacron MJ, Doiron B, Maler L, Longtin A, Bastian J (2003) Non-classical receptive field mediates switch in a sensory neuron's frequency tuning. Nature 423: 77-81.

Cloues RK, Sather WA (2003) Afterhyperpolarization regulates firing rate in neurons of the suprachiasmatic nucleus. J Neurosci 23: 1593-1604.

Deng Q, Rashid AJ, Fernandez FR, Turner RW, Maler L, Dunn RJ (2005) A C-terminal domain directs Kv3.3 channels to dendrites. J Neurosci 25: 11531-11541.

Dulka JG, Maler L, Ellis W (1995) Androgen-induced changes in electrocommunicatory behavior are correlated with changes in substance P-like immunoreactivity in the brain of the electric fish Apteronotus leptorhynchus. J Neurosci 15: 1879-1890.

Ellis LD, Mehaffey WH, Harvey-Girard E, Turner RW, Maler L, Dunn RJ (2007) SK channels provide a novel mechanism for the control of frequency tuning in electrosensory neurons. J Neurosci 27: 9491-9502.

Emptage N, Bliss TV, Fine A (1999) Single synaptic events evoke NMDA receptor-mediated release of calcium from internal stores in hippocampal dendritic spines. Neuron 22: 115-124.

Faber ES, Delaney AJ, Sah P (2005) SK channels regulate excitatory synaptic transmission and plasticity in the lateral amygdala. Nat Neurosci 8: 635-641.

Finger TE (1978) Efferent neurons of the teleost cerebellum. Brain Res 153: 608-614.

Fortune ES (2006) The decoding of electrosensory systems. Curr Opin Neurobiol 16: 474-480.

Gussin DJ, Benda J, Maler L (2007) Limits of Linear Rate Coding of Dynamic Stimuli by Electroreceptor Afferents. J Neurophysiol.

Heiligenberg W, Keller CH, Metzner W, Kawasaki M (1991) Structure and function of neurons in the complex of the nucleus electrosensorius of the gymnotiform fish Eigenmannia: detection and processing of electric signals in social communication. J Comp Physiol [A] 169: 151-164.

Heiligenberg W, Dye J (1982) Labelling of electroreceptive afferents in a gymnotoid fish by intracellular injection of HRP: The mystery of multiple maps. J Comp Physiol [A] 148: 287-296.

Ishii TM, Maylie J, Adelman JP (1997) Determinants of apamin and d-tubocurarine block in SK potassium channels. J Biol Chem 272: 23195-23200.

Jager H, Adelman JP, Grissmer S (2000) SK2 encodes the apamin-sensitive Ca(2+)-activated K(+) channels in the human leukemic T cell line, Jurkat. FEBS Lett 469: 196-202.

Kawasaki M, Maler L, Rose GJ, Heiligenberg W (1988) Anatomical and functional organization of the prepacemaker nucleus in gymnotiform electric fish: the accommodation of two behaviors in one nucleus. J Comp Neurol 276: 113-131.

Keller CH, Maler L, Heiligenberg W (1990) Structural and functional organization of a diencephalic sensory-motor interface in the gymnotiform fish, Eigenmannia. J Comp Neurol 293: 347-376.

Kohler M, Hirschberg B, Bond CT, Kinzie JM, Marrion NV, Maylie J, Adelman JP (1996) Small-conductance, calcium-activated potassium channels from mammalian brain. Science 273: 1709-1714.

Krahe R, Gabbiani F (2004) Burst firing in sensory systems. Nat Rev Neurosci 5: 13-23.

Lancaster B, Hu H, Ramakers GM, Storm JF (2001) Interaction between synaptic excitation and slow afterhyperpolarization current in rat hippocampal pyramidal cells. J Physiol 536: 809-823.

Lee WS, Ngo-Anh TJ, Bruening-Wright A, Maylie J, Adelman JP (2003) Small conductance Ca2+activated K+ channels and calmodulin: cell surface expression and gating. J Biol Chem 278: 25940-25946.

Lewis JE, Maler L (2004) Synaptic dynamics on different time scales in a parallel fiber feedback pathway of the weakly electric fish. J Neurophysiol 91: 1064-1070.

Maler L (1979) The posterior lateral line lobe of certain gymnotoid fish: quantitative light microscopy. J Comp Neurol 183: 323-363.

Maler L, Finger T, Karten HJ (1974) Differential projections of ordinary lateral line receptors and electroreceptors in the gymnotid fish, Apteronotus (Sternarchus) albifrons. J Comp Neurol 158: 363-382.

Maler L, Mugnaini E (1994) Correlating gamma-aminobutyric acidergic circuits and sensory function in the electrosensory lateral line lobe of a gymnotiform fish. J Comp Neurol 345: 224-252.

Maler L, Sas E, Johnston S, Ellis W (1991) An atlas of the brain of the electric fish Apteronotus leptorhynchus. J Chem Neuroanat 4: 1-38.

Maler L, Sas EK, Rogers J (1981) The cytology of the posterior lateral line lobe of high-frequency weakly electric fish (Gymnotidae): dendritic differentiation and synaptic specificity in a simple cortex. J Comp Neurol 195: 87-139.

Mathieson WB, Maler L (1988) Morphological and electrophysiological properties of a novel in vitro preparation: the electrosensory lateral line lobe brain slice. J Comp Physiol [A] 163: 489-506.

Middleton JW, Longtin A, Benda J, Maler L (2006) The cellular basis for parallel neural transmission of a high-frequency stimulus and its low-frequency envelope. Proc Natl Acad Sci U S A 103: 14596-14601.

Nelson ME, Xu Z, Payne JR (1997) Characterization and modeling of P-type electrosensory afferent responses to amplitude modulations in a wave-type electric fish. J Comp Physiol [A] 181: 532-544.

Ngo-Anh TJ, Bloodgood BL, Lin M, Sabatini BL, Maylie J, Adelman JP (2005) SK channels and NMDA receptors form a Ca2+-mediated feedback loop in dendritic spines. Nat Neurosci 8: 642-649.

Nolting A, Ferraro T, D'hoedt D, Stocker M (2007) An Amino Acid Outside the Pore Region Influences Apamin Sensitivity in Small Conductance Ca2+-activated K+ Channels. J Biol Chem 282: 3478-3486.

Northcutt RG (2006) Connections of the lateral and medial divisions of the goldfish telencephalic pallium. J Comp Neurol 494: 903-943.

Panofen F, Piwowarski T, Jeserich G (2002) Small conductance calcium-activated potassium channels of trout CNS: molecular structure, developmental expression, and partial biophysical characterization. Brain Res Mol Brain Res 101: 1-11.

Portavella M, Torres B, Salas C (2004) Avoidance response in goldfish: emotional and temporal involvement of medial and lateral telencephalic pallium. J Neurosci 24: 2335-2342.

Rashid AJ, Dunn RJ, Turner RW (2001) A prominent soma-dendritic distribution of Kv3.3 K+ channels in electrosensory and cerebellar neurons. J Comp Neurol 441: 234-247.

Ro S, Hatton WJ, Koh SD, Horowitz B (2001) Molecular properties of small-conductance Ca2+-activated K+ channels expressed in murine colonic smooth muscle. Am J Physiol Gastrointest Liver Physiol 281: G964-G973.

Rodriguez JA, Piddini E, Hasegawa T, Miyagi T, Dotti CG (2001) Plasma membrane ganglioside sialidase regulates axonal growth and regeneration in hippocampal neurons in culture. J Neurosci 21: 8387-8395.

Roncarati R, Decimo I, Fumagalli G (2005) Assembly and trafficking of human small conductance Ca2+activated K+ channel SK3 are governed by different molecular domains. Mol Cell Neurosci 28: 314-325.

Sah P (1996) Ca(2+)-activated K+ currents in neurones: types, physiological roles and modulation. Trends Neurosci 19: 150-154.

Sailer CA, Hu H, Kaufmann WA, Trieb M, Schwarzer C, Storm JF, Knaus HG (2002) Regional differences in distribution and functional expression of small-conductance Ca2+-activated K+ channels in rat brain. J Neurosci 22: 9698-9707.

Sailer CA, Kaufmann WA, Marksteiner J, Knaus HG (2004) Comparative immunohistochemical distribution of three small-conductance Ca2+-activated potassium channel subunits, SK1, SK2, and SK3 in mouse brain. Mol Cell Neurosci 26: 458-469.

Sas E, Maler L (1983) The nucleus praeeminentialis: a Golgi study of a feedback center in the electrosensory system of gymnotid fish. J Comp Neurol 221: 127-144.

Sas E, Maler L (1987) The organization of afferent input to the caudal lobe of the cerebellum of the gymnotid fish Apteronotus leptorhynchus. Anat Embryol (Berl) 177: 55-79.

Sawtell NB, Williams A, Bell CC (2005) From sparks to spikes: information processing in the electrosensory systems of fish. Curr Opin Neurobiol 15: 437-443.

Schumacher MA, Crum M, Miller MC (2004) Crystal Structures of Apocalmodulin and an Apocalmodulin/SK Potassium Channel Gating Domain Complex. Structure (Camb ) 12: 849-860.

Schumacher MA, Rivard AF, Bachinger HP, Adelman JP (2001) Structure of the gating domain of a Ca2+activated K+ channel complexed with Ca2+/calmodulin. Nature 410: 1120-1124.

Shmukler BE, Bond CT, Wilhelm S, Bruening-Wright A, Maylie J, Adelman JP, Alper SL (2001) Structure and complex transcription pattern of the mouse SK1 K(Ca) channel gene, KCNN1. Biochim Biophys Acta 1518: 36-46.

Stackman RW, Hammond RS, Linardatos E, Gerlach A, Maylie J, Adelman JP, Tzounopoulos T (2002) Small conductance Ca2+-activated K+ channels modulate synaptic plasticity and memory encoding. J Neurosci 22: 10163-10171.

# **CHAPTER II**

# SK CHANNELS PROVIDE A NOVEL MECHANISM FOR THE CONTROL OF FREQUENCY TUNING IN ELECTROSENSORY NEURONS

Lee D. Ellis, W. Hamish Mehaffey, Erik Harvey-Girard, Ray W. Turner, Leonard Maler, and Robert J. Dunn

Journal of Neuroscience, August 29, 2007 27: 9491-9502

# **CONTRIBUTIONS OF AUTHORS**

This study was designed by Lee Ellis and completed through the combined efforts of Lee Ellis and Hamish Mehaffey (University of Calgary). Lee Ellis composed the initial version of this manuscript with major editing by Rob Dunn and Len Maler (University of Ottawa) and further editing by Hamish Mehaffey. Lee Ellis created all of the figures for the manuscript.

Cloning of the AptSK2 channel, sequence analysis and in situ hybridization studies were all performed by Lee Ellis. The electrophysiological studies were a combined effort of Lee Ellis and Hamish Mehaffey. Hamish Mehaffey was responsible for the majority of the neurobiotin labeling that allowed for the differentiation of E and I cells. Hamish Mehaffey also designed the MatLab software used to analyze the firing coherence to random amplitude modulation stimuli.

#### **Abstract**

One important characteristic of sensory input is frequency, with sensory neurons often tuned to narrow stimulus frequency ranges. Although vital for many neural computations, the cellular basis of such frequency tuning remains largely unknown. In the electrosensory system of *A. leptorhynchus* the primary processing of important environmental and communication signals occurs in pyramidal neurons of the electrosensory lateral line lobe (ELL). Spike trains transmitted by these cells can encode low frequency prey stimuli with bursts of spikes and high frequency communication signals with single spikes. Here we demonstrate that the selective expression of SK2 channels in a subset of pyramidal neurons reduces their response to low frequency stimuli by opposing their burst responses. Apamin block of the SK2 current in this subset of cells induced bursting and increased their response to low frequency inputs. SK channel expression thus provides an intrinsic mechanism that predisposes a neuron to respond to higher frequencies and thus specific, behaviorally relevant stimuli.

#### Introduction

Sensory systems discriminate stimuli across multiple dimensions. The frequency of such signals is an important characteristic and frequency tuning has been demonstrated in the auditory (Woolley et al., 2005;Elhilali et al., 2004;Hudspeth, 2000), visual (Priebe et al., 2006) and somatosensory (Andermann et al., 2004) systems. The cell intrinsic biophysical mechanisms that shape the frequency responses are not well understood. The electrosensory system of *Apteronotus leptorhynchus* estimates the frequency content of input signals. These fish produce an electric organ discharge (EOD) to create an electric field that permits them to locate objects (electrolocation) and communicate (electrocommunication). Cutaneous electroreceptors encode amplitude modulations (AMs) of the EOD and project to pyramidal neurons in the hindbrain electrosensory lateral line lobe (ELL) (Turner and Maler, 1999;Bell and Maler, 2005). ELL pyramidal cells extract the AMs intensity and frequency. In general, prey capture is associated with low frequencies (<20 Hz) while electrocommunication signals are high

associated with low frequencies (<20 Hz) while electrocommunication signals are high frequency AMs (>50 Hz; typically male-female interactions; (Nelson and Maciver, 1999;Zakon et al., 2002).

The ELL is part of a thoroughly characterized neural network (Berman and Maler,

The ELL is part of a thoroughly characterized neural network (Berman and Maler, 1999) well suited for the study of neuronal frequency tuning. It is divided into 4 topographic maps, the lateral (LS), centrolateral (CLS), centromedial (CMS) and medial (MS) segments (Bell and Maler, 2005). While the LS, CLS and CMS receive identical inputs from tuberous electroreceptors, the MS receives input from ampullary receptors and are not evaluated in this study. The physiological and molecular makeup of the different ELL maps suggests that pyramidal neurons in the most lateral map are specialized to encode high frequency communication signals while pyramidal neurons in the more medial maps encode low frequency prey signals (Shumway, 1989;Metzner and Juranek, 1997). Within each map pyramidal cell responses to low frequency input are encoded by spike bursts, while high frequency stimuli are encoded with isolated spikes (Oswald et al., 2004). This suggests that frequency tuning of ELL pyramidal cells might depend on the biophysical control of burst generation.

Small conductance calcium activated potassium (SK) channels (Kohler et al., 1996) open in response to elevations in calcium and produce a medium after-

hyperpolarization (mAHP). SK channels can regulate numerous aspects of neuronal dynamics including: spike frequency adaptation (Pedarzani et al., 2005), spike patterning (Wolfart et al., 2001;Cloues and Sather, 2003) synaptic excitability (Stackman et al., 2002;Kramar et al., 2004), dendro-somatic coupling (Womack and Khodakhah, 2003) and long term potentiation (Behnisch and Reymann, 1998;Lancaster et al., 2001;Stackman et al., 2002;Faber et al., 2005;Ngo-Anh et al., 2005). The links between SK channel kinetics and behaviorally relevant neuronal computations have not, however, been rigorously explored.

Here we show that SK2 channels are differentially expressed across the ELL maps, with the highest levels in pyramidal neurons tuned to high frequencies. We hypothesize that frequency tuning in ELL pyramidal neurons is regulated by SK channel control of burst output. Consistent with this hypothesis, apamin was found to reduce the size of the mAHP in high frequency tuned neurons, increasing their response to low frequency input via an increase in bursting. In contrast, apamin had no effect on neurons tuned to low frequencies. We conclude that SK channels can regulate frequency selectivity in pyramidal neurons and thus tuning for prey versus communication signals.

#### **Materials and Methods**

#### Isolation of Apteronotus SK2 channel cDNA

The AptSK2 channel sequence was initially isolated using PCR and degenerate primers designed to match all possible codons for the conserved amino acid segments The primers were based on comparisons of human, rat and trout SK channel sequences. High levels of sequence conservation were found between the putative transmembrane 5° segments S1 and S6. The primers used were: forward ATCTTYGGIATGTTYGGIATIGT 3' and reverse 5' TATAGATIAGCCAIGTYTCY 3', where Y=C+T, I=inosine. PCR was performed on brain cDNA cfrom A. leptorhynchus (Bottai et al., 1997). The product of the degenerate RT-PCR (900 bp) was cloned into the pGEM-T vector (Promega, Madison, WI). Sequencing of the purified plasmids allowed the identification of sequences with high homology to known SK channels. The 5' and 3' regions of the channel were further isolated through rapid amplification of cDNA ends (RACE) using the Generacer kit from Invitrogen (Carlsbad, CA). Once the sequence of the SK2 channel was assembled, primers were designed from the 5' and 3' untranslated (UTR) sequences that could amplify the full-length channel. The channel was then amplified by PCR using Pfu polymerase, to decrease the likelihood of error introduction and the DNA sequence confirmed.

The amono acid sequence of the *Apt*SK2 channel was aligned with the rat, mouse, human and trout SK channels along with the human BK channel for the creation of a phylogenic tree. Alignments were carried out using the clustal W algorithm included in the Lasergene software package (DNAstar, Madison, WI).

## Apteronotus Brain Section Preparation For In situ Hybridization

Fish were anesthetized in tank water containing MS-222 (3-aminobenzoic acid ethyl ester) and respirated with O<sub>2</sub> bubbled MS-222 water during the perfusion procedure while surrounded in ice. Following surgical exposure of the heart 20 mL cold phosphate buffered saline (PBS) was perfused via a needle inserted into the conus arteriosus. The fish were perfused with 40 mL cold PBS containing 4% Para formaldehyde (PFA). Whole brains were surgically removed and placed in 4% PFA containing solutions. The brains were cryoprotected by placing them in a 4% PFA solution containing 10-15%

sucrose overnight at 4°C. Cryostat sections (20µm) were cut and mounted on poly-L lysine coated slides and stored at -20°C until use.

## In situ Hybridization

The hybridization probe templates were created by PCR amplification of 5' UTR + the initial 5' sequence (397 nucleotides total). The RNA synthesis reaction involved the use of a digoxin labeled UTP in the NTP mix at a ratio of 1:3 with unlabeled UTP. In situ hybridization was preformed on cryostat sections prepared as outlined above. The hybridization procedure was based on a protocol previously designed for Apteronotus slices (Bottai et al., 1997), but modified for the use of DIG labelled probes. Slides were post-fixed by placing them on a 40°C hotplate for 10 min followed by 20 min in 4% PFA/PBS at 4°C. Slides were then dehydrated in ascending alcohol (50, 70, 95, 100% - 3 min each). Unless otherwise noted all of the following steps were done at room temperature (22°C). Pre treatment of slides involved a brief rinse in PBS (5 min) followed by permeablization in 0.3% Triton-X-100/PBS for 15 min. Slides were rinsed twice in PBS (5 min) and further permeablized with Proteinase K (5 µg/mL) in TE buffer (100:50) at 37°C for 30 min. Again slides were rinsed twice with PBS (5 min) then in Triethanolamine (TEA 0.1M, 2 min) followed by acetylation with 0.25% acetic anyhydride in TEA for 5 min. Slides were dehydrated in ascending alcohol (50, 70, 95, 100% 3 min ea). Then slides were incubated for 1 hour on a slide plate (humid chamber) at 50°C with 200 µL of prehybridization solution (50% formamide, 0.75M NaCl, 25mM EDTA, 25mM PIPES, 1x Dendharts, 0.2% Tween-20, 1mg/mL salmon sperm DNA, 1mg/mL yeast tRNA). The hybridization solution included dextrane sulphate (10%) along with the specific hybridization probe. The probe solution was added and each slide was coverslipped, sealed with DPX and left overnight at the appropriate temperature. Following hybridization the slides were washed in descending sodium citrate buffer (2x SSC, 1x SSC-50% formamide, 0.2x SSC) for 20 min at the hybridization temperature. Immunodetection of the DIG labeled probe involved the following procedure: Slides were washed twice in Buffer 1 (100mM Tris pH=7.5, 150mM NaCl) for 10 min. Slides were then blocked for 30 min (Buffer 1, 01% Triton-X-100, 2% sheep serum, 1% Block (from Roche Kit #1175041), followed by incubation in a humid chamber with blocking buffer containing Anti-DIG alkaline phosphatase antibody 1:1000. Slides were washed (100 mM Tris-HCL pH 9.5, 100 mM NaCl, 50 mM MgCl<sub>2</sub>) and placed back into the humid chamber and incubated for 2-15 min with colouration solution (3% NCBI/NCT in Buffer 2). Colouration was stopped by placing slide in TE 10:1 for 10 min. Slides were subsequently coverslipped and sealed.

Optical density measurements were made using Image J software. Cells were grouped based on segment (LS, CLS, CMS) and as well as pyramidal cell sublayer (superficial or intermediate, (Bastian and Courtright, 1991;Berman et al., 1995) resulting in 6 distinct groups. Superficial neurons were considered to be those lying along the upper 25 µm of the pyramidal cell layer as previously shown (Berman et al., 1995), while intermediate cells were considered those to be > 25 µm from the stratum fibrosum (upper boundary of the pyramidal cell layer). Local background measurements were taken from the plexiform layer (pl-Fig 2) and were subtracted from cell values. Optical density histograms were created using a bin width of 10 OD units. Optical density measurements made on pyramidal cells from sense controls served as an estimate of general background labelling of pyramidal cell somata.

# Preparation of slices for electrophysiology

Fish (*A. leptorhynchus*) were obtained from local importers and maintained at 26-28°C in fresh water aquaria, in accordance with protocols approved by the University Animal Care Committee. All chemicals were obtained from SIGMA (St. Louis, MO) unless otherwise noted. Animals were anaesthetized in 0.05% phenoxy-ethanol, and ELL tissue slices of 300-400 μm thickness were prepared as previously described(Turner et al., 1994). Slices were maintained by constant perfusion of ACSF (1-2ml/min), and superfusion of humidified 95% O<sub>2</sub>, 5% CO<sub>2</sub> gas. ACSF contained, 124 mM NaCl, 3 mM KCl, 25 mM NaHCO<sub>3</sub>, 1.0 mM CaCl<sub>2</sub>, 1.5 mM MgSO<sub>4</sub> and 25 mM D-glucose, pH 7.4. HEPES-buffered ACSF for pressure ejection of pharmacological agents contained the same elements, with the following differences: 148 mM NaCl, 10 mM HEPES.

# **Recording procedures**

Glass microelectrodes were backfilled with 2 M KAc (pH 7.4; 90-120 MQ

resistance), containing 2% Neurobiotin (Vector Labs). Recordings were made from pyramidal cells from all three ELL segments receiving P-unit inputs (lateral (LS), centrolateral (CLS) and centromedial (CMS) segments). Recordings were made from the pyramidal cell layer (PCL) and digitized using a NI PCI-6030E DAQ board (National Instruments, Austin TX). Intracellular stimuli were delivered, and data was recorded in custom software using the Matlab data acquisition toolbox (Mathworks, Natick MA). Cells were held at a level just below firing threshold with a negative current injection. Random amplitude modulations (RAMs) consisting of white noise low-pass filtered to 0-60Hz were given on top of the negative current injection, and the SD of the waveform was adjusted to give firing rates of 10-25 Hz. Apamin (1-10 µM) or 1-ethyl-2-benzimidazolinone (EBIO; 1 mM) were focally ejected into the pyramidal cell layer (PCL) using electrodes of 1-2 µm tip diameter and 7-15 psi pressure ejection. Previous studies have estimate an ~10x dilution factor for ejected toxins(Turner et al., 1994). Pharmacological agents were dissolved in HEPES buffered ACSF.

## **Cell Fills**

ELL Pyramidal cells were filled after recording using sustained positive current ejection pulse (+1nA, 250ms). Following recording, slices were transferred to 4% paraformaldehyde and fixed for several days at 4°C. Slices were washed in 0.1 M phosphate buffer (PB) for several hours, and then placed in a solution of PB, Triton X-100 (0.1%), DMSO (0.5%) and streptavidin-Cy3 (1:1500) for three days. Slices were visualized under fluorescent microscopy for classification. Superficial pyramidal cells were distinguished by the extent of their dendritic arborization, and by the location of the soma within the PCL. A total of 29 cells were filled from the 3 major tuberous electrosensory maps. Cells were classified as E or I-cells depending on the presence of absence of a basilar dendrite. Of the cells, 7 were from the LS (E-cells = 3, I-cells =4), 13 from the CLS (E-cells = 7, I-cells = 6), and 9 were from the CMS (2 Superficial E-cells, two superficial I-cells, 4 intermediate E-cells, and 1 intermediate I-cell).

## **Data Analysis**

All electrophysiological data was analysed in Matlab R2006a (Mathworks,

Natick, MA). Spike threshold was taken based on the first derivative of the voltage waveform. Data was plotted in Origin (OriginLab, Northhampton MA) or Igor Pro (Wavemetrics, Lake Oswego OR). Spike trains were digitized into binary trains, and detrended. Coherence estimates were made between the digitized spike trains and the original RAM stimulus and given by:

$$C(f) = \frac{P_{sr}(f)^2}{P_{ss}(f)P_{rr}(f)}$$

where  $P_{ss}$  and  $P_{rr}$  denote the power spectrum of the stimulus and the response, and  $P_{sr}$  denotes the cross-spectrum between the stimulus and response (e.g. the spike train). Pyramidal cells displaying spontaneous slow oscillations (Turner et al., 1996) were excluded from analysis. Statistical significance was determined using paired t-tests unless otherwise noted. Cells were classified as high or low pass based on the ratio of their average coherence between 0-20 Hz, and between 30-50 Hz.

AHPs were averages of 5 spikes generated by a current injection (0.1 nA) to reach the minimum spike threshold. Spikes were averaged following alignment of spikes at threshold using clampfit 9.0 software (Axon Instruments). AHP measurements were taken at the peak of the fAHP and at 10 ms following spike peak. Significance was assessed using a paired t-test with a significance level of p < 0.05 unless otherwise noted. Statistical significance for ANOVA was determined using Tukey's HSD.

#### Results

#### Isolation of SK channel cDNA from Apteronotus

Degenerate PCR was used to isolate SK channel genes from Apteronotus brain mRNA (see methods) revealing the expression of three different SK genes, orthologous to mammalian SK1, SK2 and SK3. Of these only AptSK1 and 2 were detected in mRNA from the ELL, with AptSK2 expressed at much higher levels. At the cellular level, in situ hybridization studies showed that the expression of AptSK1 and 2 mRNAs occurs in a nearly identical segmental pattern within the ELL (data not shown); thus the differential segmental effects of apamin or EBIO might be attributed to their actions on either AptSK1 or 2 channels. However, preliminary immunohistochemical analysis has shown that AptSK2 channels are strictly somatic in these cells (Ellis, unpublished observations), well positioned to contribute to the AHPs that regulate firing patterns and burst responses. In contrast, AptSK1 channels localize nearly exclusively to distal apical dendrites (Ellis, unpublished observations). We therefore attribute the effects of the application of SK channel modulators (apamin or EBIO) onto the pyramidal cell layer (described in subsequent sections) primarily to their action on AptSK2 channels. In the localization studies described below, we have focused on AptSK2 which is the primary somatic SK channel in the ELL, although we cannot rule out a minor contribution from AptSK1 channels to the SK-mediated AHPs we record in these cells.

The *Apt*SK2 channel is highly homologous to SK2 channels from other species (Fig. 1A,B). The *Apt*SK2 channel protein shows a 96.0% identity to the trout ortholog and 86.8% identity to the human SK2 (Fig. 1A). Regions of functional importance are highly conserved, including the putative pore region, the six transmembrane segments, and two residues in the C-terminal intracellular tail (*Apt*SK2: R422, K436) that are required for the CaM interactions necessary for gating and surface expression (Lee et al., 2003). Two residues (*Apt*SK2; N334, D307) in the outer vestibule of the pore that are responsible for apamin sensitivity (Ishii et al., 1997) are also conserved. The high level of sequence conservation indicates that *Apt*SK2 should function and show drug responses similar to previously cloned SK2 channels.

# AptSK2 gene expression is regulated in a map specific manner.

The ELL receives direct input from electroreceptors on the skin and is responsible for the primary processing of electrosensory information, which is then relayed onto higher brain areas. The ELL is subdivided into 4 segments containing topographic maps of the fish body (Heiligenberg and Dye, 1982;Carr et al., 1986). The most medial segment (MS) receives input from ampullary receptors and was not assessed in this study. The three sequential lateral segments (centromedial- CMS; centrolateral-CLS, lateral-LS) receive identical inputs from tuberous receptors (reviewed by Turner and Maler, 1999). Each segment is organized in a laminar pattern with three distinct classes of pyramidal cells (superficial, intermediate and deep) defined on the basis of morphological, biochemical and physiological criteria (Bastian et al., 2002;Bastian et al., 2004;Turner and Maler, 1999). Superficial and intermediate pyramidal cells are located in the pyramidal cell layer while the granular layer contains the deep pyramidal neurons (these were not examined in this study because it is difficult to distinguish them from adjacent interneurons).

In situ hybridization was used to characterize AptSK2 mRNA levels in pyramidal neurons of the three ELL segments. The AptSK2 probe was 397 nucleotides in length, comprising 232 nucleotides of 5' UTR and 165 nucleotides of coding sequence. In control experiments, the sense probe showed low levels of non-specific staining across all segments of the ELL and other brain regions (data not shown). Mean optical density (OD) measurements were taken from individual cells sampled from across all segments for the sense controls. The average OD was  $61.5 \pm 17.1$  (n = 59 cells from 3 sections from 3 different fish), which we take to represent the value of background non-specific staining; the mean value of the sense ODs is indicated by an arrow in Fig.2C.

The staining pattern produced by the *Apt*SK2 antisense probe revealed that a large number of pyramidal neurons from both the LS and CLS were strongly labeled while in the CMS fewer cells were *Apt*SK2 positive (Fig. 2). Within the LS and CLS, both superficial and intermediate pyramidal neurons were strongly stained along with several classes of interneurons (granular cells and VML neurons; Fig. 2B). Interestingly, in the CMS, the expression of *Apt*SK2 mRNA appeared to be restricted to intermediate pyramidal neurons alone, while adjacent superficial neurons appeared unlabeled.

In order to quantify the expression of the AptSK2 probe, each segment was divided into superficial and intermediate pyramidal cell layers (resulting in 6 separate compartments) and the OD of individual cells was measured (see methods). The staining pattern for the CMS superficial layer was unimodal with a mean OD of  $66.7 \pm 25.7$  (Fig. 2C). This distribution completely overlapped and was not statistically different from that of the sense controls (t-test p > 0.05; note location of arrow in Fig. 2C), implying that this is background staining and CMS superficial pyramidal cells do not express AptSK2 mRNA. The OD histograms from the other 5 regions were bimodal showing two distinct peaks (data not shown). The first peak had mean values comparable to the sense controls, while the second peak showed much higher OD values suggesting that there were two populations of pyramidal neurons, one that expressed AptSK2 mRNA and another that did not. We picked an OD of 135 as the separating value between the two OD populations since this was the maximum OD value from the CMS superficial cells (Fig. 2C-dotted line) and a trough was present at this level in the CMS intermediate, CLS and LS OD histograms. The peaks were analyzed by averaging the data points between 0 and 135 (low OD values) and 135 and 255 (high OD values). When the two regions of the histogram were compared individually across the 5 regions that showed bimodal peaks the mean OD values were not statistically different for either the low (CMS intermediate:  $73.4 \pm 27.9$ ; CLS superficial:  $67.6 \pm 28.4$ ; CLS intermediate:  $71.9 \pm 34.3$ ; LS superficial:  $74.6 \pm 29.6$ ; LS intermediate  $75.0 \pm 34.3$ ; p = 0.65, 1-way ANOVA) or high group (CMS intermediate: 173.2  $\pm$  21.2; CLS superficial: 174.3  $\pm$  18.4; CLS intermediate:  $175.6 \pm 20.3$ ; LS superficial:  $174.3 \pm 21.5$ ; LS intermediate  $176 \pm 26.6$ ; p = 0.98, 1-way ANOVA). The 5 regions were therefore combined for further statistical analysis (Fig 2D). The summed histograms were again divided in the same way: low OD value group (0-135) and high OD value group (135-255; Fig 2D-dotted line). When the OD values of the CMS superficial group were compared to the high and low groups from the summed histogram a significant difference between the three groups was found (1way ANOVA). Posthoc analysis revealed that this was the result of differences between the high group and either the low group (Tukey's HSD; p < 0.0001) or the CMS superficial values (Tukey's HSD; p < 0.0001), while there was no significant difference between the low group and the CMS superficial values (Tukey's HSD; p = 0.46). We

conclude that the low OD group from the combined histograms was the result of background staining, which was further supported by the fact that there was no statistical difference the low OD group, the CMS superficial cells and sense control values (1-way Anova; p > 0.05).

This analysis indicates that the levels of *in situ* hybridization signal for the *Apt*SK2 mRNA are low or not present in all pyramidal neurons from the CMS superficial layer, while the other regions (CLS, LS and the intermediate cells of CMS) have 2 cell populations that are either strongly positive for *Apt*SK2 or do not express *Apt*SK2 mRNA (Fig. 2). This suggests that *Apt*SK2 channels may contribute to the response properties of only certain types of pyramidal neurons in this system. Therefore, in order to further understand the roles that the different levels of *Apt*SK2 channel expression might play in the ELL, we have used pharmacological modulation to probe pyramidal neuron responses in an *in vitro* slice preparation. The above data predicts that CMS superficial cells should not respond to drugs that modify SK channel function, while the other regions should contain both responsive and unresponsive pyramidal neurons.

# I-type pyramidal neurons lack SK channels

An interesting feature of the mRNA localization was the bimodal OD peak apparent in the CLS, LS and intermediate CMS segments. The number of positively stained neurons was approximately half of the pyramidal cell density assessed from Nissl and Golgi stains (Maler, 1979). This result suggested that *Apt*SK2 gene expression was restricted to a subclass of pyramidal neurons. Pyramidal neurons in the ELL are divided roughly equally between the E and I-types, which respond best to either increases (E-cells) or decreases (I-cells) in the amplitude of EOD distortions in the external environment (Maler, 1979;Saunders J and Bastian, 1984). E-cell types are readily identified histologically by the presence of a large basilar dendrite that receives direct excitatory input from the primary afferents. To test if SK currents were restricted to one of these cell types, we compared apamin sensitive AHPs in neurobiotin labeled E and I cells.

Intracellular recordings from pyramidal neurons in an *in vitro* slice preparation of the ELL (Mathieson and Maler, 1988;Turner et al., 1994;Berman and Maler, 1999) were

used to assess the spike responses across the ELL. Spikes were evoked though stimulation with a suprathreshold current injection. The contribution of SK channels to the AHP and firing pattern was tested by application of the channel blocker apamin (1µM) and/or the channel agonist 1-ethyl-2-benzimidazolinone (EBIO; 1mM). After recording, cells were filled with neurobiotin to allow for identification of not only pyramidal cell subtype (E or I) but also their location in relation to the pyramidal cell body layer (superficial or intermediate).

The AHP following an action potential was measured in relation to the membrane potential before spike threshold was reached. Measured at its maximum value of hyperpolarization, the AHP of identified I-cells (Fig. 3A) in all ELL segments was insensitive to either apamin (-5.7  $\pm$  0.9 mV to -6.5  $\pm$  1.0 mV; n=13; p > 0.05; paired t-test) or EBIO treatment (-7.0  $\pm$  2.1 mV to -7.6  $\pm$  3.2 mV; n=5; p > 0.05; paired t-test; Fig. 3B). Thus, the I-type pyramidal neurons, which are inhibited by stimulation of the receptive field center, are also characterized by the absence of SK channels.

# Characterization of apamin-sensitive AHPs in basilar (E-type) pyramidal neurons

The lack of apamin and EBIO sensitivity in I-type pyramidal neurons suggests that the *in situ* hybridization studies were detecting AptSK2 mRNA in E-type cells only (CLS, LS and CMS intermediate cells). Furthermore, since there was a lack of AptSK2 mRNA expression in the CMS superficial cell layer, measurements of the apamin sensitive contribution to the AHP in the E-type cells should follow the patterns of mRNA distribution shown in Figure 2 and should only be apparent in E-cells from the LS, CLS or CMS intermediate sections. This prediction was tested by analysis of the AHPs that followed current induced spike responses in neurobiotin labeled E-type pyramidal neurons (Fig. 4A) from all three segments of the ELL. The AHP, measured at its trough (1.21  $\pm$  0.73 ms after the peak of the action potential; n=16), was examined before and after the application of apamin (Fig. 4B). Since both superficial and intermediate cells of the LS and CLS showed responses to apamin, we pooled the cell data sets within these segments for analysis. Apamin reduced the AHP to 30  $\pm$  12% of pre-drug values (from 7.6  $\pm$  1.4 mV to 2.3  $\pm$  0.35 mV; n=6) of control in the LS and 60  $\pm$  9% of control (from 6.4  $\pm$  0.58 mV to 4.2  $\pm$  0.78 mV; n=8) in the CLS (Fig. 4B). Thus apamin sensitive SK

currents are present in E-type pyramidal neurons of both segments, with an apparently greater contribution to the AHP in LS neurons.

In contrast to the LS and CLS, superficial pyramidal neurons in the CMS were not labeled with the AptSK2 probe, however the adjacent intermediate E-type pyramidal cells (~10-20 µm cell to cell spacing; (Maler, 1979) were positive for AptSK2 mRNA (Fig. 2B). The absence of active SK channels in neurobiotin labeled superficial E-type neurons was confirmed when recordings revealed markedly smaller AHPs in comparison to nearby intermediate E-type cells (CMS superficial: -1.85  $\pm$  0.35; CMS intermediate: -7.6  $\pm$  1.2 mV, p<0.05; paired t-test; Fig. 4B); the AHPs of the CMS superficial E-type pyramidal cells were not reduced by apamin (112  $\pm$  7% of control; change of -0.6  $\pm$  0.45 mV; n=4). In contrast SK channels were expressed in the CMS intermediate E-type cells (Fig. 4B) with apamin reducing the average AHP to 40  $\pm$  8% (-2.0  $\pm$  0.4 mV; n=3) of control levels for labeled cells. These results confirm that SK channel activity is characteristic of intermediate, but not superficial E-type pyramidal neurons in the CMS. All changes in AHP size were significant compared to CMS superficial cells (p<0.05, 1-way ANOVA, Tukey's posthoc test).

Since all the E-type pyramidal neurons in the LS, CLS and the intermediate E-type pyramidal cells of the CMS had apamin-sensitive AHP's, we combined these populations (referred to as the SK group) for analysis of the response to the SK channel agonist EBIO. Application of EBIO lead to a significant (p < 0.01, paired t-test) increase in the size of the AHP for the SK group to  $137 \pm 42\%$  of control (-6.4  $\pm$  2.5 to -8.2  $\pm$  2.9 mV; n = 14; Fig. 4C), while CMS E-type superficial cells remained close to control levels at  $97 \pm 8\%$  (-2.15  $\pm$  0.7 to -2.1  $\pm$  0.45 mV; n = 4; Fig 4D). We therefore also pooled the CMS E-type superficial cells with the I-type cells (all segments) into a non-SK group, for evaluation of bursting and frequency tuning (see below), since in these populations the AHP was not affected by either apamin or EBIO (Figs. 3, 4).

Importantly, enhancement of the AptSK2 current with EBIO in the SK group also lead to a significant increase in the duration of the mAHP resulting in a residual hyperpolarization of  $2.8 \pm 2.5$  mV at a point 10 ms following the spike peak (Fig. 4C; p < 0.01, paired t-test), consistent with the finding that EBIO prolongs the open time of SK channels (Pedarzani et al., 2001). Thus the measurements of both apamin and EBIO

effects on the AHPs confirmed that *Apt*SK2 channels are differentially expressed among the pyramidal neurons in the ELL, as predicted by the mRNA localization studies. Further, the electrophysiology demonstrated that the cells that were negative for *Apt*SK2 expression in the LS and CLS were likely I-type pyramidal cells since they showed a lack of drug response similar to the *Apt*SK2 negative E-type superficial cells of the CMS (Fig. 4D).

# SK channels oppose burst firing in ELL pyramidal neurons

To understand how SK channel current might contribute to the response properties of E-type pyramidal neurons, the role of the depolarizing after potentials (DAPs) must be considered. Pyramidal neurons of the ELL respond to electrosensory inputs in two modes, single spikes or bursts of spikes (Gabbiani et al., 1996; Metzner et al., 1998;Oswald et al., 2004). Burst firing is driven by depolarizing current in the form of a DAP generated by current flowing back to the soma from actively back-propagating dendritic spikes. The dendritic origin of the DAP can be revealed by blocking dendritic sodium channels with the application of TTX to the apical dendrites, eliminating the dendritic spike (Mehaffey et al., 2006; Turner et al., 1994; Lemon and Turner, 2000). In superficial pyramidal neurons from the LS, TTX can block a potent DAP that lasts for 8-10 ms after spike initiation, a time course that overlaps the apamin sensitive AHP in these cells (Fig. 4E). While the DAP can be evident following a single action potential, as seen in the LS, it can also require the cumulative buildup of backpropagating spikes, as previously demonstrated in the CMS (Lemon and Turner, 2000). Furthermore, while the DAP is not always readily apparent, blockade of the dendritic spike always reveals a significant impact of the DAP on both the firing dynamics of the cell and on the AHP (Turner et al., 1994; Mehaffey et al., 2005). In general, the polarity and magnitude of spike afterpotentials reflect interplay between the depolarizing currents arising from dendritic spike backpropagation and the somatic hyperpolarizing currents arising from SK channels.

The temporal overlap of apamin-sensitive currents with the DAP suggested that SK channels would oppose burst generation in the ELL pyramidal cells through their ability to reduce the DAP. To test this idea, we examined the firing patterns of pyramidal

neurons expressing apamin-sensitive currents before and after SK channel modulation. We used the coefficient of variation (CV) of interspike intervals (ISI) as a simple measure of the variability of spike discharge in response to step depolarizations; we used the burst fraction as an equivalent measure when analyzing the response of these cells to noise injections (see below). A CV of  $\cong 1$  is indicative of random firing (Poisson process with exponentially distributed ISIs, (Softky and Koch, 1993; Bair et al., 1994; Shadlen and Newsome, 1998), while a CV>>1 is typically associated with burst discharge (Wilbur and Rinzel, 1983), allowing this measure to serve as a sensitive burst indicator. A representative E-type pyramidal neuron from the CLS responded to a step depolarization by initially firing in an irregular manner (0.3nA; Fig. 5A). Application of EBIO regularized the discharge pattern while apamin produced burst-type discharge. The entire SK group of neurons had CVs near 1 (0.95  $\pm$  0.38; n=25) suggesting that their discharge is random (Poisson process). Similar to the effect on the cell in Figure 5A, application of the SK agonist EBIO decreased the CV from 1.1  $\pm$  0.6 to 0.4  $\pm$  0.4 (p < 0.01; paired ttest, n = 11), which represents a regularization of the control Poisson-like firing pattern. The ISI histogram for the cell in Figure 5 revealed a dramatic shift to higher ISI values in response to EBIO, completely eliminating the shorter ISIs present in the original firing pattern (Fig. 5B). In the SK channel group EBIO increased the mean ISI from  $22.8 \pm 8.2$ ms to  $51.7 \pm 36.8$  ms (n=11; p < 0.02; paired t-test). In contrast, apamin (1  $\mu$ M) led to an increase in CV values from  $0.96 \pm 0.12$  to  $1.77 \pm 0.22$  (p < 0.05; paired t-test, n = 14), representing a conversion to burst firing. This was accompanied by a conversion of the ISIH to a bimodal distribution (Fig. 5B) and a decrease in the ISIs of its first peak from  $15 \pm 1.6$  ms (control) to  $7.6 \pm 0.78$  ms (the intraburst peak; p < 0.05 N=14). The conversion of pyramidal cells from a tonic to bursting mode was also demonstrated when the ISI values were plotted as a joint interval return map (Fig 5C). A random distribution of points is indicative of non-bursting units, while a tightly clustered group at short intervals combined with points along the X and Y axes stretching out to longer intervals has been previously demonstrated to represent burst firing (Turner et al., 1996). The baseline ISI values were associated with a randomly distributed return map. Following EBIO the ISI values were clustered at higher values, which was converted to a burst pattern following apamin (Fig 5C). We conclude that the AptSK2 mediated mAHP, by

reducing the DAP that drives burst firing, can inhibit burst responses in the SK positive ELL pyramidal cells.

# SK channels promote high frequency tuning of ELL pyramidal neurons

The ability for SK channels to oppose burst firing in some classes of pyramidal neurons prompted us to examine the potential for SK currents to modulate frequency responses in this system. A previous study has suggested that ELL pyramidal cells can respond to afferent input in a frequency-dependent manner: spike bursts code preferentially for low frequency signals and isolated spikes code over a broad frequency range (Oswald et al., 2004). The finding that SK channels oppose burst firing by counteracting the DAP raised the question: do SK channels, through their ability to reduce burst firing, have an effect on the frequency tuning of pyramidal cells? In order to address this question, cells were stimulated with random amplitude modulated (RAMs, 0-60 Hz Gaussian noise) current injections (Oswald et al., 2004). These stimulations are within the frequency range, and representative of, sensory input that the fish encounters during electrolocation and electrocommunication. As well, in vivo intracellular recordings (Chacron et al., 2003; Middleton et al., 2006) have demonstrated that a pyramidal cell's membrane potential can faithfully track synaptically transmitted sensory input within this frequency range. The current injections that we utilized are therefore a reasonable mimic of natural signals.

In order to quantify the frequency response a coherence ratio (ratio of the area under the coherence curve between 30-50 Hz to that under 0-20 Hz) was calculated. Labelled E-cells (see Fig. 4A) were identified in terms of their segment (CMS, CLS, LS) and position within the pyramidal cell layer (superficial or intermediate). All cells from the LS (n = 3) and CLS (n = 7) along with CMS intermediate cells (n = 4) were broadband to high-pass with a mean coherence ratio of  $1.27 \pm 0.2$  (Fig. 6A-broadband cell; n = 14). These cell types were all SK channel positive based on their responses to apamin and EBIO. In contrast, labeled I-cells (Fig. 3A, all segments) had coherence ratios of  $0.68 \pm 0.02$  (Fig. 6B; n = 13) with an upper limit to the 95% confidence interval of 0.86. While the broadband/high pass cells of the SK group do not fall within this range, the superficial E-cells in the CMS do  $(0.79 \pm 0.02;$  Fig. 6C; n=3). We use this

value to define low-pass cells (coherence ratios < 0.85); cells above this value are classified as broadband to high pass. We conclude that the frequency response characteristics of ELL pyramidal neurons can be grouped into two classes, with the I-type and CMS superficial E-type cells in the low pass non-SK group, while the E-types in the LS, CLS and intermediate CMS in the broadband-high pass SK group.

These differences allowed cells to subsequently be identified based on their frequency tuning alone (e.g. without neurobiotin labeling). We grouped cells into a functional SK group (presumptive E cells in CLS, LS and intermediate E cells in CMS) when their coherence ratios were > 0.85; when the ratio was <0.85 the cells were classified as belonging to the non-SK group presumptive superficial E cells in CMS and all I cells.

When analyzing the effects of RAM stimulation we used the burst fraction (ratio of burst spikes to all spikes) as a measure of changes in bursting, since the CV is as strongly influenced by the noise input as by the neuron's intrinsic dynamics. Bursts are defined as events with ISIs < 8 ms (corresponding to the first peak of the ISI histogram in Fig 5B) and are counted as single events based on the first spike in the group. The non-SK group had a coherence ratio of  $0.69 \pm 0.025$  and a burst fraction of  $19 \pm 1.7\%$  (n=13). In contrast the SK group (made up of a combination of high-pass and broadband cells) had an average coherence ratio of  $1.31 \pm 0.21$  and a significantly lower burst fraction of  $9.2 \pm 1.2\%$  (n=15, p<0.05; paired t-test). The difference in coherence of the non-SK (low pass) and SK (broadband/high pass) groups can therefore be associated with increased bursting within the non-SK group as measured from both the RAM (burst fraction) and step current injection (CV, see above).

When apamin was applied to the non-SK (low pass) group there was no significant change in the burst fraction (112  $\pm$  8% of control; 0.192  $\pm$  0.04 to 0.228  $\pm$  0.02, p > 0.05; paired t-test, n = 13) or coherence ratio (Fig. 6B,C, 0.690  $\pm$  0.025 to 0.677  $\pm$  0.024, p > 0.05; paired t-test, n = 13). However, when apamin was applied to the SK group (broadband/high-pass), the burst fraction increased to 210  $\pm$  30% of control values (0.127  $\pm$  0.025 to 0.206  $\pm$  0.015; p < 0.05; paired t-test, n = 13) and the coherence ratio was decreased from 1.31  $\pm$  0.21 to 0.89  $\pm$  0.05 (Fig. 6A, p < 0.05; paired t-test, n = 15), demonstrating that the cells were bursting more and responding better to low frequencies

when SK channels are blocked. This change was not due to a decreased response to high frequencies, but rather an increase in the response to low frequencies (Fig. 6A).

It was previously shown that ELL pyramidal cell bursts are good detectors of low frequency signals (Oswald et al., 2004). In order to evaluate whether the apamin induced increase in bursting (SK group) was responsible for the improvement in response to low frequency input, we first separated the spike train into bursts and isolated spikes (Fig. 6D,E; broadband cell from Fig. 6A). We then computed coherence estimates for both bursts and isolated spikes as previously described (Oswald et al., 2004). The increase in burst fraction was associated with an increase in the mean burst coherence of the low-frequency component of the input (0-20 Hz) to  $175 \pm 7\%$  of control (p < 0.05; paired t-test, n = 14, Fig. 6F). The isolated spike coherence remained unchanged (Fig. 6G) and isolated spikes coded equally well for all frequencies. We conclude that an SK generated mAHP contributes to frequency tuning in LS and CMS cells by reducing the magnitude of the DAP; this in turn increases the burst threshold and subsequently decreases the pyramidal cell's response to low frequency input. Conversely, the lack of SK currents in the superficial cells of the CMS and in all I-type cells permits them to generate burst responses and respond well to low frequency input.

# Discussion

Sensory systems are tuned to the natural environmental and communication signal's that have shaped their evolution. In senses such as audition and vision a key feature of such signals is their frequency. Tuning to the frequency content of tones is a fundamental aspect of auditory physiology. Visual cortex neurons are tuned to both temporal and spatial frequencies and, as a consequence, to stimulus velocity (Priebe et al., 2006). Models of frequency tuning in the CNS generally invoke network and synaptic dynamics to account for frequency tuning (Krukowski and Miller, 2001). However, the potential contribution of single cell dynamics as determined by ionic conductances, such as Ca2+ activated K+ channels, has not been investigated in as much detail (Stocker and Pedarzani, 2000). The electrosensory system of A. leptorhynchus is adapted to detect AMs arising from communication signals and the motion of prey. This requires tuning to AM frequencies ranging from ~1 to 300 Hz (Nelson and Maciver, 1999;Benda and Herz, 2003) and spatial frequencies of 0.2 to 2 cycles/cm (Nelson and Maciver, 1999). We have demonstrated that SK channels are required for high frequency tuning of ELL pyramidal neurons. We show that SK channels oppose burst firing in a subset of these neurons, resulting in a selective reduction in low frequency tuning. This allows for control of the relative sensitivity of ELL pyramidal cells to the low (prey detection) and high (electrocommunication) frequency signals.

SK channels are expressed in the mammalian CNS and mediate a Ca<sup>2+</sup>-dependent mAHP that becomes activated within 1-5 ms and can persist for up to 200 ms (Xia et al., 1998). Their activity has been reported to affect numerous apparently unrelated neuronal processes, which may reflect differences in the Ca<sup>2+</sup> source or may be the result of the concurrent activity of other voltage and/or ligand gated channels (Marder and Goaillard, 2006). We have cloned the SK2 channel from *A. leptorhynchus* and demonstrated evolutionary conservation with respect to the amino acid sequences involved in K<sup>+</sup> ion selectivity, calmodulin binding and apamin sensitivity. The distribution of *Apt*SK2 mRNA in pyramidal neurons of the ELL was polarized, with high levels expressed in pyramidal neurons that detect high frequency communication signals (LS, CLS E-type cells) in comparison to the low levels expressed in the cell types specialized for low frequencies (CMS superficial E-type cells and I-type cells in all segments). *In vivo* I-

cells, which do not express SK channels, are also tuned to lower frequencies than E-type cells (CLS, LS; Chacron et al., 2005). This strengthens the notion that the cellular properties found *in vitro* contribute to the functional properties of the intact circuitry *in vivo*. In particular our results suggest that frequency tuning of pyramidal cells might be controlled in part by *Apt*SK2 channels.

An analysis of the properties of the spike induced AHPs confirmed the differential expression of AptSK2 channels indicated by the localization of its mRNA. An apamin and EBIO-sensitive mAHP was detected in the pyramidal neurons that express the AptSK2 mRNA. In contrast, all I-type and CMS superficial E-type pyramidal neurons failed to respond to SK channel modulation. Thus, the differential expression of AptSK2 mRNA results in a non-uniform distribution of functional SK channels in pyramidal neurons of the ELL.

The functional significance of these differences in SK channel expression became evident when the frequency response properties of these neurons were analyzed. Neurons were stimulated with RAM current injections, and the frequency dependence of their spike responses was analyzed. The results showed that AptSK2 positive pyramidal cells were responsive to a broad range of frequencies (0-60 Hz), while AptSK2 negative cells were more responsive to low frequencies. Furthermore, in AptSK2 positive neurons, the cell's response to low frequencies could be increased following apamin application, while the response to high frequencies was not affected. Thus, SK channels are required to limit the low frequency response in these cells and the absence of SK channel activity biases their response to low frequencies.

The ability of SK channels to reduce the low frequency response is accomplished through their action of opposing burst firing in these cells. We have previously demonstrated that bursts are caused by DAPs that arise from actively backpropagating spikes in ELL pyramidal cell apical dendrites (Turner et al., 1994;Lemon and Turner, 2000;Fernandez et al., 2005) and that bursts are selectively tuned for low frequency stimuli (Oswald et al., 2004;Oswald et al., 2007;Doiron et al., 2007). We have now shown that the SK mediated mAHP temporally overlaps and opposes the DAP, reducing burst firing. In this way, SK channels selectively decrease the low frequency response by increasing the threshold for burst firing. As predicted, apamin treatment had no effect on

the AHPs or frequency tuning of SK2-negative pyramidal cells of the CMS or I-type cells. Consistent with this mechanism, measurement of the burst fractions of pyramidal cells demonstrated a negative correlation with SK2 expression and apamin sensitivity. Apamin sensitive cells showed a significantly lower burst fraction (9.2  $\pm$  2%) than apamin insensitive cells (19  $\pm$  1.7 %, p < 0.05; paired t-test). These results demonstrate that the differential expression of SK channels plays an important role in determining the frequency selectivity of ELL pyramidal neurons.

It is likely that there are numerous network and biophysical mechanisms that regulate the relative size of the DAP and mAHP, allowing them to control bursting and thus low frequency tuning. At the network level it has already been established in vivo that frequency tuning is controlled by feedback input to ELL pyramidal cells (Chacron et al., 2005). Further support for this comes from in vitro studies showing that the DAP amplitude and bursting can be regulated by these feedback pathways (Mehaffey et al., 2005). The necessity for cell intrinsic regulation of bursting is suggested by the greater prominence of the DAP in LS (see Fig. 4A). Thus in order to prevent bursting in the LS a large opposing SK current would be required, as is seen in Figure 4B. An additional player in the balancing act between the mAHP and DAP are persistent Na+ currents (I<sub>NaP</sub>), which have previously been implicated in the production of DAPs and control of bursting (Azouz et al., 1996; Yue et al., 2005). I<sub>NaP</sub> is prominent in ELL pyramidal cells (Doiron et al., 2003; Turner et al., 1994; Berman et al., 2001). Therefore, as recently discussed (Marder and Goaillard, 2006; Izhikevich, 2006), the function of SK channels cannot be predicted from their dynamics alone. Rather, in this case, information transmission by ELL pyramidal cells likely depends on the complex dynamical interactions of at least SK channels, DAPs generated by dendritic Na<sup>+</sup> channels, somatic persistent Na<sup>+</sup> channels and feedback from synaptic input.

The regulation of bursting through the interplay of the mAHP and DAP is not unique to the ELL. It has previously been shown that apamin blockade of a mAHP can lead to bursting through an unmasking of a DAP (Ping and Shepard, 1999). In mammalian neurons the DAP has been attributed to a number of active ionic currents, that may include backpropagation of dendritic spikes (Nishimura et al., 2001). The regulation of DAP amplitude by an SK current may therefore be a common mechanism

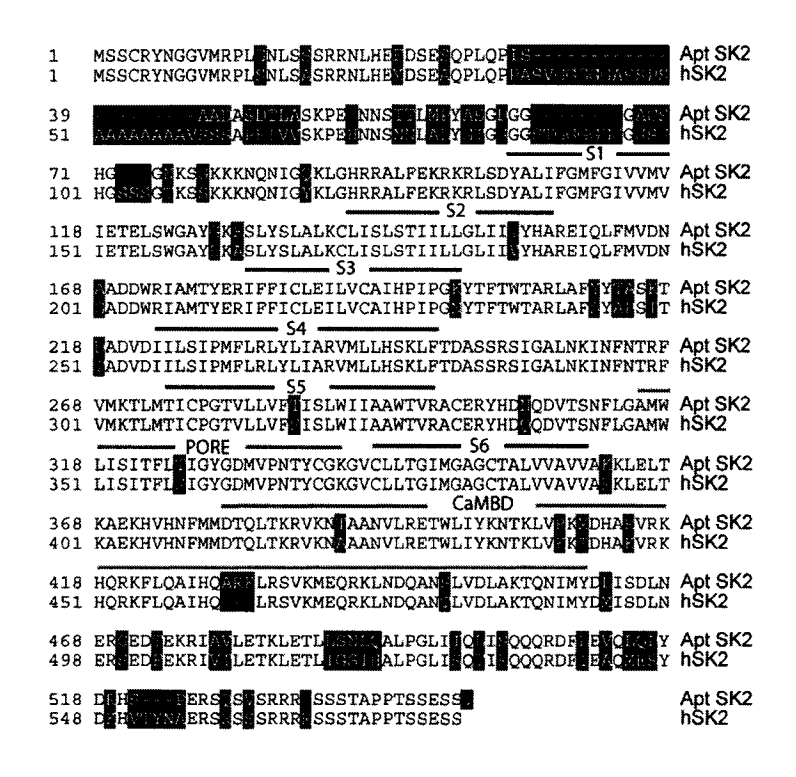
through which neurons can regulate bursting. Burst regulation in these neurons has not, however, been linked to specific neural computations such as frequency tuning. Here we have shown that control of bursting plays a specific role in the higher order processing abilities of a neuron, and possibly an animal's subsequent response to specific sets of environmental stimuli (prey).

In ELL pyramidal cells bursts are believed to function as feature detectors for low frequency/jamming stimuli (Gabbiani et al., 1996). Previous in vivo work (Shumway, 1989; Chacron et al., 2005; Metzner and Juranek, 1997) along with our results suggest that CMS pyramidal cells (E and I) will be tuned to the low frequencies induced by these signals while the LS (E cells) will be tuned to high frequency communication signals. However, LS pyramidal cells are also the most sensitive to weak signals (Shumway, 1989) which suggests that they are essential in detecting distant prey (Nelson and Maciver, 1999). The velocity (V), spatial (SF) and temporal (TF) frequencies associated with prey capture are simply related:  $TF(cycles/s) = SF(cycles/cm) \times V(cm/s)$ . Therefore a reduction in the fish's speed from >20 to <1 cm/s during prey acquisition will result in a concomitant reduction in the temporal frequencies produced by prey (down to ~1 Hz; Nelson and Maciver, 1999). Electroreceptors are not very sensitive to such low frequencies (Chacron et al., 2005). We therefore hypothesize that, when the fish engages in low speed scanning, enhancing the detection of the weak low frequency signals could occur through the inhibition of SK channels, which would cause an up-regulation of burst firing. This could be accomplished through a number of second messenger systems (Nicoll, 1988; Ren et al., 2006; Grunnet et al., 2004). Preliminary results suggest that serotonergic (5-HT) and cholinergic (Maler et al., 1981; Phan and Maler, 1983) input to the ELL can regulate bursting (Ellis, unpublished observations), although direct links to SK channels have not yet been established.

The fact that cortical pyramidal cells strongly express SK2 channels (Stocker and Pedarzani, 2000; Sailer et al., 2002; Villalobos et al., 2004) and that at least a subset of these are bursty, suggests that similar mechanisms to those described here may be operative in the control of velocity tuning of pyramidal cells in visual cortex (Priebe et al., 2006). Direct evidence with regard to SK channel control of frequency tuning is currently lacking for mammalian neurons expressing SK channels (including cortical

pyramidal cells). The work presented here strongly suggests that the differential expression of SK channels may help to regulate frequency-dependent higher order sensory processing and, more generally, information processing via spike bursts.





B.

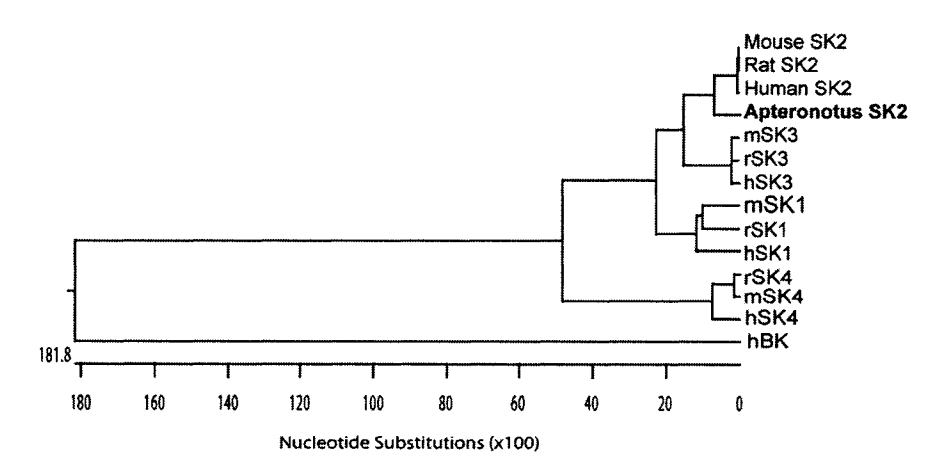


Figure 1. Sequence evaluation of SK2. (A) Alignment of the amino acid sequences from the cloned SK2 channel from *Apteronotus* (*Apt*) with the human channel (hSK2). Sequence variations are highlighted. The six predicted transmembrane segments (S1-S6) are indicated (black lines) along with the channel pore and predicted calmodulin-binding domain (CaMBD; grey lines). (B) Phylogenic comparison of the *Apt*SK2 channel with the human (h), rat (r), mouse (m) SK channels and the human BK channel shows that the *Apt*SK2 channel is homologous to the previously cloned mammalian channels. Analysis was with the Clustal W method within the Lasergene software package.

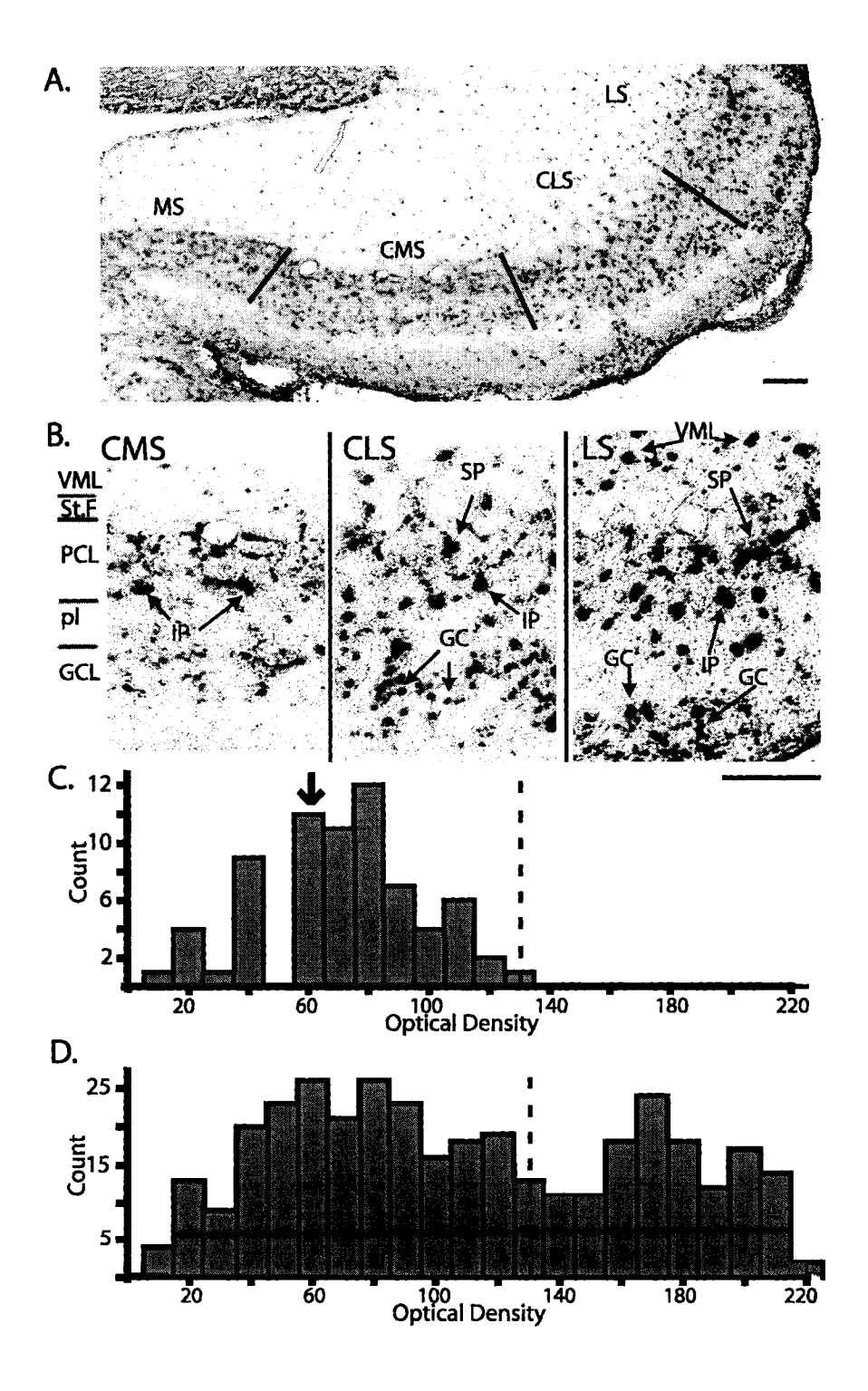
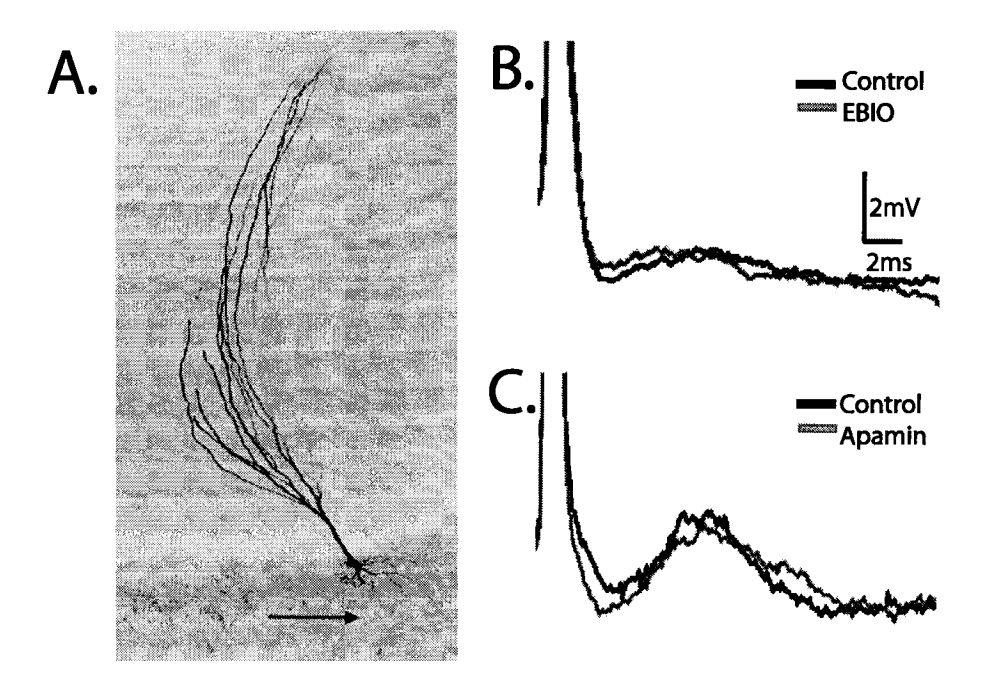


Figure 2. Compartmental expression pattern of AptSK2 in the ELL. (A) In situ hybridization analysis of AptSK2 in the ELL. Lines indicate segment divisions of the sensory maps in the ELL. The highest expression is found in the lateral segment (LS), with a lower level found in the centrolateral (CLS) and centromedial segments (CMS). Undetectable levels are found in the medial segment (MS). (B) Magnified view of the segmental localization pattern. Superficial (SP) and intermediate (IP) pyramidal neurons are strongly labeled in the LS and CLS along with ventral molecular layer (VML) interneurons and granule cells (GC). In the CMS only intermediate pyramidal neurons display strong SK2 expression. Scale bars: 100μm. (C) Optical density histogram of cells from the superficial layer of the CMS showing a single peak. Bin width was 10 OD units. Arrow points to the location of the mean OD of the sense controls; the distribution of sense controls OD values overlaps that of the CMS superficial cells. (D) Bimodal optical density histogram from cells in the LS, CLS and intermediated CMS segments. Dotted lines represent the separation of low and high OD levels for the bimodal histogram in D; note that this value corresponds to the maximum value of the histogram in C.



**Figure 3.** I-cells do not respond to SK channel modulation. (A) Neurobiotin labeled I-cell showing the lack of a basilar dendrite (arrow). (B, C) Superimposed spike averages from single I-cells showing no change in the AHP following either EBIO (B) or apamin (C) application.

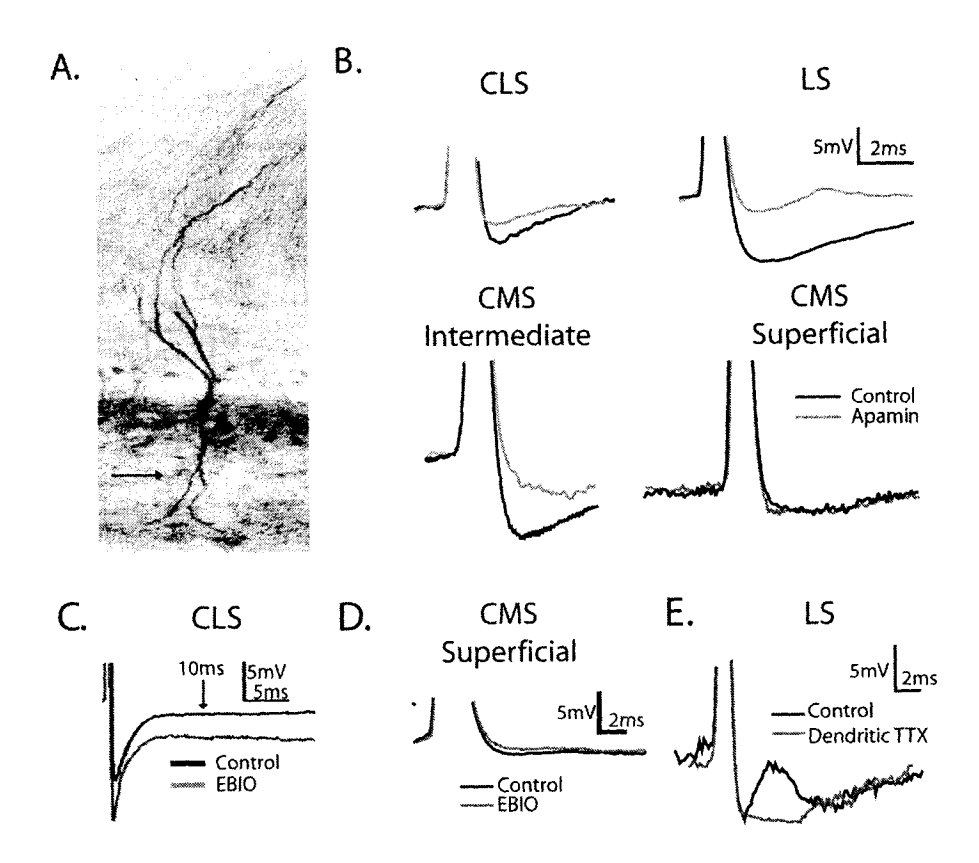


Figure 4. E-cell responses to apamin match the *Apt*SK2 distribution patterning. (A) An E-cell labeled with neurobiotin showing the presence of a basilar dendrite (arrow). (B) Single cell AHP averages generated via intracellular current injection (0.1 nA) superimposed before and after drug treatment. Neurons in the LS, CLS along with CMS intermediate cells respond to apamin (grey) with a decrease in the size of the AHP. CMS superficial cells do not show a response to apamin. (C) A representative CLS cell showing an increased and persistent AHP following EBIO. (D) A CMS superficial cell showing no response to EBIO. (E) Elimination of the DAP following TTX application to the apical dendrites reveals that the time course of the DAP overlaps that of the apamin sensitive AHP.

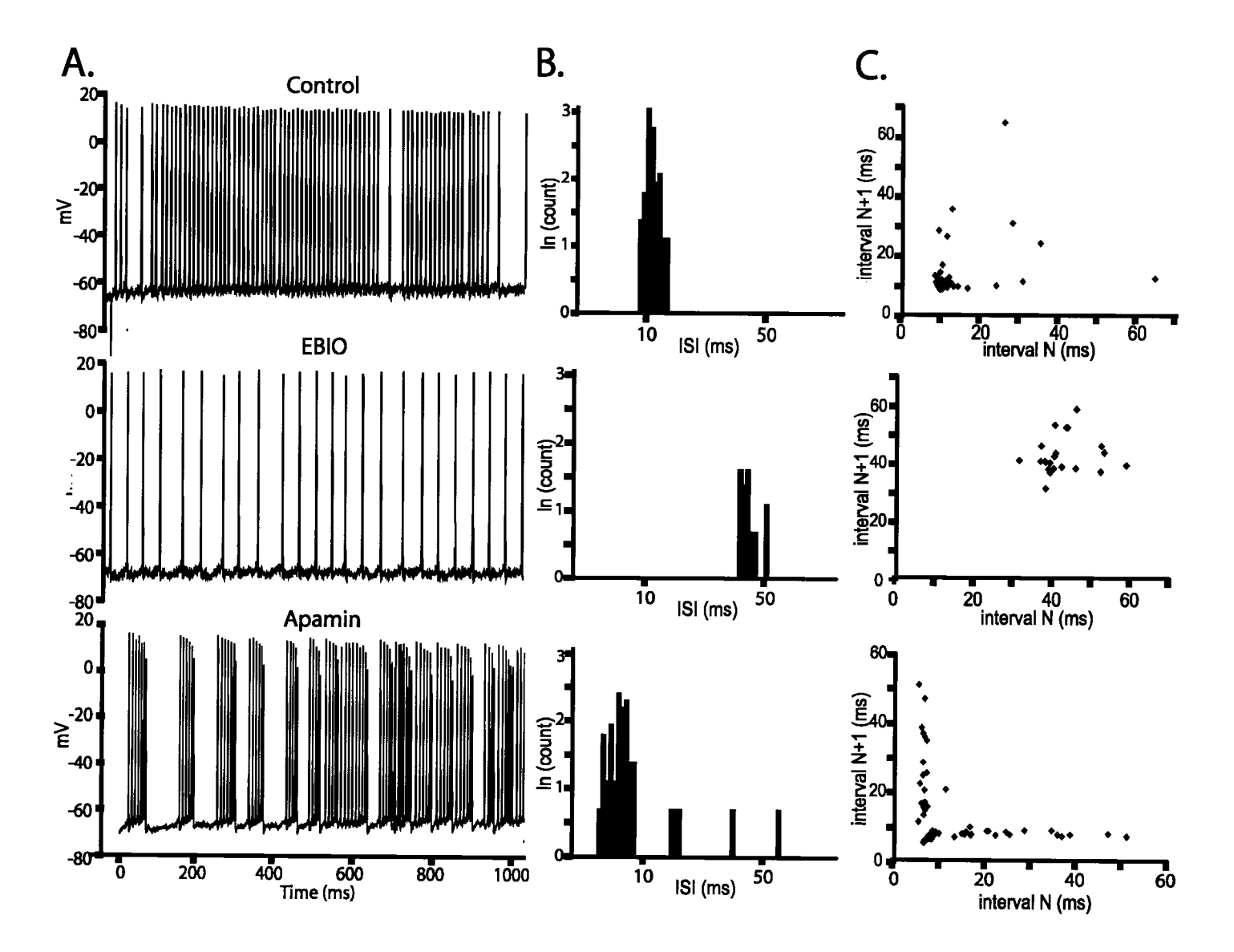


Figure 5. SK channels control the firing mode of a CLS cell. (A) Representative traces from a CLS E-cell (0.3nA current injection) showing a regularization of the firing pattern following EBIO (1mM) and the subsequent conversion to a burst-firing mode following application of apamin (1 $\mu$ M). (B) Plotting the natural logarithm of the interspike intervals (ISI) representing the traces in (A) shows a shift of the ISI distribution to longer intervals in response to EBIO along with a decrease in the spike count. The ISI distribution is shifted to shorter intervals and becomes clearly bi-modal following apamin. The first peak of the apamin ISIH contains the burst spikes. (C) Joint interval return maps showing randomly distributed points under baseline conditions confirm a non-bursting firing mode; the shortest ISIs are typically >10 ms. EBIO leads to an increase in ISI values and a regularization that is demonstrated by the presence of a single cluster of long ISIs. Apamin leads to a separation of the return map into a burst cluster (ISIs <10 ms) and broadly distributed longer ISI returns representing variable inter-burst intervals as previously shown (Turner et al., 1996).

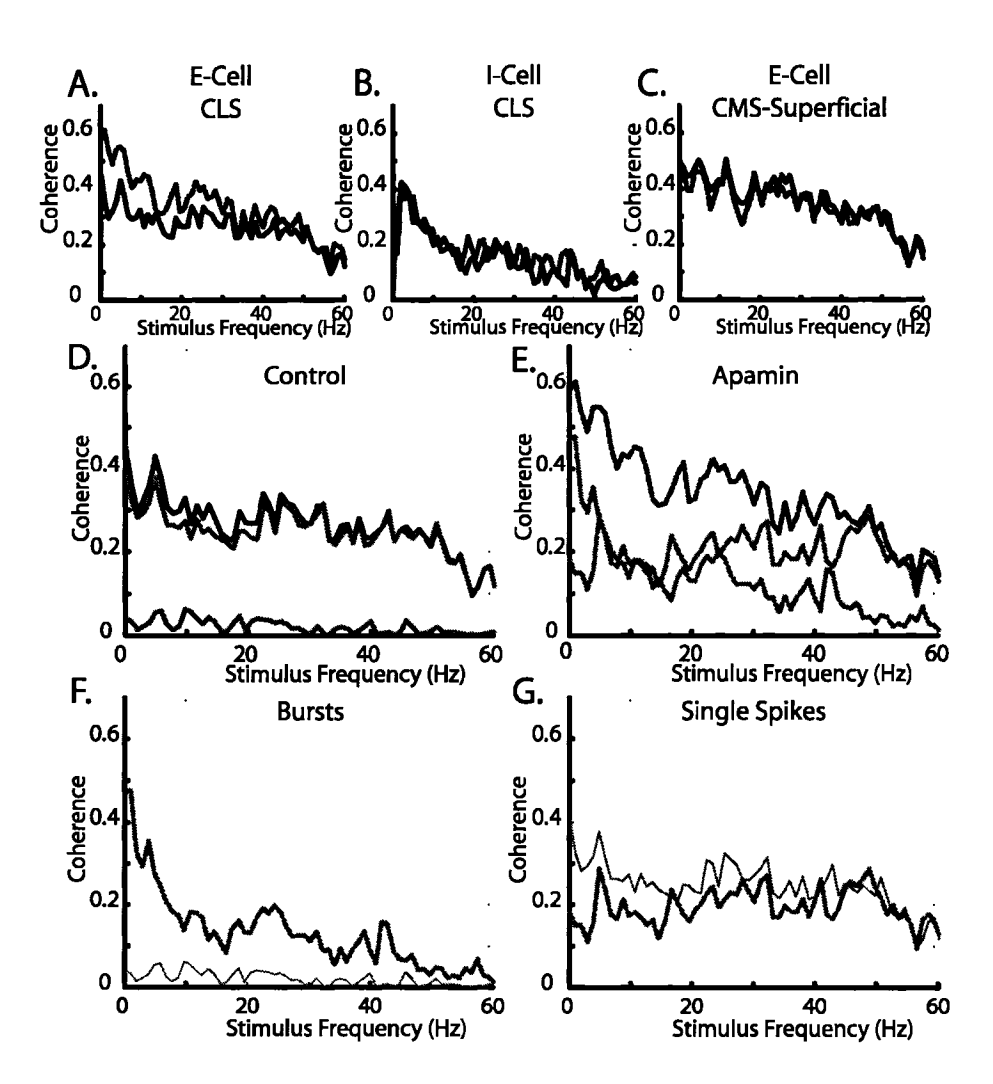


Figure 6. Increased response to low frequency stimuli follow SK channel block. Neurons were given a random amplitude modulation (RAM) current injection of 0-60 Hz Gaussian noise representative of naturalistic stimuli. (A) Coherence plot of a representative broadband CLS cell showing an increased response to low frequencies following apamin (blue). (B,C). Neither I-cells (B) nor CMS superficial cells (C) show frequency-response changes to the RAM following application of apamin (1uM; blue). (D+E) Separation of the coherence response of the CLS cell from A under control conditions (D; black;) and apamin (E; blue) into components attributable to single spikes (red) or bursts (green). (F) Overlay of burst component from D (thin trace) and E (thick trace) showing an increased burst response to low frequencies. (G) Overlay of the isolated spike component from D (thin trace) and E (thick trace) showing only minor response changes.

#### References

Andermann ML, Ritt J, Neimark MA, Moore CI (2004) Neural correlates of vibrissa resonance; band-pass and somatotopic representation of high-frequency stimuli. Neuron 42: 451-463.

Azouz R, Jensen MS, Yaari Y (1996) Ionic basis of spike after-depolarization and burst generation in adult rat hippocampal CA1 pyramidal cells. J Physiol 492 ( Pt 1): 211-223.

Bair W, Koch C, Newsome W, Britten K (1994) Power spectrum analysis of bursting cells in area MT in the behaving monkey. J Neurosci 14: 2870-2892.

Bastian J, Chacron MJ, Maler L (2002) Receptive field organization determines pyramidal cell stimulus-encoding capability and spatial stimulus selectivity. J Neurosci 22: 4577-4590.

Bastian J, Chacron MJ, Maler L (2004) Plastic and nonplastic pyramidal cells perform unique roles in a network capable of adaptive redundancy reduction. Neuron 41: 767-779.

Bastian J, Courtright J (1991) Morphological correlates of pyramidal cell adaptation rate in the electrosensory lateral line lobe of weakly electric fish. J Comp Physiol [A] 168: 393-407.

Behnisch T, Reymann KG (1998) Inhibition of apamin-sensitive calcium dependent potassium channels facilitate the induction of long-term potentiation in the CA1 region of rat hippocampus in vitro. Neurosci Lett 253: 91-94.

Bell and Maler (2005) Central neuroanatomy of electrosensory systems in fish. In: Springer Handbook of Auditory Research: Electroreception (Bullock TH, Hopkins C.D., Popper A.N., Fay R.R., eds), pp 68-111. New York.: Springer.

Benda J, Herz AV (2003) A universal model for spike-frequency adaptation. Neural Comput 15: 2523-2564.

Berman N, Dunn RJ, Maler L (2001) Function of NMDA receptors and persistent sodium channels in a feedback pathway of the electrosensory system. J Neurophysiol 86: 1612-1621.

Berman NJ, Hincke MT, Maler L (1995) Inositol 1,4,5-trisphosphate receptor localization in the brain of a weakly electric fish (Apteronotus leptorhynchus) with emphasis on the electrosensory system. J Comp Neurol 361: 512-524

Berman NJ, Maler L (1999) Neural architecture of the electrosensory lateral line lobe: adaptations for coincidence detection, a sensory searchlight and frequency-dependent adaptive filtering. J Exp Biol 202: 1243-1253.

Bottai D, Dunn RJ, Ellis W, Maler L (1997) N-methyl-D-aspartate receptor 1 mRNA distribution in the central nervous system of the weakly electric fish Apteronotus leptorhynchus. J Comp Neurol 389: 65-80.

Carr CE, Maler L, Taylor B (1986) A time-comparison circuit in the electric fish midbrain. II. Functional morphology. J Neurosci 6: 1372-1383.

Chacron MJ, Doiron B, Maler L, Longtin A, Bastian J (2003) Non-classical receptive field mediates switch in a sensory neuron's frequency tuning. Nature 423: 77-81.

Chacron MJ, Maler L, Bastian J (2005) Feedback and feedforward control of frequency tuning to naturalistic stimuli. J Neurosci 25: 5521-5532.

Cloues RK, Sather WA (2003) Afterhyperpolarization regulates firing rate in neurons of the suprachiasmatic nucleus. J Neurosci 23: 1593-1604.

Doiron B, Oswald AM, Maler L (2007) Interval Coding II: Dendrite Dependent Mechanisms. J Neurophysiol.

Doiron B, Noonan L, Lemon N, Turner RW (2003) Persistent Na+ current modifies burst discharge by regulating conditional backpropagation of dendritic spikes. J Neurophysiol 89: 324-337.

Elhilali M, Fritz JB, Klein DJ, Simon JZ, Shamma SA (2004) Dynamics of precise spike timing in primary auditory cortex. J Neurosci 24: 1159-1172.

Faber ES, Delaney AJ, Sah P (2005) SK channels regulate excitatory synaptic transmission and plasticity in the lateral amygdala. Nat Neurosci 8: 635-641.

Fernandez FR, Mehaffey WH, Turner RW (2005) Dendritic Na+ current inactivation can increase cell excitability by delaying a somatic depolarizing afterpotential. J Neurophysiol 94: 3836-3848.

Gabbiani F, Metzner W, Wessel R, Koch C (1996) From stimulus encoding to feature extraction in weakly electric fish. Nature 384: 564-567.

Grunnet M, Jespersen T, Perrier JF (2004) 5-HT1A receptors modulate small-conductance Ca2+-activated K+ channels. J Neurosci Res 78: 845-854.

Heiligenberg W, Dye J (1982) Labelling of electroreceptive afferents in a gymnotoid fish by intracellular injection of HRP: The mystery of multiple maps. J Comp Physiol [A] 148: 287-296.

Hudspeth AJ (2000) Hearing. In: Principles of Neural Science (Kandel ER, Shwartz JH, Jessell TM, eds), McGraw-Hill.

Ishii TM, Maylie J, Adelman JP (1997) Determinants of apamin and d-tubocurarine block in SK potassium channels. J Biol Chem 272: 23195-23200.

Izhikevich EM (2006) Dynamic Systems in Neuroscience: The Geometry of Excitability and Bursting. MIT Press.

Kohler M, Hirschberg B, Bond CT, Kinzie JM, Marrion NV, Maylie J, Adelman JP (1996) Small-conductance, calcium-activated potassium channels from mammalian brain. Science 273: 1709-1714.

Kramar EA, Lin B, Lin CY, Arai AC, Gall CM, Lynch G (2004) A novel mechanism for the facilitation of theta-induced long-term potentiation by brain-derived neurotrophic factor. J Neurosci 24: 5151-5161.

Krukowski AE, Miller KD (2001) Thalamocortical NMDA conductances and intracortical inhibition can explain cortical temporal tuning. Nat Neurosci 4: 424-430.

Lancaster B, Hu H, Ramakers GM, Storm JF (2001) Interaction between synaptic excitation and slow afterhyperpolarization current in rat hippocampal pyramidal cells. J Physiol 536: 809-823.

Lee WS, Ngo-Anh TJ, Bruening-Wright A, Maylie J, Adelman JP (2003) Small conductance Ca2+-activated K+ channels and calmodulin: cell surface expression and gating. J Biol Chem 278: 25940-25946.

Lemon N, Turner RW (2000) Conditional spike backpropagation generates burst discharge in a sensory neuron. J Neurophysiol 84: 1519-1530.

Maler L (1979) The posterior lateral line lobe of certain gymnotoid fish: quantitative light microscopy. J Comp Neurol 183: 323-363.

Maler L, Collins M, Mathieson WB (1981) The distribution of acetylcholinesterase and choline acetyl transferase in the cerebellum and posterior lateral line lobe of weakly electric fish (Gymnotidae). Brain Res 226: 320-325.

Marder E, Goaillard JM (2006) Variability, compensation and homeostasis in neuron and network function. Nat Rev Neurosci 7: 563-574.

Mathieson WB, Maler L (1988) Morphological and electrophysiological properties of a novel in vitro preparation: the electrosensory lateral line lobe brain slice. J Comp Physiol [A] 163: 489-506.

Mehaffey WH, Doiron B, Maler L, Turner RW (2005) Deterministic multiplicative gain control with active dendrites. J Neurosci 25: 9968-9977.

Mehaffey WH, Fernandez FR, Rashid AJ, Dunn RJ, Turner RW (2006) Distribution and function of potassium channels in the electrosensory lateral line lobe of weakly electric apteronotid fish. J Comp Physiol A Neuroethol Sens Neural Behav Physiol 192: 637-648.

Metzner W, Juranek J (1997) A sensory brain map for each behavior? Proc Natl Acad Sci U S A 94: 14798-14803.

Metzner W, Koch C, Wessel R, Gabbiani F (1998) Feature extraction by burst-like spike patterns in multiple sensory maps. J Neurosci 18: 2283-2300.

Middleton JW, Longtin A, Benda J, Maler L (2006) The cellular basis for parallel neural transmission of a high-frequency stimulus and its low-frequency envelope. Proc Natl Acad Sci U S A 103: 14596-14601.

Nelson ME, Maciver MA (1999) Prey capture in the weakly electric fish Apteronotus albifrons: sensory acquisition strategies and electrosensory consequences. J Exp Biol 202: 1195-1203.

Ngo-Anh TJ, Bloodgood BL, Lin M, Sabatini BL, Maylie J, Adelman JP (2005) SK channels and NMDA receptors form a Ca2+-mediated feedback loop in dendritic spines. Nat Neurosci 8: 642-649.

Nicoll RA (1988) The coupling of neurotransmitter receptors to ion channels in the brain. Science 241: 545-551.

Nishimura Y, Asahi M, Saitoh K, Kitagawa H, Kumazawa Y, Itoh K, Lin M, Akamine T, Shibuya H, Asahara T, Yamamoto T (2001) Ionic mechanisms underlying burst firing of layer III sensorimotor cortical neurons of the cat: an in vitro slice study. J Neurophysiol 86: 771-781.

Oswald AM, Chacron MJ, Doiron B, Bastian J, Maler L (2004) Parallel processing of sensory input by bursts and isolated spikes. J Neurosci 24: 4351-4362.

Oswald AM, Doiron B, Maler L (2007) Interval Coding I: Burst Inter-spike Intervals as indicators of Stimulus Intensity. J Neurophysiol.

Pedarzani P, McCutcheon JE, Rogge G, Jensen BS, Christophersen P, Hougaard C, Strobaek D, Stocker M (2005) Specific enhancement of SK channel activity selectively potentiates the afterhyperpolarizing current I(AHP) and modulates the firing properties of hippocampal pyramidal neurons. J Biol Chem 280: 41404-41411.

Pedarzani P, Mosbacher J, Rivard A, Cingolani LA, Oliver D, Stocker M, Adelman JP, Fakler B (2001) Control of electrical activity in central

neurons by modulating the gating of small conductance Ca2+-activated K+ channels. J Biol Chem 276: 9762-9769.

Phan M, Maler L (1983) Distribution of muscarinic receptors in the caudal cerebellum and electrosensory lateral line lobe of gymnotiform fish. Neurosci Lett 42: 137-143.

Ping HX, Shepard PD (1999) Blockade of SK-type Ca2+-activated K+ channels uncovers a Ca2+-dependent slow afterdepolarization in nigral dopamine neurons. J Neurophysiol 81: 977-984.

Priebe NJ, Lisberger SG, Movshon JA (2006) Tuning for spatiotemporal frequency and speed in directionally selective neurons of macaque striate cortex. J Neurosci 26: 2941-2950.

Ren Y, Barnwell LF, Alexander JC, Lubin FD, Adelman JP, Pfaffinger PJ, Schrader LA, Anderson AE (2006) Regulation of surface localization of the small conductance Ca2+activated potassium channel, Sk2, through direct phosphorylation by cAMP-dependent protein kinase. J Biol Chem 281: 11769-11779.

Sailer CA, Hu H, Kaufmann WA, Trieb M, Schwarzer C, Storm JF, Knaus HG (2002) Regional differences in distribution and functional expression of small-conductance Ca2+-activated K+ channels in rat brain. J Neurosci 22: 9698-9707.

Saunders J, Bastian J (1984) The physiology and morphology of two classes of electrosensory neurons in the weakly electric fish Apteronotus Leptorhynchus. J Comp Physiol 154: 199-209.

Shadlen MN, Newsome WT (1998) The variable discharge of cortical neurons: implications for connectivity, computation, and information coding. J Neurosci 18: 3870-3896.

Shumway CA (1989) Multiple electrosensory maps in the medulla of weakly electric gymnotiform fish. I. Physiological differences. J Neurosci 9: 4388-4399.

Softky WR, Koch C (1993) The highly irregular firing of cortical cells is inconsistent with temporal integration of random EPSPs. J Neurosci 13: 334-350.

Stackman RW, Hammond RS, Linardatos E, Gerlach A, Maylie J, Adelman JP, Tzounopoulos T (2002) Small conductance Ca2+-activated K+ channels modulate synaptic plasticity and memory encoding. J Neurosci 22: 10163-10171.

Stocker M, Pedarzani P (2000) Differential distribution of three Ca(2+)-activated K(+) channel subunits, SK1, SK2, and SK3, in the adult rat central nervous system. Mol Cell Neurosci 15: 476-493.

Turner RW, Maler L (1999) Oscillatory and burst discharge in the apteronotid electrosensory lateral line lobe. J Exp Biol 202: 1255-1265.

Turner RW, Maler L, Deerinck T, Levinson SR, Ellisman MH (1994) TTX-sensitive dendritic sodium channels underlie oscillatory discharge in a vertebrate sensory neuron. J Neurosci 14: 6453-6471.

Turner RW, Plant JR, Maler L (1996) Oscillatory and burst discharge across electrosensory topographic maps. J Neurophysiol 76: 2364-2382.

Villalobos C, Shakkottai VG, Chandy KG, Michelhaugh SK, Andrade R (2004) SKCa channels mediate the medium but not the slow calcium-activated afterhyperpolarization in cortical neurons. J Neurosci 24: 3537-3542.

Wilbur WJ, Rinzel J (1983) A theoretical basis for large coefficient of variation and bimodality in neuronal interspike interval distributions. J Theor Biol 105: 345-368.

Wolfart J, Neuhoff H, Franz O, Roeper J (2001) Differential expression of the small-conductance, calcium-activated potassium channel SK3 is critical for pacemaker control in dopaminergic midbrain neurons. J Neurosci 21: 3443-3456.

Womack MD, Khodakhah K (2003) Somatic and dendritic small-conductance calcium-activated potassium channels regulate the output of cerebellar purkinje neurons. J Neurosci 23: 2600-2607.

Woolley SM, Fremouw TE, Hsu A, Theunissen FE (2005) Tuning for spectro-temporal modulations as a mechanism for auditory discrimination of natural sounds. Nat Neurosci 8: 1371-1379.

Xia XM, Fakler B, Rivard A, Wayman G, Johnson-Pais T, Keen JE, Ishii T, Hirschberg B, Bond CT, Lutsenko S, Maylie J, Adelman JP (1998) Mechanism of calcium gating in small-conductance calcium-activated potassium channels. Nature 395: 503-507.

Yue C, Remy S, Su H, Beck H, Yaari Y (2005) Proximal persistent Na+ channels drive spike afterdepolarizations and associated bursting in adult CA1 pyramidal cells. J Neurosci 25: 9704-9720.

Zakon H, Oestreich J, Tallarovic S, Triefenbach F (2002) EOD modulations of brown ghost electric fish: JARs, chirps, rises, and dips. J Physiol Paris 96: 451-458.

# **CHAPTER III**

# MUSCARINIC RECEPTORS CONTROL FREQUENCY TUNING THROUGH THE DOWNREGULATION OF AN A-TYPE POTASSIUM CURRENT

Lee D. Ellis, Rüdiger Krahe, Charles W. Bourque, Robert J. Dunn and Maurice J. Chacron

Journal of Neurophysiology, September 2007 98: 1526-37

# **CONTRIBUTIONS OF AUTHORS**

This manuscript was composed by Lee Ellis and Maurice Chacron, with editing by Rudiger Krahe and Rob Dunn. Lee Ellis created all of the figures for the manuscript.

The initial *in vivo* experiments that evaluated the effects of muscarinic acetylcholine receptor (mAChR) activation on the response properties of pyramidal neurons were a combined effort by Maurice Chacron and Rudiger Krahe. The subsequent *in vitro* experiments that linked mAChR activation to the modulation of an A-type current were designed and performed by Lee Ellis. Maurice Chacron is responsible for the creation of the mathematical model in its entirety.

#### **Abstract**

The functional role of cholinergic input in the modulation of a sensory response, specifically the frequency response of pyramidal neurons, was studied using a combination of *in vivo* and *in vitro* electrophysiology supplemented by mathematical modeling. The electrosensory system of *Apteronotus leptorhynchus* recognizes different environmental stimuli by their unique alteration of a self-generated electric field. Variations in the patterns of stimuli are primarily distinguished based their frequency. Pyramidal neurons in the electrosensory lateral line lobe (ELL) are often tuned to respond to specific input frequencies. Alterations in the tuning of the pyramidal neurons may allow *Apteronotus* to preferentially select for certain stimuli. Here we show that muscarinic receptor activation *in vivo* enhances the excitability, burst firing, and subsequently the response of pyramidal cells to naturalistic sensory input. Through a combination of *in vitro* electrophysiology and mathematical modeling, we reveal that this enhanced excitability and bursting likely results from the down-regulation of an A-type potassium current. Further, we provide an explanation of the mechanism by which these currents can mediate frequency tuning.

#### Introduction

It is well known that sensory neurons can give vastly different responses to the same sensory stimulus based on the behavioral context and there is great interest in understanding the mechanisms by which this occurs (Abbott L.F., 2005).

Cholinergic pathways can regulate information processing in several brain areas (reviewed in; Everitt and Robbins, 1997;Sarter et al., 2005) and studies have shown that cholinergic input can enhance a neuron's response to specific types sensory input (Bakin and Weinberger, 1996;Kilgard and Merzenich, 1998;Weinberger, 2003;Tang et al., 1997;Gu, 2003;Sarter et al., 2005). Cholinergic input can control a cell's firing properties in a number of different ways, possibly through the regulation of several ion channels or through the modulation of synaptic properties (review; Lucas-Meunier et al., 2003). However, direct links between the cholinergic modulation of an individual neuron and the effects that such changes would have on responses to external sensory stimuli at the systems level have been more difficult to make.

Weakly electric fish sense distortions in their self-generated electric field caused by nearby objects (Figs. 1A, 1B). Electroreceptive neurons on their skin encode these perturbations through changes in firing rate (Bastian, 1981) and this information is then relayed to the pyramidal cells within the ELL (for a review of the electrosensory system see: Turner and Maler, 1999, Fig. 1C). The electrosensory system displays many similarities with mammalian sensory systems (Berman and Maler, 1999; Krahe and Gabbiani, 2004; Sadeghi et al., 2007) and benefits from detailed neuroanatomy (Maler et al., 1991), well characterized physiology (both at the systems and single neuron level) and distinct response patterns to natural sensory input (Bastian et al., 2002; Chacron et al., 2005; Chacron, 2006; Berman and Maler, 1998a; Berman and Maler, 1998c; Berman and Maler, 1998b). Previous studies have shown that descending glutamatergic pathways could control pyramidal cell responses to sensory input (Chacron et al., 2005; Mehaffey et al., 2005). Here we focus on descending cholinergic input, which likely emanates from a unique pathway (Fig. 1C; Maler et al., 1981). We show that activation of muscarinic acetylcholine receptors can increase a neurons response to low frequency input through an increase in firing rate and burst fraction that is the result of the down-regulation of an A-type potassium current.

#### **Materials and Methods**

### In vivo electrophysiology

### **Experimental setup**

The weakly electric fish *Apteronotus leptorhynchus* was used exclusively in this study. Fish were housed in groups of 3-10 in 150 L tanks, water temperature was maintained between 26-28 °C and water resistivity varied between 2000 and 5000  $\Omega$ -cm. Experiments were performed in a 39 × 44 × 12 cm deep plexiglass aquarium with water recirculated from the animal's home tank. Animals were artificially respirated with a continuous water flow of 10 ml/min. Surgical techniques were the same as those described previously (Bastian, 1996a;Bastian, 1996b) and all procedures were in accordance with animal care and use guidelines of McGill University.

## Recording

Extracellular recordings from pyramidal neurons were made with metal-filled micropipettes (Frank and Becker, 1964). Recording sites as determined from surface landmarks and recording depth were limited to the centrolateral and lateral segments of the ELL only. Extracellular signals were recorded at 10 kHz using a CED 1401 amplifier with spike2 software (Cambridge electronic design, Cambridge, UK). Spikes were detected with custom written software in Matlab (Mathworks, Natick, MA).

### **Stimulation**

The stimulation protocol was described previously in detail (Bastian et al., 2002). Stimuli consisted of random amplitude modulations (RAM's) of the animal's own electric organ discharge (EOD) and were generated by multiplying a Gaussian band limited (0-120 Hz, 8-th order Butterworth) white noise with an EOD mimic that consisted of a train of single-cycle sinusoids with frequency slightly higher than that of the EOD and phase locked to the zero-crossings of the animal's own EOD. The resulting signal was then presented via two silver-silver-chloride electrodes located 19 cm on each side of the animal, giving rise to stimuli that were spatially diffuse (Fig. 1B). Stimulus intensities were similar to those previously used (Bastian et al., 2002;Chacron et al., 2005;Chacron, 2006) and typical contrasts used ranged between 5-20%. Each stimulus presentation

lasted 100 sec in order to obtain sufficient amounts of data. It should be noted that male fish routinely gave behavioral responses (chirps) when the noise stimulus was presented as described previously (Doiron et al., 2003a).

## Pharmacology

Previously established micropressure ejection techniques were used to focally apply drugs within the ELL dorsal molecular layer containing the apical dendritic trees of pyramidal cells (Bastian, 1993;Bastian and Nguyenkim, 2001;Bastian et al., 2004;Chacron et al., 2005;Chacron, 2006). Multibarrel pipettes were pulled to a fine tip and subsequently broken to a total tip diameter of 10 µm. One barrel was filled with a 1mM solution of carbachol, the other filled with a 1mM solution of atropine, while a third was filled with a 1 mM glutamate solution. After a recording from a well-isolated pyramidal cell was established, the pressure pipette was slowly advanced into an appropriate region of the ELL molecular layer while periodically ejecting "puffs" of glutamate (duration=100 msec, pressure=40 psi). As described previously, proximity to a recorded cell will result in short-latency excitation of that cell. After correct placement, carbachol or atropine were then delivered as a series of 10 pulses (duration=100 msec, pressure=40 psi). This treatment typically resulted in altered pyramidal cell activity lasting 2-3 minutes.

### Data analysis

Responses to random AMs were accumulated as sequences of spike times for each cell. ISI sequences were computed as the time between consecutive spikes and ISI histograms were built with a binwidth of 1 msec. We divided the counts by the total count number times the binwidth in order to obtain the ISI probability density P(I). We obtained a binary sequence X(t) from the spike train sampled a 2 kHz. X(t) and the stimulus S(t) (also sampled at 2 kHz) were then used to estimate the mutual information rate density as: I(t) = -log2[1-C(t)] (in bits/sec/Hz) (Borst and Theunissen, 1999). Here  $C(t) = |P_{rs}(t)|2/[P_{ss}(t)|P_{rr}(t)]$  is the stimulus-response coherence (Roddey et al., 2000), where  $P_{rs}$  denotes the stimulus-response cross spectrum,  $P_{ss}$  is the power spectrum of the stimulus, and  $P_{rr}$  is the power spectrum of the spike train. All spectral quantities were

estimated using multitaper estimation techniques (Jarvis and Mitra, 2001). To account for the fact that the mutual information rate density increases with firing rate (Borst and Haag, 2001), we normalized it by the mean firing rate  $f_r$  (measured in spk/sec) during stimulation:  $MI(f)=I(f)/f_r$ . MI(f) is thus measured in bits/spk/Hz. All values are reported as mean  $\pm$  standard deviation.

### In vitro electrophysiology

### **Preparation of slices**

Fish (*A. leptorhynchus*) were obtained from local importers and maintained at 26-28°C in fresh water aquaria, in accordance with protocols approved by the McGill University Animal Care Committee. All chemicals were obtained from SIGMA (St. Louis, MO) unless otherwise noted. Animals were anaesthetized in 0.05% phenoxyethanol, and ELL tissue slices of 300-400 μm thickness were prepared as previously described (Turner et al., 1994). Slices were maintained by constant perfusion of ACSF (1-2ml/min), and superfusion of humidified 95% O<sub>2</sub>, 5% CO<sub>2</sub> gas. ACSF contained, 124 mM NaCl, 3 mM KCl, 25 mM NaHCO<sub>3</sub>, 1.0 mM CaCl<sub>2</sub>, 1.5 mM MgSO<sub>4</sub> and 25 mM D-glucose, pH 7.4. HEPES-buffered ACSF for pressure ejection of pharmacological agents contained the same elements, with the following differences: 148 mM NaCl, 10 mM HEPES.

### **Recording procedures**

Glass microelectrodes were filled with 2 M KAc (pH 7.4; 90-120 MΩ resistance). Recordings were made from the somata of pyramidal neurons in the centrolateral segment and digitized using a NI PCI-6030E DAQ board (National Instruments, Austin TX). Intracellular stimuli were delivered, and data were recorded with Clampex 9.0 software (Axon Instruments). Cells were held at a voltage level just below firing threshold. Negative current injections (0.3 nA) were given every 5s to measure resistance changes during drug application. All drugs (Carbachol (1 mM), Atropine (1 mM), 4-AP (1 mM) and TEA (1 mM)) were focally ejected into the dorsal molecular layer (DML) using electrodes of 1-2 μm tip diameter and 7-15 psi pressure ejection.

Previous studies have estimated a ~10x dilution factor for ejected toxins (Turner et al., 1994). Pharmacological agents were dissolved in HEPES buffered ACSF.

### Data analysis

Data were analyzed using Clampfit 9.0 software (Axon Instruments). Baseline depolarizations were measured as the difference between 1 s membrane potential averages before drug application and after a depolarization plateau had been reached. Burst fractions were the proportion of ISI's that were <10 ms, representing a previously defined burst threshold (Oswald et al., 2004). The interspike interval histogram (ISIH) was created from the sum of ISI events (bin width=0.5 ms) from a 1s depolarization (0.3nA) for 3 cells in which carbachol was washed out. The ISIH values were normalized as a fraction of the total event number to account for the increased firing rate following carbachol. Resistance was measured as the average hyperpolarization value 40-50 ms following a negative current injection (0.3nA). Significance was evaluated using the Students t-test (p=0.05). ISI sequences were computed as the time between consecutive spikes and ISI histograms were built with a binwidth of 1 msec. We divided the counts by the total count number times the binwidth in order to obtain the ISI probability density P(I). All values are reported as mean ± standard deviation.

#### Model description

We used a previously described two-compartment model of an ELL pyramidal cell (Doiron et al., 2002;Oswald et al., 2004) that contains all the essential elements to reproduce bursting seen experimentally (Lemon and Turner, 2000;Doiron et al., 2001). The model neuron is comprised of an isopotential soma (s) and a single dendritic compartment that are joined through an axial resistance of  $1/g_c$  ( $g_c$ : coupling conductance) allowing for the electrotonic diffusion of currents from the soma to dendrite (d) and vice versa. Both compartments contain the essential spiking currents; fast inward  $Na^+$  ( $I_{Na,s}$ ,  $I_{Na,d}$ ) and outward delayed rectifying (Dr)  $K^+$  ( $I_{Dr,s}$ ,  $I_{Dr,d}$ ), and passive leak currents ( $I_{leak}$ ). The presence of spiking currents in the dendrite enables the active backpropagation of somatic action potentials required for bursting. The membrane potentials at the soma,  $V_s$ , and the dendrite,  $V_d$ , are determined using a Hodgkin–Huxley

like formalism (Koch, 1999). The original model (Doiron et al., 2002) comprised six nonlinear differential equations. This study expands on this model by incorporating an A-type  $K^+$  current,  $I_{a,d}$ , into the dendritic compartment. We note that an A-type potassium current was previously incorporated into a multicompartmental model of pyramidal neuron activity on which the reduced model used here is based(Doiron et al., 2001). The kinetics for the A-type potassium current are qualitatively similar to those used previously.  $V_s$  and  $V_d$  are described by the following equations:

$$C_{m} \frac{dV_{s}}{dt} = I_{0} + g_{Na,s} \cdot m_{\infty}^{2} \cdot (1 - n_{s}) \cdot (V_{Na} - V_{s}) + \eta_{1}(t) + g_{Dr,s} \cdot n_{s}^{2} \cdot (V_{K} - V_{S}) + \frac{g_{c}}{\kappa} \cdot (V_{d} - V_{s}) + g_{leak} \cdot (V_{l} - V_{s}) + S(t)$$

$$C_{m} \frac{dV_{d}}{dt} = g_{Na,d} \cdot m_{d}^{2} \cdot h_{d} \cdot (V_{Na} - V_{d}) + g_{a,d} \cdot m_{a,d}^{2} \cdot h_{a} \cdot (V_{K} - V_{d}) + g_{Dr,d} \cdot n_{d}^{2} \cdot p_{d} \cdot (V_{K} - V_{d}) + \frac{g_{c}}{1 - \kappa} \cdot (V_{s} - V_{d}) + g_{leak} \cdot (V_{l} - V_{d}) + \eta_{2}(t)$$

$$(2)$$

 $\eta_1(t)$  and  $\eta_2(t)$  are Ornstein-Uhlenbeck processes (Gardiner, 1985) to account for sources of intrinsic noise described by:

$$\frac{d\eta_{1,2}}{dt} = -\frac{\eta_{1,2}}{\tau_n} + \sqrt{D}\xi_{1,2}$$

where  $\xi_{1,2}(t)$  are independent Gaussian random variables with zero mean and unit standard deviation. Here S(t) is a time varying stimulus which is either low pass filtered (8<sup>th</sup> order Butterworth, 120 Hz cutoff frequency) Gaussian white noise or a sinusoid with a given frequency. The parameter g is a maximal conductance ( $g_{max}$ , mS/cm<sup>2</sup>), while m and g are activation parameters and g are inactivation parameters. Each is described by the following equation:

$$\frac{dx}{dt} = \frac{x_{\infty}(V) - x}{\tau} \tag{3}$$

where  $x_{\infty}(V)$  is the infinite conductance curve and  $\tau$  is the time constant. The infinite conductance curve is modeled as a sigmoid:

$$x_{\infty}(V) = \frac{1}{1 + e^{-(V - V_{1/2})/k}} \tag{4}$$

and the values for  $\tau$ ,  $V_{1/2}$ , and k for each current are given in table 1. Other parameter values are: the ratio of somatic to total area:  $\kappa = 0.8$ ; the reversal potentials:  $V_{Na}=40$  mV,  $V_{K}=-88.5$  mV,  $V_{leak}=-70$  mV; membrane capacitance:  $C_m=1$   $\mu F/cm^2$ ;  $g_{leak}=0.18$  mS/cm<sup>2</sup> and  $g_c=0.21$  mS/cm<sup>2</sup>; time constant of the noise:  $\tau_{\eta}=20$  msec; intensity of the noise: D=0.01 (msec)<sup>-2</sup>. The model equations were integrated using an Euler-Maruyama algorithm with a time step of 0.5  $\mu$ sec.

Table 1: Model Parameters

Current	g <sub>max</sub>	V <sub>1/2</sub>	k	τ
	(mS/cm <sup>2</sup> )	(mV)		(msec)
$I_{Na,s}(m_{\infty,s}(V_s))$	35	-50	3	N/A
$I_{Dr,s}(n_s(V_s))$	15	-50	3	0.19
$I_{Na,d}(m_{,d}(V_d)/h_d(V_d))$	4	-40/-52	5/-5	0.3/1.0
$I_{a,d}(m_a(V_d)/h_a(V_d))$	2	-69/-69	4/1	1/10
$I_{Dr,d}(n_d (V_d)/p_d(V_d))$	15	-40/-65	5/-6	0.9/3

#### Results

### Carbachol increases burst firing in vivo

We obtained extracellular recordings from ELL pyramidal neurons *in vivo*. The stimulation consisted of random amplitude modulations of the animal's own electric field that were spatially diffuse, mimicking distortions caused by conspecifics (see Fig 1B; Bastian et al., 2002;Chacron et al., 2005;Chacron, 2006). In order to look at the effects of cholinergic input onto pyramidal neurons, we used previously established pharmacological techniques (Bastian et al., 2004;Bastian, 1993;Chacron et al., 2005;Chacron, 2006) to apply carbachol, a cholinergic receptor agonist, within the ELL dorsal molecular layer (DML) where cholinergic binding sites are located (Phan and Maler, 1983). In all cases, this lead to an increased firing rate that recovered to control conditions (Fig 2; control:  $15.57 \pm 6.42$  Hz; carbachol:  $20.12 \pm 9.34$  Hz; recovery:  $13.56 \pm 6.62$  Hz). The firing rate under carbachol was significantly higher than the firing rate under control conditions (p=0.005, paired t-test, n=14). For the cells that were followed to recovery, the firing rate after receovery was not significantly different than the firing rate under control conditions (p=0.35, paired t-test, n=6).

The increased firing rate was accompanied by an increased fraction of high frequency ISIs (<10 ms; Fig. 3A). It has been shown previously that ISI's with a value below 10 ms were primarily caused by an intrinsic burst mechanism (Doiron et al., 2003b;Oswald et al., 2004). We thus computed the burst fraction (i.e. the fraction of ISIs below 10 msec) as done previously (Oswald et al., 2004; see methods). On average, carbachol application more than doubled the burst fraction with respect to values under control conditions (Fig. 3C; control:  $0.11 \pm 0.10$ ; carbachol:  $0.24 \pm 0.15$ , p=0.001, paired t-test, n=14). For the cells that were followed to recovery, the burst fraction values after recovery were not significantly different than those obtained under control conditions (Fig. 3C; recovery:  $0.07 \pm 0.08$ , p=0.82, paired t-test, n=6).

Since carbachol can activate both nicotinic and muscarinic AChR's, we applied atropine, a muscarinic acetylcholine receptor (mAChR) antagonist, to determine which receptor subtype was primarily activated. Atropine alone did not affect the firing rate (p=0.56, paired t-test, n=5) or the burst fraction (compare panels C and D of figure 3, p=0.65, paired t-test, n=5) of the pyramidal neurons. Atropine did, however, prevent the

carbachol from having an effect on the firing rate (control:  $12.96 \pm 3.35$  Hz; carbachol following atropine:  $11.58 \pm 3.58$  Hz; p=0.21, paired t-test, n=7), the interspike interval distribution (Fig 3B), or the burst fraction (Fig 3D; control:  $0.14 \pm 0.13$ ; carbachol following atropine:  $0.13 \pm 0.13$ ; p=0.72, paired t-test, n=5).

### Muscarinic receptor activation alters pyramidal cell tuning in vivo

In order to quantify the effects of mAChR activation on pyramidal neuron responses to sensory input, we used information theory (Cover and Thomas, 1991; Shannon, 1948) to compute the mutual information rate density between the sensory stimulus and the pyramidal cell's spike train in response to that stimulus (Borst and Theunissen, 1999). The mutual information rate density is normalized by the neuron's firing rate and is measured in bits/spk/Hz: thereby quantifying the information transmitted by each action potential as a function of frequency per unit time. Application of carbachol primarily increased the information rate density at low frequencies (Fig 4A). We computed  $M_{low}$ , the average mutual information rate density for the frequency range 0-20 Hz (Chacron et al., 2003; Chacron et al., 2005) to assess the cell's low frequency response and found that carbachol lead to a significant increase in  $M_{low}$  (control: 0.004  $\pm$ 0.001 bits/spk/Hz; carbachol:  $0.006 \pm 0.001$ ; p=0.009, paired t-test, n=14). There was no significant change overall in the response to high frequency stimuli (Fig. 4B) as quantified by M<sub>high</sub>, the average mutual information rate density for the frequency range 40-60 Hz (p=0.52, paired t-test, n=14). Activation of cholinergic input unto pyramidal cells can thus increase their response to low frequency sensory stimuli.

### Application of carbachol in vitro increases bursting

mAChR activation has been found to alter the firing properties of individual neurons through the modulation of a number of individual ionic conductances (Delgado-Lezama et al., 1997;Svirskis and Hounsgaard, 1998;Tai et al., 2006;Mittmann and Alzheimer, 1998;Stocker et al., 1999;Akins et al., 1990;Nakajima et al., 1986;Chen and Johnston, 2004). In order to determine if the effects of mAChR activation resulted from the regulation of one or several ion channels, we used an *in vitro* ELL slice preparation (Turner et al., 1994;Turner et al., 1996).

Intracellular sharp electrode recordings were obtained from ELL pyramidal Most of the pyramidal neurons recorded from spontaneously fired action potentials at their resting membrane potential. In order to silence cell firing, negative current injections were used to hold the membrane potential below the firing threshold (average holding potential:  $-73 \pm 6$  mV; n=13). Carbachol (1 mM) was applied to the DML and this resulted on average in a 3.8  $\pm$  1.8 mV depolarization of the membrane potential (p<0.001; paired t-test; n=20; Fig 5A), which often caused the action potential threshold to be reached. Application of atropine (1 mM) prior to carbachol prevented this depolarization (Fig 5B;  $-76.5 \pm 4.4$  mV to  $-77.2 \pm 4.2$  mV; p=0.11; paired t-test; n=4), suggesting the effect is due in large part to mAChR activation. When applied on its own atropine had no effect on the membrane properties (data not shown). Step current injections revealed an increase in firing rate following carbachol (Fig. 5C, control: 39 ± 14; carbachol:  $67 \pm 23$  Hz; p<0.001; paired t-test; n=13) as well as an increase in burst fraction (Fig 5D;  $0.26 \pm 0.29$  to  $0.39 \pm 0.26$ ; p<0.01; paired t-test; n=13). The effects of carbachol on the in vitro slice preparations were thus found to be qualitatively similar to those obtained in vivo as, in both cases, carbachol lead to increased spiking and bursting activity and its effects were prevented by atropine.

The membrane depolarization caused by carbachol application *in vitro* suggests an effect on subthreshold membrane properties, which could be mediated by regulation of one or multiple ion channels. The effects of carbachol were most likely not due to voltage gated  $Ca^{2+}$ , high-threshold  $K^+$  or  $Ca^{2+}$ -activated  $K^+$  channels, since these channels are not typically active at these potentials. In order to further characterize the changes caused by carbachol, negative current pulses (0.3 nA) were applied at regular intervals in order to measure subthreshold membrane resistance changes in response to drug application. Carbachol increased the membrane resistance on average by 37% (Fig 5E; control: 15.7  $\pm$  7.1 M $\Omega$ ; carbachol: 20.1  $\pm$  7.7 M $\Omega$ ; p<0.001; paired t-test; n=12) suggesting the downregulation of an outward current. The carbachol effect is then unlikely to be mediated by subthreshold inward currents, such as persistent sodium.

It was then hypothesized that subthreshold K<sup>+</sup> currents were responsible for the effects of carbahol. The negative current injections showed no evidence of a depolarizing rectification characteristic of H-type currents (I<sub>h</sub>) (Maccaferri et al., 1993), and previous

studies have been unable to demonstrate the presence of H-type potassium currents in pyramidal neurons. However, evidence does exist for an A-type K<sup>+</sup> current (I<sub>A</sub>) in pyramidal neurons (Mathieson and Maler, 1988;Berman and Maler, 1999), which lead us to speculate that a down-regulation of I<sub>A</sub> was responsible for the effects observed.

# Down-regulation of a 4-AP sensitive K<sup>+</sup> current by muscarinic input

In order to determine if the effects of mAChR activation were due to the downregulation of an A-type current, we made use of the potassium channel antagonist 4aminopyridine (4-AP). Previous results have shown that 4-AP can block the Kv1 and Kv4 channels linked to A-type currents (Coetzee et al., 1999) and 4-AP has already been shown to alter the firing properties of ELL pyramidal neurons (Mathieson and Maler, 1988). If mAChR activation down-regulates I<sub>A</sub> then 4-AP should result in similar changes to the subthreshold membrane kinetics as those seen following carbachol application. When 4-AP (1 mM) was applied to the DML the membrane potential was depolarized (Fig 6A;  $2.8 \pm 0.8$  mV; p<0.001; paired t-test; n=5) from a holding potential just below threshold (-73  $\pm$  2 mV). Application of 4-AP also increased the resistance, on average, by 48% (Fig 6B;  $16.9 \pm 8.9 \text{ M}\Omega$  to  $23.5 \pm 10.7 \text{ M}\Omega$ ; p=0.015; paired t-test; n=7). Neither of the changes following 4-AP were statistically different than the changes seen following carbachol (depolarization p=0.11; resistance p=0.30; t-tests). Since 4-AP can block a number of K<sup>+</sup> channels not typically associated with I<sub>A</sub>, we also used TEA to evaluate the effects of blocking these channels (Coetzee et al., 1999). TEA (1 mM) had no significant effect on the holding potential (Fig 6C; control: -74.0  $\pm$  1.2 mV; TEA: –  $74.1 \pm 1.5 \text{ mV}$ ; p= 0.36; paired t-test; n=8) or the membrane resistance (Fig 6D; control:  $19.8 \pm 8.9 \text{ M}\Omega$ ; TEA:  $19.3 \pm 9.7 \text{ M}\Omega$ ; p=0.38; paired t-test; n=7). However, when carbachol was applied following TEA, a depolarization leading to firing still occurred (2.8 ± 2.0 mV, p=0.001; paired t-test; n=7) along with an average 40 % increase in membrane resistance (control:  $17.5 \pm 7.0 \text{ M}\Omega$ ; TEA+carbachol:  $23.8 \pm 8.1 \text{ M}\Omega$ ; p=0.002; paired t-test, n=5). These effects were not statistically different than those obtained with carbachol application alone (membrane depolarization p=0.22; resistance p=0.12; t-tests). Importantly when 4-AP was applied after carbachol, it did not lead to a further depolarization or change in membrane resistance, when the membrane potential was reset

to pre-carbachol values (-73.1  $\pm$  2.5 to -72.8  $\pm$  2.6; p=0.18; 25.8  $\pm$  3.8 M $\Omega$  to 25.6  $\pm$  3.9 M $\Omega$ ; p=0.35; n=7). The similarities between the effects of carbachol and 4-AP suggests that the effects of mAChR activation by carbachol are mediated by the down-regulation of K<sup>+</sup> channels that are blocked by 4-AP and not TEA, such as those linked to I<sub>A</sub>.

In ELL pyramidal neurons, the 4-AP sensitive A-type K<sup>+</sup> current was previously shown to control the first spike latency following a step depolarization (Mathieson and Maler, 1988). The latent period is controlled by the membrane potential value preceding the depolarization as more hyperpolarized levels will remove the inactivation of I<sub>A</sub> and thereby increase first spike latency (Connor and Stevens, 1971;McCormick, 1991;Schoppa and Westbrook, 1999). Similar control of first spike latency was shown for ELL pyramidal neurons (Mathieson and Maler, 1988).

As such, we investigated whether 4-AP, TEA or carbachol had effects on first spike latency. The membrane potential was set at the same value (typically -73 mV) both before and after drug application. Carbachol and 4-AP each led to a similar reduction in first spike latency after a step depolarization (Fig 7A: Control:  $44.4 \pm 22.6$  msec; Carbachol:  $10.4 \pm 4.4$  msec; p<0.001; paired t-test; n=11; Fig 7B: Control:  $49.1 \pm 19.4$  msec; 4-AP:  $19.4 \pm 10.5$  msec; p<0.001; paired t-test; n=7). Conversely, first spike latency was not affected by TEA (Fig 7C; control:  $37.4 \pm 21.9$  ms; TEA:  $43.2 \pm 34.9$  ms; p=0.13; paired t-test; n=8), but could be reduced by a subsequent application of carbachol (Fig 7D; control:  $29.4 \pm 19.4$  ms; TEA+Carbachol:  $10.8 \pm 8.7$  ms; p=0.01; paired t-test; n=5). These results support the hypothesis that mAChR activation leads to an inactivation of I<sub>A</sub>.

#### Modeling the in vitro effects of IA

Since there is not a specific regulator of I<sub>A</sub> and, as mentioned, 4-AP is a non-specific potassium channel antagonist, it was important to determine if a down-regulation of I<sub>A</sub> is sufficient to cause the effects following carbachol application. We subsequently incorporated an A-type current into a two-compartment numerical model that was previously developed for ELL pyramidal neurons (Doiron et al., 2002;Oswald et al., 2004). We mimicked the effects of carbachol and 4-AP in the model by setting the maximum conductance of the A-type current to zero from its control value (2 mS/cm<sup>2</sup>).

This resulted in a ~5 mV depolarization of the membrane potential (holding potential =  $^{-7}$  mV) that induced spiking (Fig 8A). The membrane resistance was larger by 33% without I<sub>A</sub>, similar to the effects obtained *in vitro* with carbachol or 4-AP application (compare Fig. 8B with Fig 5E+6B). We also obtained a greater first spike latency following a step depolarization with I<sub>A</sub> present (Figs. 8C and 8D; with I<sub>A</sub>: 79.26 ± 15.64 ms; without I<sub>A</sub>: 11.34 ± 5.56 ms). Finally, the model neuron had a much greater tendency to burst without I<sub>A</sub> (Fig. 8E). This was quantified by the burst fraction (Fig. 8F), which was much greater without I<sub>A</sub> (with I<sub>A</sub>: 0.02; without I<sub>A</sub>: 0.35). Therefore, our results show that the removal of an I<sub>A</sub> current in a model pyramidal cell can account for all the effects observed with carbachol and 4-AP application *in vitro*.

In order to understand how IA affects signal transmission, we used noise current injections in the model to mimic sensory stimulation in vivo as done previously (Oswald et al., 2004). It was found that I<sub>A</sub> significantly reduced the model neuron's response to low frequency input, consistent with the *in vivo* results (Fig. 9A). In order to understand this effect, we used sinusoidal current injections of different frequencies. For 1 Hz, it was found that removal of I<sub>A</sub> had little effect on the firing rate (Figs. 9B and 9C). This can be understood as follows: During the negative portion of the sinusoid, the membrane is hyperpolarized and this will tend to de-inactivate I<sub>A</sub>, however, because of the large period (1 sec) I<sub>A</sub> will subsequently inactivate before the onset of spiking, resulting in no net effect. In contrast, removal of I<sub>A</sub> significantly increased the firing rate for a 5 Hz sinusoid (Fig. 9D). In this case, I<sub>A</sub> does not fully inactivate during the shorter depolarizing portion of the sinusoid and thus can have a significant effect on firing rate. Finally, removal of IA had little effect on the firing rate for a 40 Hz sinusoid (Fig. 9E). In this case, the short hyperpolarization is unlikely to de-inactivate the A-type channels. A plot of the model neuron's firing rate with and without IA as a function of frequency revealed an effect for frequencies contained between 1 and 40 Hz (Fig. 9F).

Our modeling results have thus shown that A-type currents can have significant effects on the tuning of neurons in the low frequency range. As such, our modeling results provide an explanation for why mAChR activation *in vivo* increased the cell's response to low frequency input only.

#### **Discussion**

We have shown that activation of muscarinic receptors can significantly alter the response of ELL pyramidal neurons to sensory input. *In vivo* application of the cholinergic agonist carbachol increased pyramidal neuron excitability, leading to an increase in spiking and bursting activity. Moreover, it was found that carbachol application onto pyramidal neurons increased the transmission of the low frequency components of an external electrosensory signal. The effects of carbachol could be prevented by the muscarinic antagonist atropine, suggesting carbachol was primarily activating muscarinic acetylcholine receptors (mAChR).

In order to understand the cellular mechanisms that mediate these altered responses, we investigated the consequences of cholinergic receptor activation in vitro. We found that carbachol application also increased pyramidal cell excitability and burst firing and that these effects were also prevented by atropine. Activation of mAChR's in vitro led to a ~4 mV membrane depolarization from a level below threshold, accompanied by an increase in the subthreshold membrane resistance. These results suggested that cholinergic receptor activation down-regulates an outward current that is active in the subthreshold regime. Since the presence of an A-type current was previously shown in ELL pyramidal neurons (Mathieson and Maler, 1988), we set out to determine if this current was being down regulated by mAChR activation. It was found that the K<sup>+</sup> channel antagonist 4-AP had effects on the subthreshold membrane kinetics similar to those of carbachol. Furthermore, carbachol could prevent the subthreshold effects of 4-AP, suggesting that mAChR activation down-regulates 4-AP sensitive channels. Since 4-AP is a non-specific potassium channel blocker, we also used the K<sup>+</sup> channel blocker TEA to confirm that the effects of carbachol were confined to the K<sup>+</sup> channels that are known to mediate A-type currents. TEA had no significant effect on either the holding potential or the membrane resistance while application of carbachol in the presence of TEA led to changes in holding potential and membrane resistance that were comparable to those seen with carbachol application alone. Since previous studies had shown that blocking A-type currents with 4-AP could have a significant effect on first spike latency (Mathieson and Maler, 1988), we measured the effects of carbachol and 4-AP on first spike latency. We confirmed the effect of 4-AP previously shown and additionally

demonstrated that carbachol could lead to similar decreases in first spike latency, whereas TEA had no significant effect.

### Control of a neuron's frequency tuning by A-type currents

We used a two-compartmental mathematical model to assess if the removal of an A-type current could replicate the effects of carbachol. The model showed that the removal of an A-type current can result in similar changes in burst firing, holding potential, membrane resistance, and first spike latency as those seen under experimental activation of mAChR's, supporting the in vitro findings (Fig 8). Additionally it was shown that when the model was presented with a noise current injection to mimic sensory stimulation in vivo, removal of IA resulted in an increased response to low frequency input, which was similar to that seen following carbachol application in vivo. In order to understand this effect, we used sinusoidal current injections. It was shown that for very low frequencies (< 1 Hz) removal of I<sub>A</sub> had no effect on neuronal response properties. We propose that this is due to the length of the depolarizing phase of the sinewave, which should result in a complete inactivation of IA by the time spike threshold is reached, thus eliminated it's effect. Further, it was shown that at frequencies greater than 40 Hz, the removal of IA again had no effect since the period of hyperpolarization is insufficient to de-inactivate the A-type channels. As such, our modeling results suggest that the downregulation of A-type potassium channels is sufficient to explain the increase in the low frequency tuning, in the range between 1 and 40 Hz, of pyramidal neurons found in vivo following pharmacological activation of mAChRs.

# A pyramidal neuron's response to low frequencies is behaviorally relevant

We have shown that mAChR activation leads to an increased pyramidal neuron response to the low temporal frequency components of sensory input. A number of natural sensory stimuli contain low temporal frequencies. The jamming avoidance response (JAR; reviewed in: Heiligenberg, 1991) is a well-described behavior that is triggered by low temporal frequency spatially diffuse electrosensory stimuli. Specifically, the JAR occurs when a fish encounters a conspecific with an EOD frequency close to its own. These signals can interfere with electrolocation if the frequency difference is less

than 8 Hz (Heiligenberg, 1991). The fish with the highest EOD frequency increases its EOD frequency until the signals will interfere less with electrolocation. However, previous *in vivo* studies have shown that pyramidal neurons generally display poor responses to low frequency global stimuli (Bastian et al., 2002;Bastian et al., 2004;Chacron et al., 2003;Chacron et al., 2005;Chacron, 2006). Our results show that cholinergic input has the capacity to make pyramidal neurons more responsive these stimuli.

Alternatively, prey can also cause low-frequency stimuli. However, these signals are more spatially localized (Nelson and Maciver, 1999). It is therefore also possible that the cholinergic pathway can increase the response of pyramidal neurons to prey stimuli, thereby improving the animal's prey detection abilities. While further studies are needed to understand how and when cholinergic input becomes active, it is likely descending input from a higher brain area (see below) and can be activated in response to behaviorally relevant stimuli.

### Muscarinic control of the A-type current

A number of higher order functions can be controlled by cholinergic input including, but not limited to: attention (Bucci et al., 1998;Voytko et al., 1994), learning (Miranda and Bermudez-Rattoni, 1999;Fine et al., 1997) & memory (Hasselmo et al., 1992;Sarter et al., 2005). These types of modulations often elevate sensory responsiveness and occur when a cholinergic pathway is activated in conjunction with an external sensory stimulus. An example of such control occurs in the somatosensory cortex where a stimulus response can be enhanced by stimulating descending cholinergic pathways from the cortex during the presentation of an external cue (Donoghue and Carroll, 1987;Rasmusson and Dykes, 1988). In the visual system, cholinergic input can lead to potentiation through an enhancement of the signal to noise ratio (Gu, 2003). In the hippocampus LTP may be facilitated when a backpropagating spike is paired with an EPSP (Magee and Johnston, 1997).

It has been shown that the down-regulation of an A-type current can increase the backpropagation of dendritic spikes (Hoffman et al., 1997). It is likely that the down-regulation of I<sub>A</sub> can lead to an increase in the strength of the backpropagating spike and

thus facilitate LTP, when paired with an EPSP as described above. This may be one mechanism through which I<sub>A</sub> can regulate higher order processes, such as learning. The dendritic modification of I<sub>A</sub> by mAChRs that we have shown here results in an increased response to low frequency input through an increase in bursting. The reduction of I<sub>A</sub> may result in an increase in backpropagation of dendritic spikes, in a similar way to that described for the facilitation of LTP. The backpropagation of dendritic spikes has been shown to control bursting in ELL pyramidal neurons (Turner et al., 1994;Lemon and Turner, 2000) and since bursts are strong encoders of low frequencies in this system (Oswald et al., 2004), control of backpropagation by I<sub>A</sub> may be the mechanism whereby the frequency response is modulated. In fact mathematical modeling has suggested that the removal of a low threshold potassium current (IK<sub>LT</sub>) from pyramidal neurons has the same effect as decreasing the size of a sodium spike (Fernandez et al., 2005a), which has been shown to modulate burst frequency (Fernandez et al., 2005b).

Downregulation of A-type currents by cholinergic receptor activation has already been demonstrated in other systems such as the hippocampus (Nakajima et al., 1986) and neostriatum (Akins et al., 1990;Nakamura et al., 1997). Activation of M1 receptors leads to an increase in protein kinase C (PKC) that can lead to a decrease in Kv4 generated currents. The kinetics of Kv4 type channels suggest they can generate an A-type current (Coetzee et al., 1999;Song, 2002). Interestingly it has also been shown that PKC may modulate I<sub>A</sub> through a positive shift in the activation curve (Hoffman and Johnston, 1998) instead of the direct reduction in I<sub>A</sub> that was previously described. In *Apteronotus* it has been suggested that a positive shift in the I<sub>A</sub> activation curve can prevent its influence on bursting (Fernandez et al., 2005a). It then appears that regardless of whether I<sub>A</sub> is directly reduced or if the activation curve is shifted, mAChR modulation may produce the alterations in bursting described in this study through the activation of a PKC pathway.

### The cholinergic input pathway

Cholinergic input unto pyramidal cells most likely originates from eurydendroid cells within the caudal lobe of the cerebellum (Phan and Maler, 1983;Maler et al., 1981;Mathieson and Maler, 1988;Berman and Maler, 1999). The circuitry within the caudal lobe of the cerebellum is similar to that of the deep cerebellar nuclei in

mammalian systems (Finger, 1978). While the general morphology (Guest RM, 1983) and some of the cellular projections (Carr et al., 1986) of eurydendroid cells have been investigated, the sensory responsiveness of this cell type is unknown and may be activated by input from higher brain centers, similar to the cholinergic pathways in mammalian systems. The results presented here make the analysis of this input pathway a critical component required to understand its effects on sensory processing.

A recent review has highlighted the similarities between ELL pyramidal neurons and LGN relay cells in terms of burst firing (Krahe and Gabbiani, 2004). LGN relay cells have a well-characterized burst mechanism (Sherman, 2001) and in the LGN bursts transmit information about low frequency stimuli (Lesica and Stanley, 2004). The results presented here along with previous work showing an increase in burst firing can increase a neurons response to low frequencies (Oswald et al., 2004) are consistent with the results from the LGN. Since A-type potassium currents are present in LGN relay cells (Budde et al., 1992) and since acetylcholine has been shown to increase their excitability (Kemp and Sillito, 1982;Sillito et al., 1983), it is possible that regulation of burst firing by A-type channels regulates information transmission in the LGN in a manner similar to that observed in ELL.

Overall, control of frequency tuning through the regulation of A-type currents is likely to be found in other systems and may be a general mechanism by which neural responses to sensory input are regulated. Enhanced processing of specific sensory information through increases in excitability mediated by the down-regulation of an I<sub>A</sub> current may thus be a general feature of sensory processing regulating higher cognitive functions such as attention in mammals.

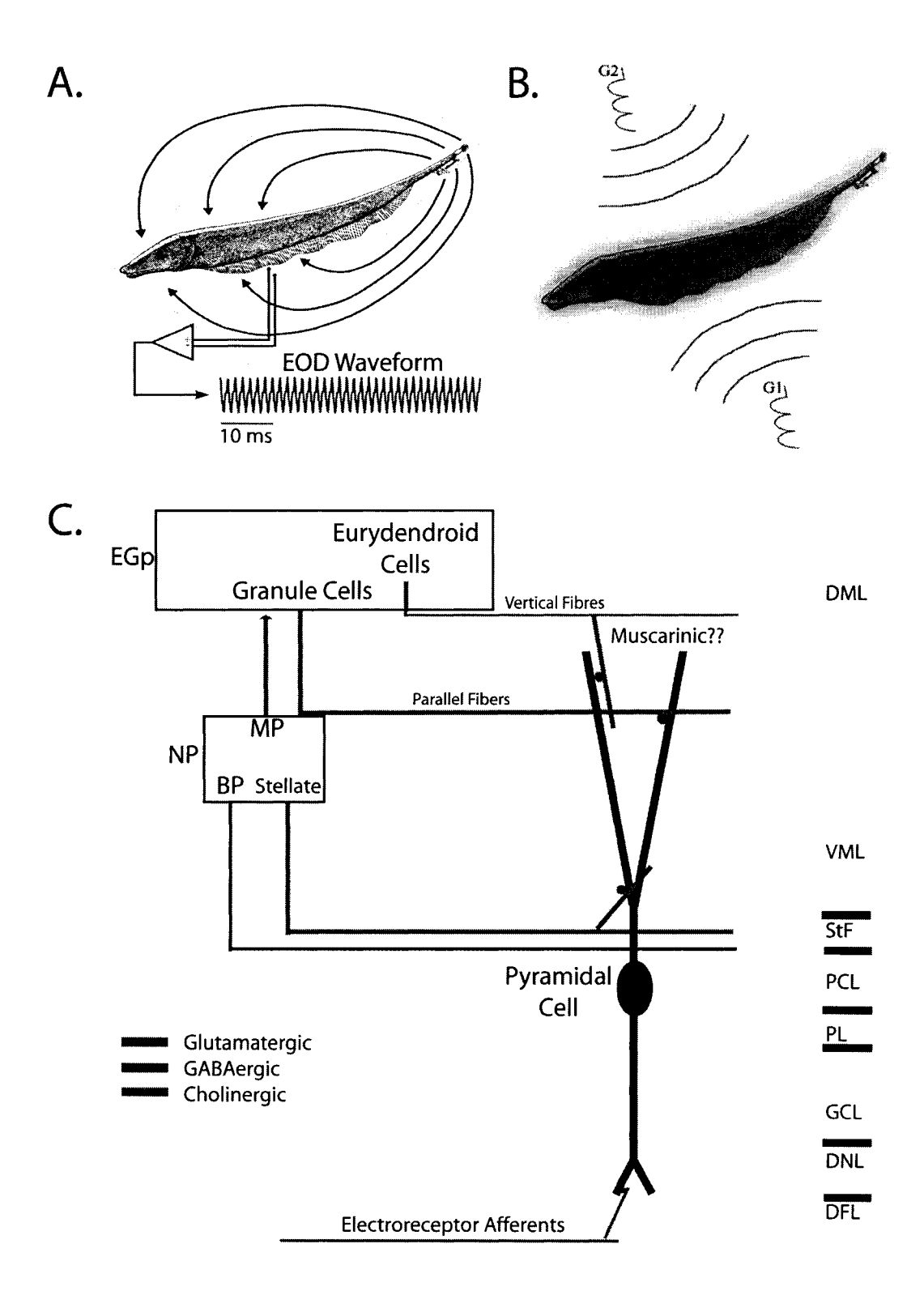
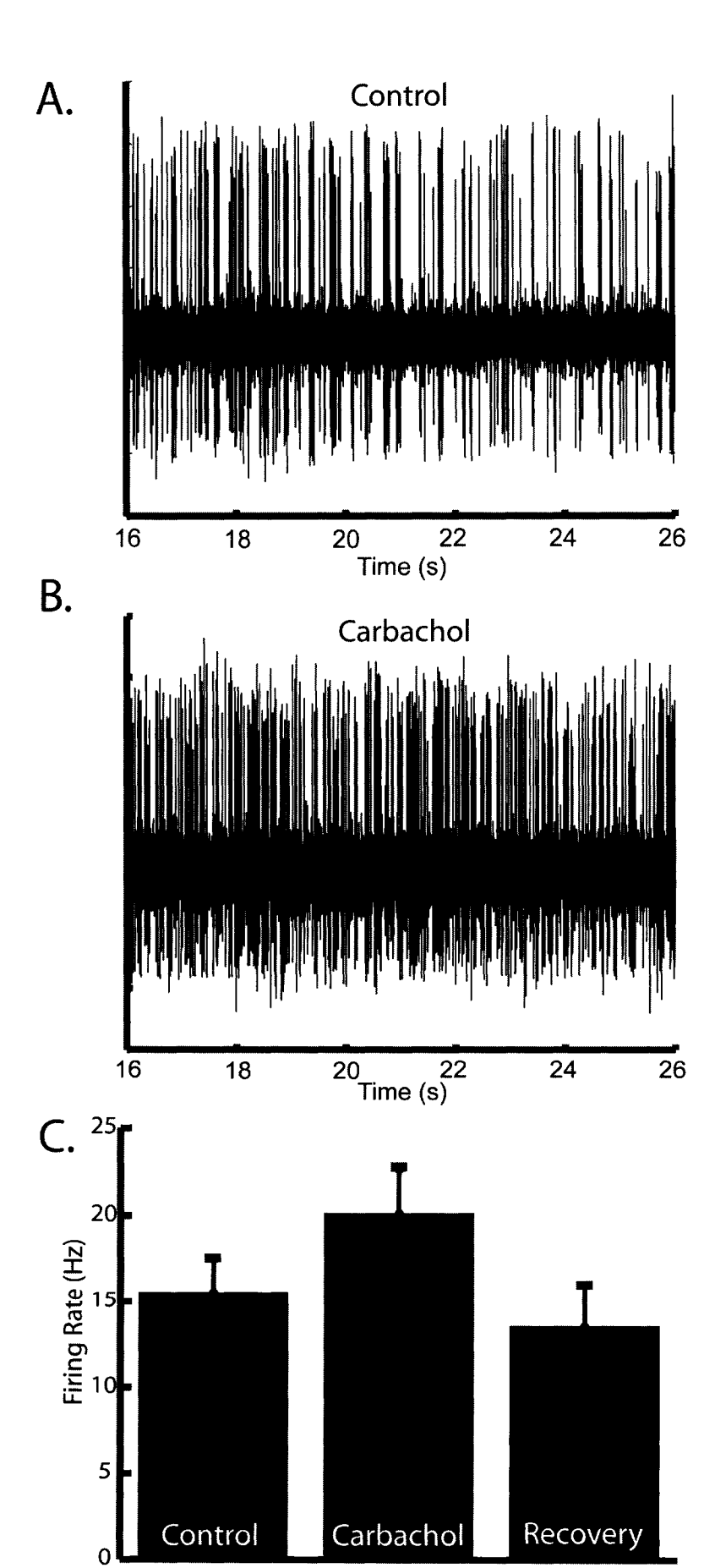


Figure 1. The electrosensory system. (A) Weakly electric fish generate an electric field around their body in order to electrolocate objects. For Apteronotus Leptorhynchus, the EOD waveform recorded at one point in space is quasi-sinusoidal with a frequency of 600-1000 Hz (green trace). (B) Illustration of the Global stimulation geometry used. Amplitude modulations of the animals own EOD are delivered via two silver-silverchloride electrodes (G1 and G2) located 19 cm away on each side of the animal. The perturbations of the EOD created are roughly spatially homogeneous on the animal's skin surface. (C) Illustration of the relevant circuitry. Electroreceptor afferents on the animal's skin detect amplitude modulations of the EOD and synapse unto pyramidal cells within the electrosensory lateral line lobe. Pyramidal cells project to the nucleus praeminentialis (NP). Bipolar cells (BP) and stellate cells feedback, from the NP, unto pyramidal cells by way of the stratum tractus fibrosum (StF). Multipolar cells (MP) project to granule cells (GC) within the eminentia granularis posterior (EGP). These granule cells also feedback unto pyramidal cells via parallel fibers. Finally, pyramidal cells are thought to receive cholinergic input from eurydendroid cells within the EGP via vertical fibers. Other abbreviations: DML: dorsal molecular layer, VML: ventral molecular layer, PCL: pyramidal cell layer, PL: plexiform layer, DNL: deep neuropil layer.



**Figure 2.** Carbachol leads to increased cellular excitability *in vivo*. (A) Extracellular recording of spontaneous activity of an ELL pyramidal neuron. (B) Increased firing in response to application of carbachol. (C) Carbachol leads to a significant increase in the average firing rate (control:  $15.57 \pm 6.42$  Hz; carbachol  $20.12 \pm 9.34$  Hz; p=0.005, paired t-test, n=14), which returns to control levels after recovery period ( $13.56 \pm 6.62$  Hz, p=0.35, paired t-test, n=6).

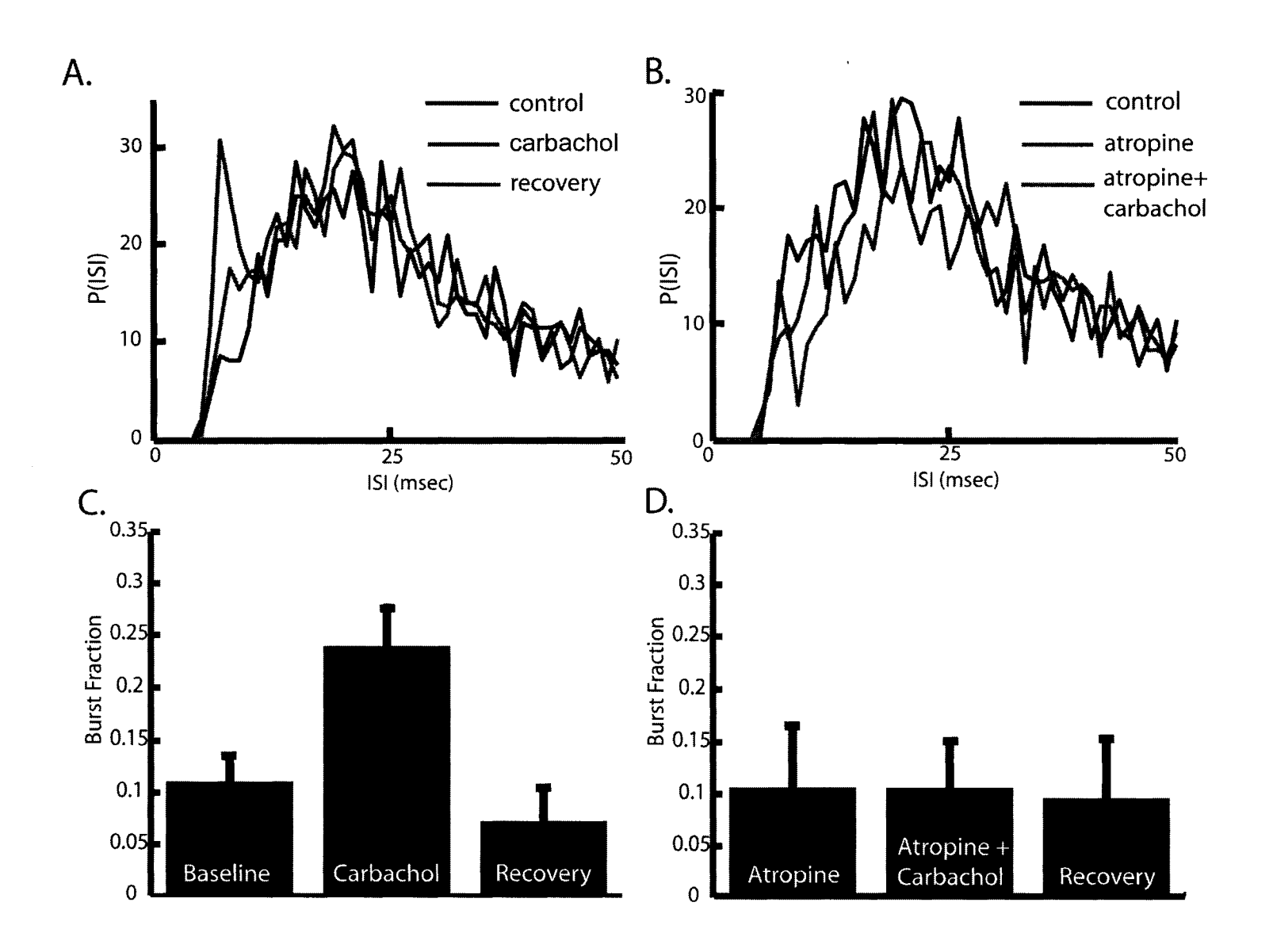
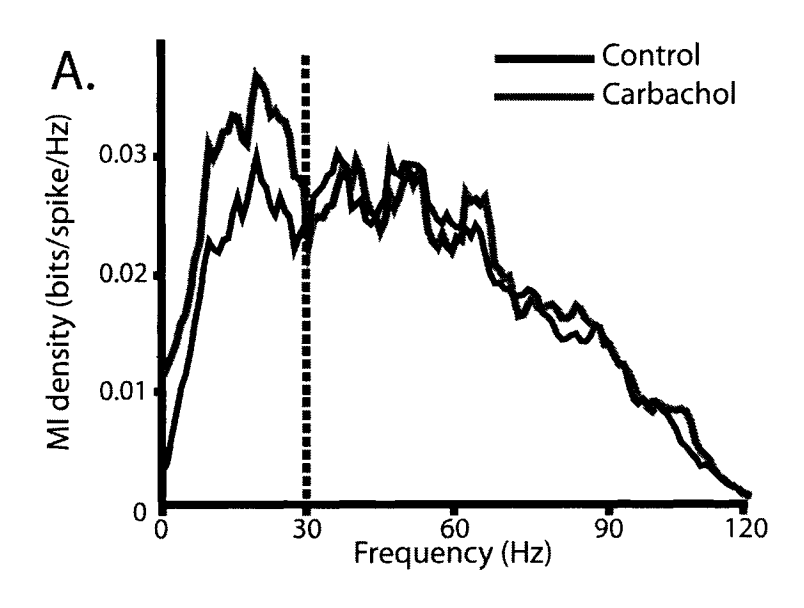
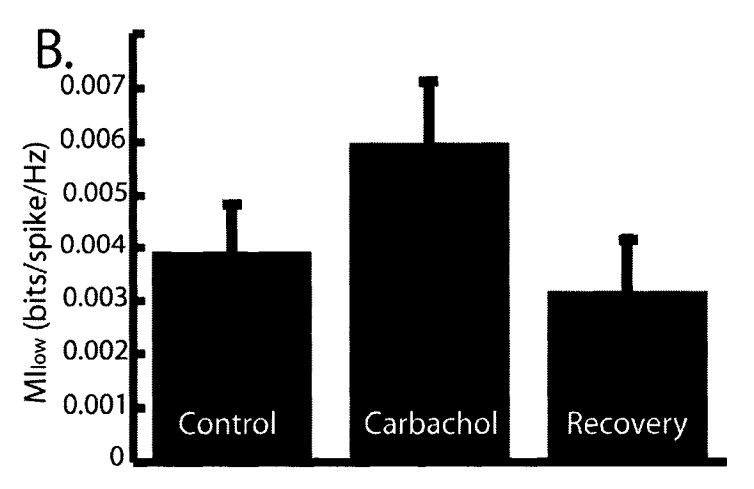


Figure 3. Muscarinic receptor activation leads to an increase in burst firing *in vivo*. (A) ISI histograms before (blue), during (red), and after (green) application of carbachol. Carbachol leads to an increase in ISIs below 10 msec. (B) ISI histograms before (blue), during (red), and after (green) application of carbachol in the presence of atropine. Atropine prevents the effect of carbachol revealing muscarinic receptor activation by carbachol. (C) Bar graph representing the average increase of the burst fraction (fraction of ISIs<10 msec; control:  $0.11 \pm 0.10$ ; carbachol:  $0.24 \pm 0.15$ , p=0.001, paired t-test, n=14) following carbachol and return to control levels following recovery period. (D) Atropine prevents an increase in burst fraction for the population of cells tested.





**Figure 4.** Muscarinic receptor activation increases the response to low frequency sensory stimuli *in vivo*. (A) Mutual information rate density showing an increased response to frequencies <30 Hz. (B) Bar graph showing the average mutual information rate density for low frequencies ( $M_{low}$ ).  $M_{low}$  increased after carbachol application and then returned to control levels (control:  $0.004 \pm 0.001$  bits/spk/Hz; carbachol:  $0.006 \pm 0.001$ ; p=0.009, paired t-test, n=14).

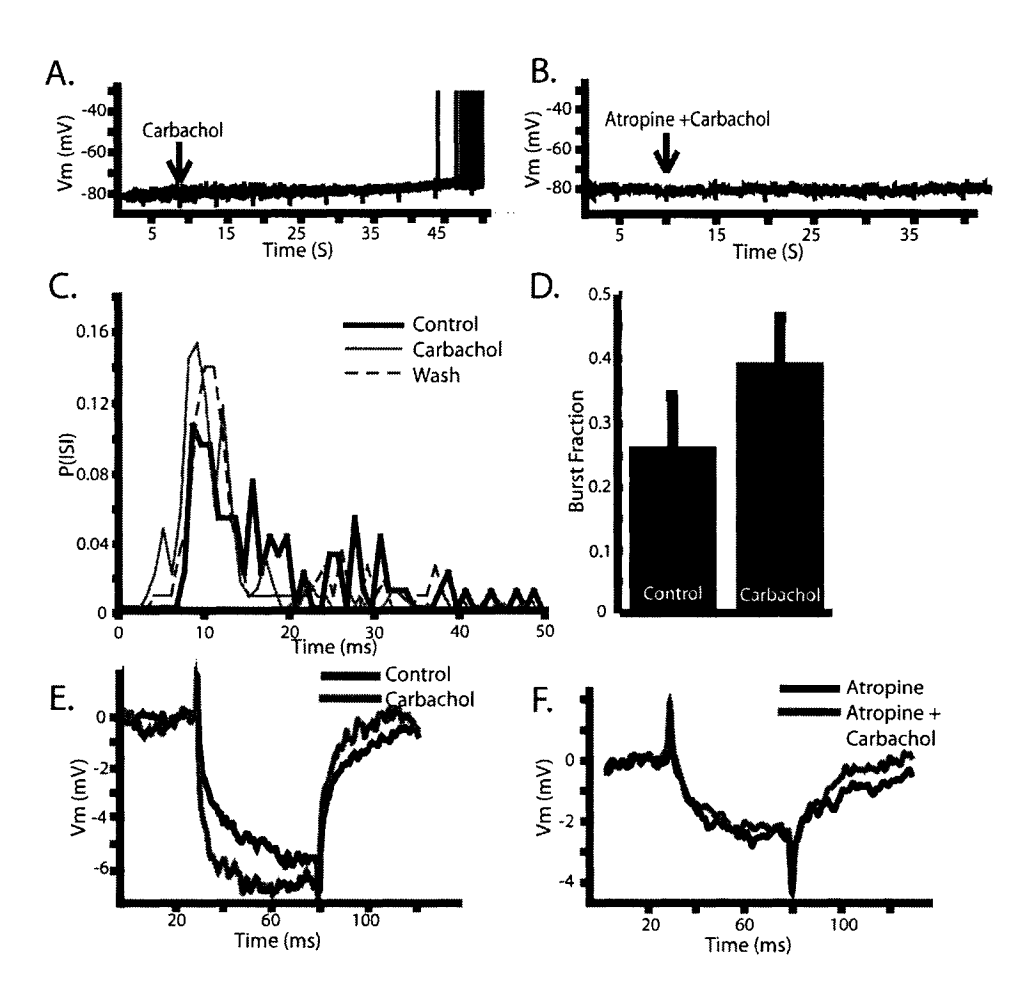
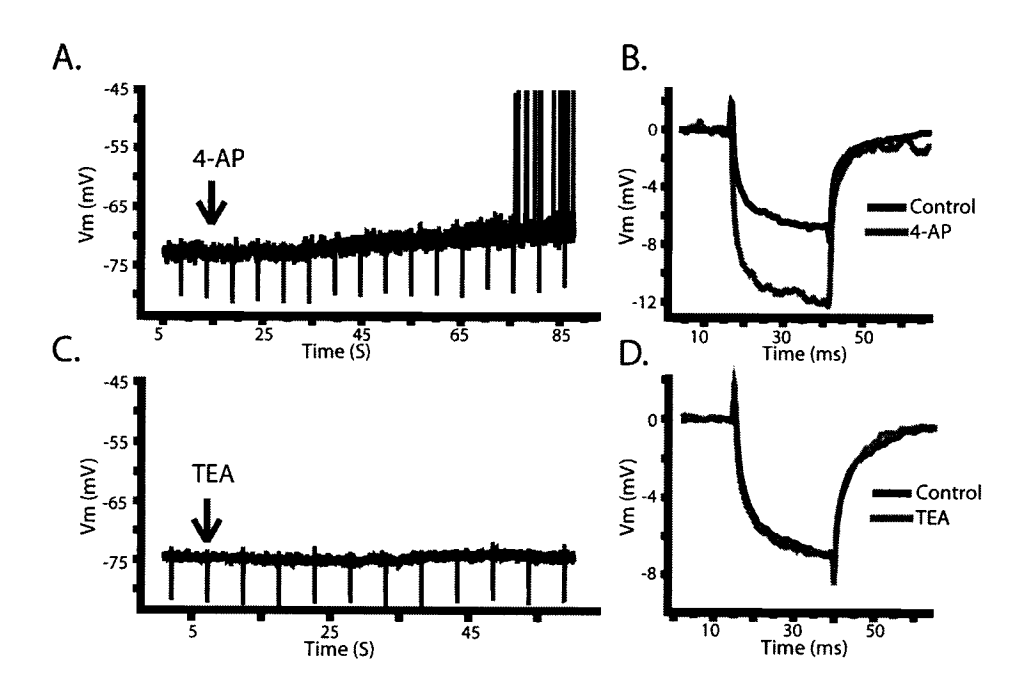


Figure 5. Carbachol activates muscarinic receptors *in vitro*. (A) Carbachol leads to a ~4 mV depolarization of the membrane potential from a subthreshold level leading to spiking (Spikes truncated at -35 mV). (B) Atropine eliminates the effects of carbachol, suggesting mAChR activation. (C) ISI histogram showing an increase in ISI's <10 ms following carbachol application. (D) A significant increase in the burst fraction (fraction of ISIs<10 msec) following carbachol application. (E) Carbachol also leads to an increased membrane resistance. (F) Carbachol in the presence of atropine does not increase the membrane resistance.



**Figure 6.** A potassium channel blocker can mirror the effects of carbachol. (A+B) The potassium channel antagonist 4-AP leads to a depolarization of the membrane potential (A) and an increase in resistance (B). (C+D) The potassium channel blocker TEA does not affect either the membrane potential (C) or resistance (D).

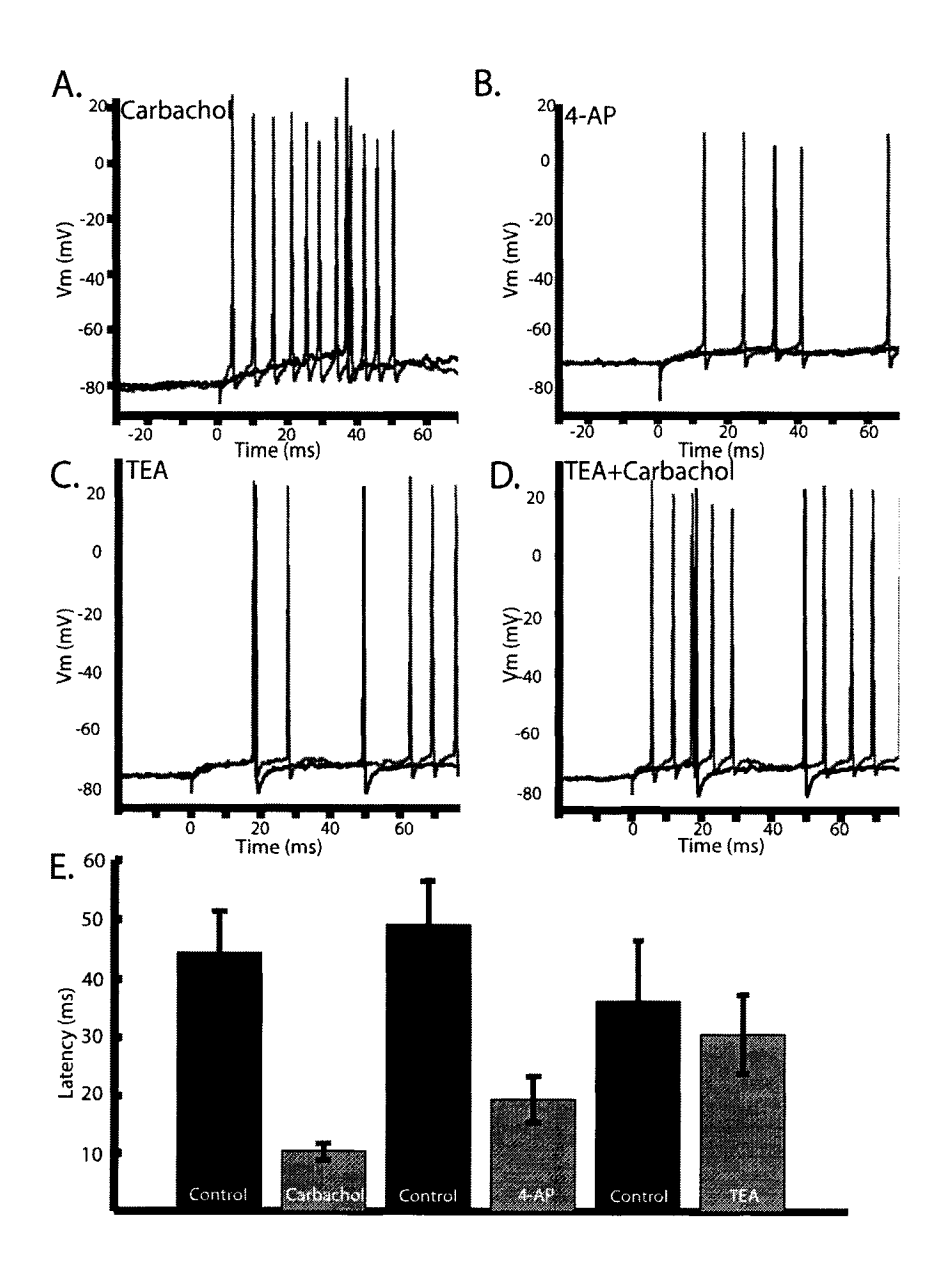
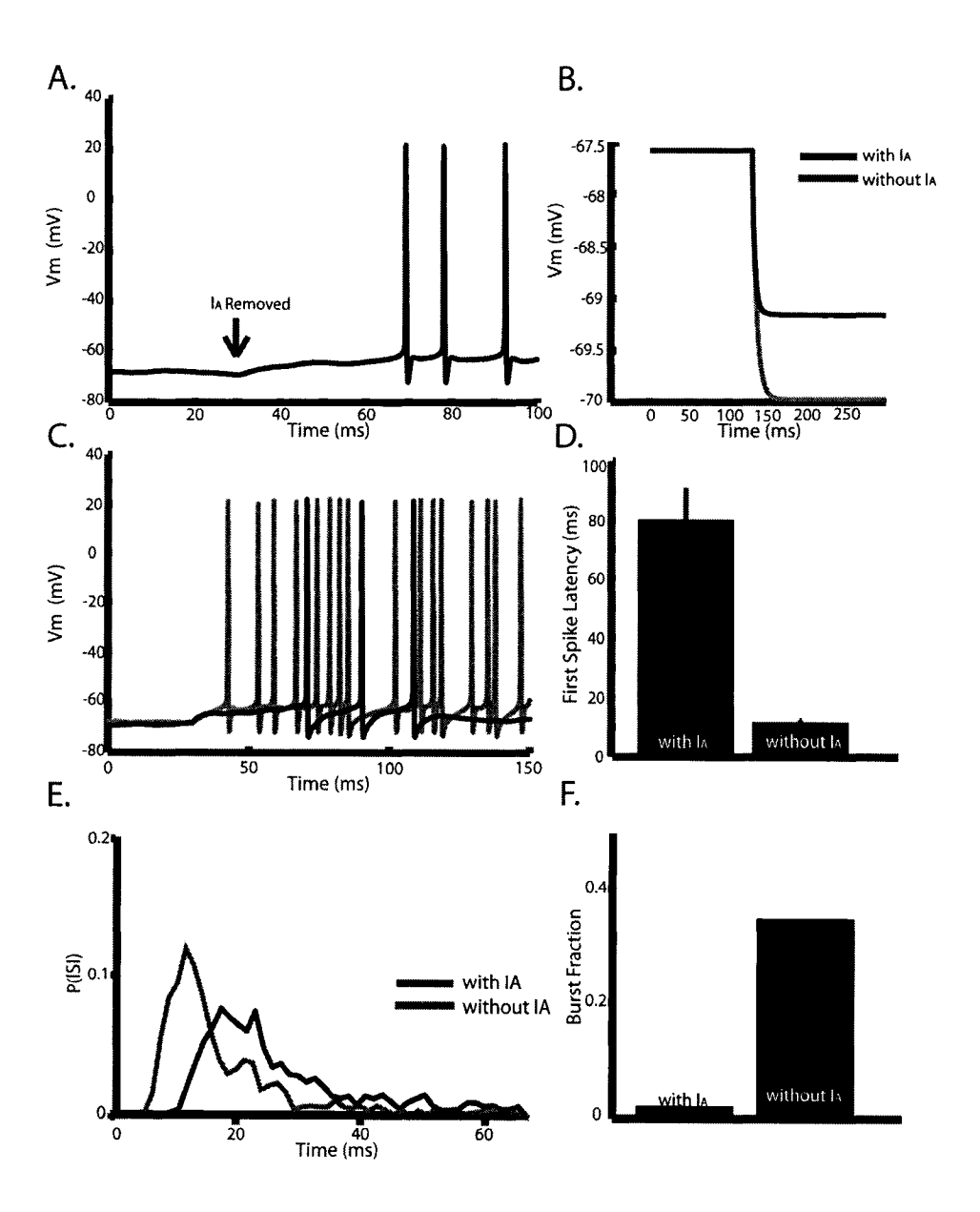
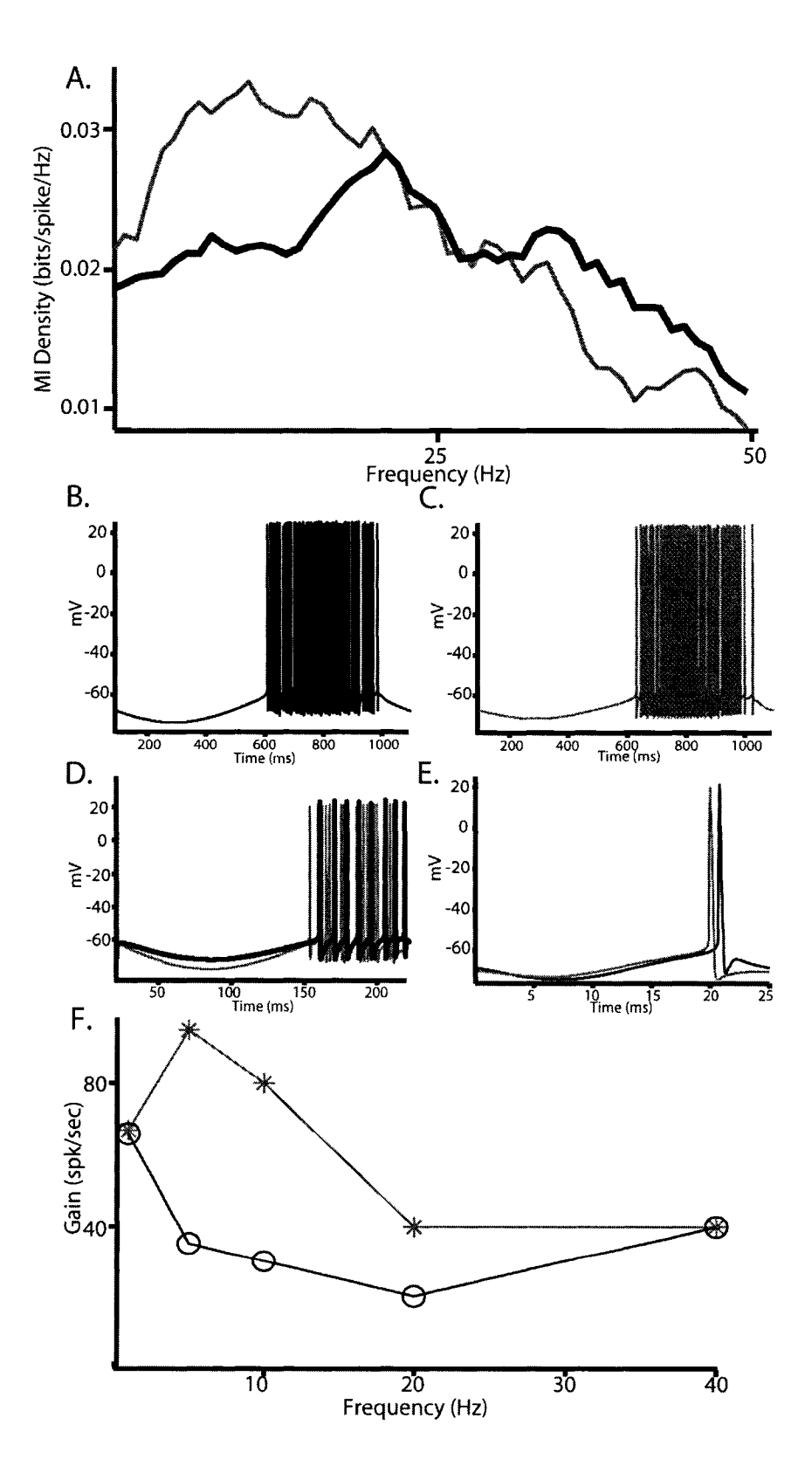


Figure 7. Carbachol and 4-AP lead to a decreased first spike latency, suggesting the involvement of an A-type current. (A) Carbachol leads to a reduced spike latency following a step current injection (0.2nA). (B) 4-AP mirrors the effect of carbachol reducing first spike latency in a representative cell. (C) TEA does not alter the spike latency. (D) Carbachol decreases latency even when applied after TEA. (E) Bar graphs showing a significant decrease in latency following carbachol and 4-AP (Control:  $44.4 \pm 22.6$  msec; Carbachol:  $10.4 \pm 4.4$  msec; p<0.001; paired t-test; n=11: Control:  $49.1 \pm 19.4$  msec; 4-AP:  $19.4 \pm 10.5$  msec; p<0.001; paired t-test; n=7), while TEA did not show a significant decrease in latency (control:  $37.4 \pm 21.9$  ms; TEA:  $43.2 \pm 34.9$  ms; p=0.13; paired t-test; n=8).



**Figure 8.** Modeling the effects of blocking A-type channels. (A) Removal of  $I_A$  leads to a ~5 mV depolarization and spiking. At t=130 ms, we set  $g_A$  from 2 mS/cm<sup>2</sup> to 0. We had  $I_0$ =1.3. (B) Step hyperpolarization with  $g_A$ =2 mS/cm<sup>2</sup> (black) and  $g_A$ =0 (grey) showing a 33% increase in resistance with D=0. This was obtained by setting  $I_0$  from 1.375 to 0.875. (C) Step depolarizations with (black,  $g_A$ =2 mS/cm<sup>2</sup>) and without (grey,  $g_A$ =0)  $I_A$ . At t=130 ms, we increased  $I_0$  from 0.5 to 1.7 (grey) and from 1 to 2.3 (black). (D) Mean latencies obtained under repeated step depolarizations as described in C. (E) ISI probability densities obtained under repeated step depolarizations as described in C. (F) Burst fraction obtained from the ISI probability. Note that S(t)=0 for all panels.



**Figure 9.** Modeling the effects of A-type channels on signal processing. (A) Mutual information density with (black) and without (grey)  $I_A$ . Removal of  $I_A$  leads to increased information at low (<20 Hz) frequencies. In both cases we injected zero mean low pass filtered (8<sup>th</sup> order butterworth, 120 Hz cutoff) Gaussian white noise with standard deviation 0.5. Other parameters were the same as in figure 7 except  $I_0$ =0.7,  $g_A$ =0 (grey) and  $I_0$ =2,  $g_A$ =2 mS/cm² (black). (B) Membrane potential with  $I_A$  and a 1 Hz sinusoidal current injection. (C) Membrane potential without  $I_A$  and a 1 Hz sinusoidal current injection. (D) Membrane potential with (black) and without (grey)  $I_A$  with a 5 Hz sinusoidal current injection. (E) Membrane potential with (black) and without (grey)  $I_A$  with a 40 Hz sinusoidal current injection. (F) Firing rate as a function of the sinusoidal current's frequency with (black) and without (grey)  $I_A$ . For all simulations with sinusoidal current, we had  $I_0$ =0.4 (black) and  $I_0$ =1.4 (grey) as well as D=0 and the sinusoid's amplitude was set to 2 for all frequencies.

#### References

Abbott L.F. (2005) Where are the Switches on This Thing? In: 23 Problems in Systems Neuroscience (van Hemmen J.L, Sejnowski T.J., eds), pp 423-431. Oxford University Press; USA.

Akins PT, Surmeier DJ, Kitai ST (1990) Muscarinic modulation of a transient K+conductance in rat neostriatal neurons. Nature 344: 240-242.

Bakin JS, Weinberger NM (1996) Induction of a physiological memory in the cerebral cortex by stimulation of the nucleus basalis. Proc Natl Acad Sci U S A 93: 11219-11224.

Bastian, J. Electrolocation I. How the electroreceptors of Apteronotus albifrons code for moving objects and other electrical stimuli. 144, 465-479. 1981. Ref Type: Generic

Bastian J (1993) The role of amino acid neurotransmitters in the descending control of electroreception. J Comp Physiol [A] 172: 409-423.

Bastian J (1996a) Plasticity in an electrosensory system. I. General features of a dynamic sensory filter. J Neurophysiol 76: 2483-2496.

Bastian J (1996b) Plasticity in an electrosensory system. II. Postsynaptic events associated with a dynamic sensory filter. J Neurophysiol 76: 2497-2507.

Bastian J, Chacron MJ, Maler L (2002) Receptive field organization determines pyramidal cell stimulus-encoding capability and spatial stimulus selectivity. J Neurosci 22: 4577-4590.

Bastian J, Chacron MJ, Maler L (2004) Plastic and nonplastic pyramidal cells perform unique roles in a network capable of adaptive redundancy reduction. Neuron 41: 767-779.

Bastian J, Nguyenkim J (2001) Dendritic modulation of burst-like firing in sensory neurons. J Neurophysiol 85: 10-22.

Berman NJ, Maler L (1998a) Distal versus proximal inhibitory shaping of feedback

excitation in the electrosensory lateral line lobe: implications for sensory filtering. J Neurophysiol 80: 3214-3232.

Berman NJ, Maler L (1998b) Inhibition evoked from primary afferents in the electrosensory lateral line lobe of the weakly electric fish (Apteronotus leptorhynchus). J Neurophysiol 80: 3173-3196.

Berman NJ, Maler L (1998c) Interaction of GABAB-mediated inhibition with voltage-gated currents of pyramidal cells: computational mechanism of a sensory searchlight. J Neurophysiol 80: 3197-3213.

Berman NJ, Maler L (1999) Neural architecture of the electrosensory lateral line lobe: adaptations for coincidence detection, a sensory searchlight and frequency-dependent adaptive filtering. J Exp Biol 202: 1243-1253.

Borst A, Haag J (2001) Effects of mean firing on neural information rate. J Comput Neurosci 10: 213-221.

Borst A, Theunissen FE (1999) Information theory and neural coding. Nat Neurosci 2: 947-957.

Bucci DJ, Holland PC, Gallagher M (1998) Removal of cholinergic input to rat posterior parietal cortex disrupts incremental processing of conditioned stimuli. J Neurosci 18: 8038-8046.

Budde T, Mager R, Pape HC (1992) Different Types of Potassium Outward Current in Relay Neurons Acutely Isolated from the Rat Lateral Geniculate Nucleus. Eur J Neurosci 4: 708-722.

Carr CE, Maler L, Taylor B (1986) A time-comparison circuit in the electric fish midbrain. II. Functional morphology. J Neurosci 6: 1372-1383.

Chacron MJ (2006) Nonlinear information processing in a model sensory system. J Neurophysiol 95: 2933-2946.

Chacron MJ, Doiron B, Maler L, Longtin A, Bastian J (2003) Non-classical receptive field mediates switch in a sensory neuron's frequency tuning. Nature 423: 77-81.

Chacron MJ, Maler L, Bastian J (2005) Feedback and feedforward control of frequency tuning to naturalistic stimuli. J Neurosci 25: 5521-5532.

Chen X, Johnston D (2004) Properties of single voltage-dependent K+ channels in dendrites of CA1 pyramidal neurones of rat hippocampus. J Physiol 559: 187-203.

Coetzee WA, Amarillo Y, Chiu J, Chow A, Lau D, McCormack T, Moreno H, Nadal MS, Ozaita A, Pountney D, Saganich M, Vega-Saenz dM, Rudy B (1999) Molecular diversity of K+channels. Ann N Y Acad Sci 868: 233-285.

Connor JA, Stevens CF (1971) Voltage clamp studies of a transient outward membrane current in gastropod neural somata. J Physiol 213: 21-30.

Cover T, Thomas J (1991) Elements of Information Theory. New York: Wiley.

Delgado-Lezama R, Perrier JF, Nedergaard S, Svirskis G, Hounsgaard J (1997) Metabotropic synaptic regulation of intrinsic response properties of turtle spinal motoneurones. J Physiol 504 (Pt 1): 97-102.

Doiron B, Chacron MJ, Maler L, Longtin A, Bastian J (2003a) Inhibitory feedback required for network oscillatory responses to communication but not prey stimuli. Nature 421: 539-543.

Doiron B, Laing C, Longtin A, Maler L (2002) Ghostbursting: a novel neuronal burst mechanism. J Comput Neurosci 12: 5-25.

Doiron B, Longtin A, Turner RW, Maler L (2001) Model of gamma frequency burst discharge generated by conditional backpropagation. J Neurophysiol 86: 1523-1545.

Doiron B, Noonan L, Lemon N, Turner RW (2003b) Persistent Na+ current modifies burst discharge by regulating conditional backpropagation of dendritic spikes. J Neurophysiol 89: 324-337.

Donoghue JP, Carroll KL (1987) Cholinergic modulation of sensory responses in rat primary somatic sensory cortex. Brain Res 408: 367-371.

Everitt BJ, Robbins TW (1997) Central cholinergic systems and cognition. Annu Rev Psychol 48: 649-684.

Fernandez FR, Mehaffey WH, Molineux ML, Turner RW (2005a) High-threshold K+ current increases gain by offsetting a frequency-dependent increase in low-threshold K+ current. J Neurosci 25: 363-371.

Fernandez FR, Mehaffey WH, Turner RW (2005b) Dendritic Na+ current inactivation can increase cell excitability by delaying a somatic depolarizing afterpotential. J Neurophysiol 94: 3836-3848.

Fine A, Hoyle C, Maclean CJ, Levatte TL, Baker HF, Ridley RM (1997) Learning impairments following injection of a selective cholinergic immunotoxin, ME20.4 IgG-saporin, into the basal nucleus of Meynert in monkeys. Neuroscience 81: 331-343.

Finger TE (1978) Efferent neurons of the teleost cerebellum. Brain Res 153: 608-614.

Frank K, Becker MC (1964) Microelectrodes for recording and stimulation. In: Physical Techniques in Biological Research, Part A New York, Academic.

Gardiner CW (1985) Handbook of Stochiastic Methods. Berlin: Springer.

Gu Q (2003) Contribution of acetylcholine to visual cortex plasticity. Neurobiol Learn Mem 80: 291-301.

Guest RM. Alternate Cerebellar Circuitry - The Morphology of the Caudal Cerebellar Lobe of the Weakly Electric Fish. 1983. University of Ottawa-Department of Anatomy. Ref Type: Thesis/Dissertation

Hasselmo ME, Anderson BP, Bower JM (1992) Cholinergic modulation of cortical associative memory function. J Neurophysiol 67: 1230-1246.

Heiligenberg W (1991) Sensory control of behavior in electric fish. Curr Opin Neurobiol 1: 633-637.

Hoffman DA, Johnston D (1998) Downregulation of transient K+ channels in dendrites of hippocampal CA1 pyramidal neurons by activation of PKA and PKC. J Neurosci 18: 3521-3528.

Hoffman DA, Magee JC, Colbert CM, Johnston D (1997) K+ channel regulation of signal propagation in dendrites of hippocampal pyramidal neurons. Nature 387: 869-875.

Jarvis MR, Mitra PP (2001) Sampling properties of the spectrum and coherency of sequences of action potentials. Neural Comput 13: 717-749.

Kemp JA, Sillito AM (1982) The nature of the excitatory transmitter mediating X and Y cell inputs to the cat dorsal lateral geniculate nucleus. J Physiol 323: 377-391.

Kilgard MP, Merzenich MM (1998) Cortical map reorganization enabled by nucleus basalis activity. Science 279: 1714-1718.

Koch C (1999) Biophysics of Computation. New York: University Press.

Krahe R, Gabbiani F (2004) Burst firing in sensory systems. Nat Rev Neurosci 5: 13-23.

Lemon N, Turner RW (2000) Conditional spike backpropagation generates burst discharge in a sensory neuron. J Neurophysiol 84: 1519-1530.

Lesica NA, Stanley GB (2004) Encoding of natural scene movies by tonic and burst spikes in the lateral geniculate nucleus. J Neurosci 24: 10731-10740.

Lucas-Meunier E, Fossier P, Baux G, Amar M (2003) Cholinergic modulation of the cortical neuronal network. Pflugers Arch 446: 17-29.

Maccaferri G, Mangoni M, Lazzari A, DiFrancesco D (1993) Properties of the hyperpolarization-activated current in rat hippocampal CA1 pyramidal cells. J Neurophysiol 69: 2129-2136.

Magee JC, Johnston D (1997) A synaptically controlled, associative signal for Hebbian plasticity in hippocampal neurons. Science 275: 209-213.

Maler L, Collins M, Mathieson WB (1981) The distribution of acetylcholinesterase and choline acetyl transferase in the cerebellum and posterior

lateral line lobe of weakly electric fish (Gymnotidae). Brain Res 226: 320-325.

Maler L, Sas E, Johnston S, Ellis W (1991) An atlas of the brain of the electric fish Apteronotus leptorhynchus. J Chem Neuroanat 4: 1-38.

Mathieson WB, Maler L (1988) Morphological and electrophysiological properties of a novel in vitro preparation: the electrosensory lateral line lobe brain slice. J Comp Physiol [A] 163: 489-506.

McCormick DA (1991) Functional properties of a slowly inactivating potassium current in guinea pig dorsal lateral geniculate relay neurons. J Neurophysiol 66: 1176-1189.

Mehaffey WH, Doiron B, Maler L, Turner RW (2005) Deterministic multiplicative gain control with active dendrites. J Neurosci 25: 9968-9977.

Miranda MI, Bermudez-Rattoni F (1999) Reversible inactivation of the nucleus basalis magnocellularis induces disruption of cortical acetylcholine release and acquisition, but not retrieval, of aversive memories. Proc Natl Acad Sci U S A 96: 6478-6482.

Mittmann T, Alzheimer C (1998) Muscarinic inhibition of persistent Na+ current in rat neocortical pyramidal neurons. J Neurophysiol 79: 1579-1582.

Nakajima Y, Nakajima S, Leonard RJ, Yamaguchi K (1986) Acetylcholine raises excitability by inhibiting the fast transient potassium current in cultured hippocampal neurons. Proc Natl Acad Sci U S A 83: 3022-3026.

Nakamura TY, Coetzee WA, Vega-Saenz dM, Artman M, Rudy B (1997) Modulation of Kv4 channels, key components of rat ventricular transient outward K+ current, by PKC. Am J Physiol 273: H1775-H1786.

Nelson ME, Maciver MA (1999) Prey capture in the weakly electric fish Apteronotus albifrons: sensory acquisition strategies and electrosensory consequences. J Exp Biol 202: 1195-1203.

Oswald AM, Chacron MJ, Doiron B, Bastian J, Maler L (2004) Parallel processing of sensory

input by bursts and isolated spikes. J Neurosci 24: 4351-4362.

Phan M, Maler L (1983) Distribution of muscarinic receptors in the caudal cerebellum and electrosensory lateral line lobe of gymnotiform fish. Neurosci Lett 42: 137-143.

Rasmusson DD, Dykes RW (1988) Long-term enhancement of evoked potentials in cat somatosensory cortex produced by co-activation of the basal forebrain and cutaneous receptors. Exp Brain Res 70: 276-286.

Roddey JC, Girish B, Miller JP (2000) Assessing the performance of neural encoding models in the presence of noise. J Comput Neurosci 8: 95-112.

Sadeghi SG, Chacron MJ, Taylor MC, Cullen KE (2007) Neural variability, detection thresholds, and information transmission in the vestibular system. J Neurosci 27: 771-781.

Sarter M, Hasselmo ME, Bruno JP, Givens B (2005) Unraveling the attentional functions of cortical cholinergic inputs: interactions between signal-driven and cognitive modulation of signal detection. Brain Res Brain Res Rev 48: 98-111.

Schoppa NE, Westbrook GL (1999) Regulation of synaptic timing in the olfactory bulb by an Atype potassium current. Nat Neurosci 2: 1106-1113.

Shannon CE (1948) The mathematical theory of communication. pp 379-423. Bell Systems Technical Journal.

Sherman SM (2001) Tonic and burst firing: dual modes of thalamocortical relay. Trends Neurosci 24: 122-126.

Sillito AM, Kemp JA, Berardi N (1983) The cholinergic influence on the function of the cat dorsal lateral geniculate nucleus (dLGN). Brain Res 280: 299-307.

Song WJ (2002) Genes responsible for native depolarization-activated K+ currents in neurons. Neurosci Res 42: 7-14.

Stocker M, Krause M, Pedarzani P (1999) An apamin-sensitive Ca2+-activated K+ current in

hippocampal pyramidal neurons. Proc Natl Acad Sci U S A 96: 4662-4667.

Svirskis G, Hounsgaard J (1998) Transmitter regulation of plateau properties in turtle motoneurons. J Neurophysiol 79: 45-50.

Tai C, Kuzmiski JB, MacVicar BA (2006) Muscarinic enhancement of R-type calcium currents in hippocampal CA1 pyramidal neurons. J Neurosci 26: 6249-6258.

Tang Y, Mishkin M, Aigner TG (1997) Effects of muscarinic blockade in perirhinal cortex during visual recognition. Proc Natl Acad Sci U S A 94: 12667-12669.

Turner RW, Maler L (1999) Oscillatory and burst discharge in the apteronotid electrosensory lateral line lobe. J Exp Biol 202: 1255-1265.

Turner RW, Maler L, Deerinck T, Levinson SR, Ellisman MH (1994) TTX-sensitive dendritic sodium channels underlie oscillatory discharge in a vertebrate sensory neuron. J Neurosci 14: 6453-6471.

Turner RW, Plant JR, Maler L (1996) Oscillatory and burst discharge across electrosensory topographic maps. J Neurophysiol 76: 2364-2382.

Voytko ML, Olton DS, Richardson RT, Gorman LK, Tobin JR, Price DL (1994) Basal forebrain lesions in monkeys disrupt attention but not learning and memory. J Neurosci 14: 167-186.

Weinberger NM (2003) The nucleus basalis and memory codes: auditory cortical plasticity and the induction of specific, associative behavioral memory. Neurobiol Learn Mem 80: 268-284.

# **DISCUSSION**

It has now been shown that two distinct potassium currents, one that is generated by a small-conductance calcium activated potassium channel (SK) and another from a low threshold A-type potassium channel can control a sensory neuron's response to specific types of input.

Cloning and localization revealed both unique and partially overlapping expression patterns for the 3 different SK subtypes throughout the brain. The major focus of this study was the electrosensory lateral line lobe (ELL; since it has been the most highly studied) where only the AptSK1 and 2 channels were present. It appears that both channels may be expressed in the same cell types however; the AptSK1 channels are primarily dendritic, while the AptSK2 channels show a somatic compartmentalization. In vitro electrophysiological characterization of ELL pyramidal neurons has revealed that only a subset of pyramidal neurons express functional SK channels. The presence of functional SK channels was cell and segment specific and the distribution pattern matched well with the localization of both AptSK2 protein and mRNA. electrophysiological analysis has shown that AptSK currents are associated with neurons that respond best to high frequency sensory stimuli, while those that respond strongly to the low frequency components of the stimuli are devoid of SK currents. Importantly, pharmacological block of the SK channels in neurons with broadband/high-pass characteristics elevated their response to low frequency stimuli. These results seem to suggest that the presence of the AptSK2 channel in ELL pyramidal neurons may help to set their baseline frequency response pattern.

Metabotropic receptors have the potential to modulate individual ionic conductances. A preliminary study had revealed that the cholinergic agonist carbachol led to an enhancement of a neuron's response to low frequencies similar to that seen following AptSK channel block in vitro. Through the use of the in vitro slice preparation I have now shown that this effect is not the result of AptSK modulation but rather, it is likely the result of the down-regulation of an A-type potassium current. Blocking the A-type current in vitro lead to a similar increase in low frequency response as that seen in vivo following mAChR activation.

Sensory nuclei use frequency as one of the major characteristics to distinguish between various environmental stimuli. Examples of this lie in the auditory system, which responds to the frequency of tones, and in vision, where the sensory nuclei respond to both temporal and spatial frequencies. In both systems frequency tuning is thought to be primarily regulated by network and synaptic dynamics (Krukowski and Miller, 2001; Oswald et al., 2006). Pyramidal neurons in the ELL use frequency to distinguish between two broad categories of electrosensory input generated by either prey or communication signals. Prey-type signals result in low frequency perturbations of the electric field, while communication-type signals primarily result in high frequency changes (Nelson and Maciver, 1999; Zakon et al., 2002). Similar to the auditory and visual systems frequency tuning in the ELL can be controlled by synaptic feedback both in vivo (Chacron et al., 2005) and in vitro (Mehaffey et al., 2005). We have now shown that the baseline frequency response properties of a pyramidal neuron can be set by an individual ionic conductance. Additionally, we have shown that altering the activity of an individual ion channel can modulate a neuron's sensory processing ability. The regulation of the A-type conductance by a second messenger pathway has revealed that metabotropic receptor activation can regulate a neuron's frequency response properties in addition to the ionotropic modifications that were previously shown. Importantly, this also provides a mechanism whereby second messenger cascades initiated by cell intrinsic mechanisms, such as may occur during development or stress, could potentially control a neurons sensory response.

# AptSK channel distribution patterns suggest multiple roles in electrosensory processing.

I have shown that the *Apt*SK channels show a high degree of sequence homology and the mRNA from the *Apt*SK1 and 2 channels is expressed at high levels in subsets of ELL pyramidal cells, showing at least a partial, if not completely overlapping distribution pattern. However, immunohistochemistry revealed that the two channels appear to show differential compartmentalization within individual pyramidal neurons. The *Apt*SK1 channels are localized primarily to dendrites, while the *Apt*SK2 channels appear to be somatic. Similar subcellular compartmental distribution patterns have been found for the

Kv3.1 and 3.3 subtypes (Deng et al., 2005). The Kv3.3 channels are rapidly inactivating, while the Kv3.1 channels show a prolonged activation. These kinetic differences may allow for distinct control of cellular firing properties, which could explain why they are differentially distributed. SK channel subtypes on the other hand show very similar activation/inactivation kinetics and conductance properties. This then raises the question: why have two different AptSK channels? Since SK channels are activated soley by calcium, the reason may be a requirement for co-localization with a calcium source. It has been suggested that, due to calcium diffusion co-efficients and chelation, an SK channel must be localized within 50-150 µm of it's source (Marrion and Tavalin, 1998). For ELL pyramidal neurons it is likely that SK channels in the soma (AptSK2) are activated by VGCCs, although the possible subtypes are currently unknown (for a review of SK channel co-localization with VGCCs see Sah and Davies, 2000). It does appear that AptSK1 channels are present in the dentritic spines of pyramidal neurons, making it likely that they are activated by calcium influx from NMDARs, similar to findings in the amygdala and hippocampus (Faber et al., 2005; Ngo-Anh et al., 2005). In this way AptSK1 channels could be controlling the threshold for synaptic plasticity, something that has been shown for SK2 channels in the mammalian hippocampus (Stackman et al., 2002). This type of regulation has the ability to control learning and memory (Bond et al., 2004; Hammond et al., 2006). While the evaluation of learning in Apteronotus has just begun (Maler L., personal communication), it is plausible that the expression of AptSK1 in dendritic spines may limit plastic changes to ELL pyramidal neurons. If this is the case then the map specific expression pattern of AptSK1 would be of great interest, since the lower expression found in the CMS may allow for CMS pyramidal neurons to be more readily modified by feedback onto the apical dendrites, while LS neurons are perhaps more static, or require larger amounts of feedback to undergo plastic changes.

While AptSK1 channels do appear to localize to dendritic spines of ELL pyramidal neurons, it has not been ruled out that they are also present along the shaft of the dendrites. The presence of AptSK1 in the shaft of the dendrites can be important as previous studies have linked SK channel activity to the repolarization of back-propagating plateau potentials in cerebellar purkinje neurons (Cai et al., 2004). In this respect there may be a dual role for AptSK1 channels in the dendrites of pyramidal

neurons, one involving the regulation of synaptic activity and another in which they play a role in the control of actively back-propagating spikes. As mentioned the mechanism of burst generation in ELL pyramidal neurons relies on back-propagating spikes (Turner et al., 1994;Lemon and Turner, 2000). Again, the selective expression of *Apt*SK1 in the LS and CLS over the CMS may impart distinct kinetics onto back-propagating spikes. Since, as demonstrated in this thesis, bursts help to control frequency tuning, *Apt*SK1 channels localized to the dendritic shaft may also be playing a role in controlling frequency tuning.

One final aspect of the distribution pattern of AptSK1 channels must be discussed. It appears that the AptSK1 channels are also localized to the basilar dendrites of E-type pyramidal neurons. The basilar dendrites receive the sensory input from electroreceptors. The presence of AptSK1 could then regulate the strength of this input by opposing the synaptic input. As the input level increased so then would the calcium level, leading to an ever increasing AptSK1 channel activation, which may help to set an upper limit on the amount of feedforward input.

# Functional role of A-type currents

Strong evidence exists in other systems that expression levels of A-type channels increases with distance from the soma (Hoffman et al., 1997;Johnston et al., 2000;Migliore et al., 1999). When this dendritic I<sub>A</sub> blocked pharmacologically (Hoffman et al., 1997) or is knocked down genetically (Chen et al., 2006) the amplitude (and thus strength) of back propagating somatic spikes are increased, allowing for an increase in rebound APs rendering the soma hyper-excitable. Burst firing in ELL pyramidal neurons is controlled through back-propagating dendritic spikes, which, as in the aforementioned systems show a decrease in spike height with an increasing distance from the soma (Turner et al., 2002;Lemon and Turner, 2000). It has been suggested that a cumulative inactivation of Kv3 channels in the dendrites prevents complete de-inactivation of sodium channels, leading to their cumulative inactivation, thus decreasing the dendritic spike height (Fernandez et al., 2005). Since I<sub>A</sub> is a low-threshold current, it should theoretically be active before the back-propagating spike reaches the distal dendrite. In this way the A-type current may also help to reduce the back propagating spike height. If

as in other systems the A-type channels show an increasing expression pattern with increasing distance from the soma, this would seem to place them optimally to oppose the back-propagating spike.

# Future Work I: AptSK channels

Since the contributions of the AptSK2 channels to the frequency filtering properties of ELL pyramidal neurons have been shown to be of substantial interest, evaluation of the role(s) that AptSK1 plays becomes important. As suggested the AptSK1 channels may be co-localized in dendritic spines with NMDA receptors. NMDA receptors have been shown to be present in the dendritic spines of ELL pyramidal neurons where they are involved in the late phase of feedback generated EPSPs (Berman et al., 2001). In order to evaluate the possible links between AptSK1 channels and NMDARs a combination of electrophysiology and immunohistochemistry is required. While antibodies exist for both NR1 (Berman et al., 2001) and AptSK1 channels, they are both polyclonal (rabbit) antibodies, which makes assessment of their co-localization in dendritic spines impossible. This problem could be solved through the creation of a monoclonal (mouse) antibody to either protein. Physiological analysis could be accomplished through intracellular somatic recordings in which the neuronal response properties to NMDAR activation could be assessed in the presence or absence of both SK channel antagonists (apamin) or agonists (EBIO). The creation of the monoclonal antibody and the co-localization study would be quite laborious, so the physiological study should be performed first and then supported by the co-localization study.

# Dendritic distribution of AptSK1 channels

The most straightforward way to evaluate the expression patterns of AptSK1 channels would be through co-staining of the AptSK1 antibody with a synaptic marker and subsequent evaluation with high-powered confocal imaging. If there is no staining in the dendritic shaft then this will be immediately evident. If however there is staining in the shaft of the dendrite this may indicate the expression of AptSK1 channels, however it may simply be AptSK1 channels in transport to the dendritic spines. If there was AptSK1 in the shaft of the dendrite the surface expression could be evaluated by marking an

extracellular loop of an *Apt*SK1 channel clone with an antigenic peptide. The clone could then be delivered using the semiliki forest virus, which has been previously shown to deliver potassium channels to pyramidal cell dendrites (Deng et al., 2005). Antibodies to the antigenic peptide could then be used to assess the presence or absence of the *Apt*SK1 clones along the shaft of the dendrite by applying the antibody without first permeablizing the cells. This should then only stain proteins on the membrane surface.

# Secondary modulation of AptSK channels

While the activation of mAChRs did not result in a modulation of *Apt*SK channels, it is entirely plausible that another neurotransmitter, or second messenger could result in the modulation of *Apt*SK channels either on the surface or along the dendrites of pyramidal neurons. The list of candidates for secondary modulation of SK channels is long and some care would need to be taken when choosing appropriate candidates. This should primarily be based on transmitters found to be present in the ELL such as serotonin (Johnston et al., 1990) or glutamate (Maler and Monaghan, 1991;Bastian, 1993).

# Future work II: A-type potassium currents

Since previous studies have shown that cholinesterase activity was primarily located within the dorsal molecular layer of the ELL(Maler et al., 1981) (Carr et al., 1986) and the G-protein coupled regulatory effects mediated by muscarinic input act locally, we hypothesized that the A-type potassium current in ELL pyramidal neurons is localized to apical dendrites. The two-compartmental model created by Dr. Maurice Chacron is based on a dendritically localized I<sub>A</sub> and can convincingly mimic the effects of mAChR activation. Cloning and localization of the A-type channel may provide insights into some of the questions previously raised regarding the functional role of the A-type currents.

Importantly, it should be noted that in the studies described in this thesis  $I_A$  was never actually measured. In order to fully understand both the modulation and role of  $I_A$  it would be important to measure the current directly. This would require all other currents to be pharmacologically blocked before  $I_A$  could be measured on it's own. Activation and inactivation kinetics could then be measured without the influence of currents generated during an action potential. The kinetic's of  $I_A$  are important to determine the amount of  $I_A$  present at the resting membrane potential. This would allow for an evaluation of the mechanism by which mAChR activation regulates  $I_A$ . If there is a simple block of A-type channels then  $I_A$  should be eliminated at all voltages, however it has been shown that mAChR activation can shift the inactivation of A-type channels to more hyperpolarized voltages (Akins et al., 1990). Measuring  $I_A$  directly could also enable the levels of dendritic current to be assessed by patch clamping dendrites at various distances from the soma. If, as suggested, there is an increasing level of  $I_A$  when moving distally from the soma this should be reflected by a larger current present at the resting membrane potential.

#### REFERENCES

Akins PT, Surmeier DJ, Kitai ST (1990) Muscarinic modulation of a transient K+conductance in rat neostriatal neurons. Nature 344: 240-242.

Bastian J (1993) The role of amino acid neurotransmitters in the descending control of electroreception. J Comp Physiol [A] 172: 409-423.

Berman N, Dunn RJ, Maler L (2001) Function of NMDA receptors and persistent sodium channels in a feedback pathway of the electrosensory system. J Neurophysiol 86: 1612-1621.

Bond CT, Herson PS, Strassmaier T, Hammond R, Stackman R, Maylie J, Adelman JP (2004) Small conductance Ca2+-activated K+ channel knock-out mice reveal the identity of calcium-dependent afterhyperpolarization currents. J Neurosci 24: 5301-5306.

Cai X, Liang CW, Muralidharan S, Kao JP, Tang CM, Thompson SM (2004) Unique roles of SK and Kv4.2 potassium channels in dendritic integration. Neuron 44: 351-364.

Carr CE, Maler L, Taylor B (1986) A time-comparison circuit in the electric fish midbrain. II. Functional morphology. J Neurosci 6: 1372-1383.

Chacron MJ, Maler L, Bastian J (2005) Feedback and feedforward control of frequency tuning to naturalistic stimuli. J Neurosci 25: 5521-5532.

Chen X, Yuan LL, Zhao C, Birnbaum SG, Frick A, Jung WE, Schwarz TL, Sweatt JD, Johnston D (2006) Deletion of Kv4.2 gene eliminates dendritic A-type K+ current and enhances induction of long-term potentiation in hippocampal CA1 pyramidal neurons. J Neurosci 26: 12143-12151.

Deng Q, Rashid AJ, Fernandez FR, Turner RW, Maler L, Dunn RJ (2005) A C-terminal domain directs Kv3.3 channels to dendrites. J Neurosci 25: 11531-11541.

Faber ES, Delaney AJ, Sah P (2005) SK channels regulate excitatory synaptic

transmission and plasticity in the lateral amygdala. Nat Neurosci 8: 635-641.

Fernandez FR, Mehaffey WH, Turner RW (2005) Dendritic Na+ current inactivation can increase cell excitability by delaying a somatic depolarizing afterpotential. J Neurophysiol 94: 3836-3848.

Hammond RS, Bond CT, Strassmaier T, Ngo-Anh TJ, Adelman JP, Maylie J, Stackman RW (2006) Small-conductance Ca2+-activated K+channel type 2 (SK2) modulates hippocampal learning, memory, and synaptic plasticity. J Neurosci 26: 1844-1853.

Hoffman DA, Magee JC, Colbert CM, Johnston D (1997) K+ channel regulation of signal propagation in dendrites of hippocampal pyramidal neurons. Nature 387: 869-875.

Johnston D, Hoffman DA, Magee JC, Poolos NP, Watanabe S, Colbert CM, Migliore M (2000) Dendritic potassium channels in hippocampal pyramidal neurons. J Physiol 525 Pt 1: 75-81.

Johnston SA, Maler L, Tinner B (1990) The distribution of serotonin in the brain of Apteronotus leptorhynchus: an immunohistochemical study. J Chem Neuroanat 3: 429-465.

Krukowski AE, Miller KD (2001) Thalamocortical NMDA conductances and intracortical inhibition can explain cortical temporal tuning. Nat Neurosci 4: 424-430.

Lemon N, Turner RW (2000) Conditional spike backpropagation generates burst discharge in a sensory neuron. J Neurophysiol 84: 1519-1530.

Maler L, Collins M, Mathieson WB (1981) The distribution of acetylcholinesterase and choline acetyl transferase in the cerebellum and posterior lateral line lobe of weakly electric fish (Gymnotidae). Brain Res 226: 320-325.

Maler L, Monaghan D (1991) The distribution of excitatory amino acid binding sites in the brain of an electric fish, Apteronotus leptorhynchus. J Chem Neuroanat 4: 39-61.

Marrion NV, Tavalin SJ (1998) Selective activation of Ca2+-activated K+ channels by colocalized Ca2+ channels in hippocampal neurons. Nature 395: 900-905.

Mehaffey WH, Doiron B, Maler L, Turner RW (2005) Deterministic multiplicative gain control with active dendrites. J Neurosci 25: 9968-9977.

Migliore M, Hoffman DA, Magee JC, Johnston D (1999) Role of an A-type K+ conductance in the back-propagation of action potentials in the dendrites of hippocampal pyramidal neurons. J Comput Neurosci 7: 5-15.

Nelson ME, Maciver MA (1999) Prey capture in the weakly electric fish Apteronotus albifrons: sensory acquisition strategies and electrosensory consequences. J Exp Biol 202: 1195-1203.

Ngo-Anh TJ, Bloodgood BL, Lin M, Sabatini BL, Maylie J, Adelman JP (2005) SK channels and NMDA receptors form a Ca2+-mediated feedback loop in dendritic spines. Nat Neurosci 8: 642-649.

Oswald AM, Schiff ML, Reyes AD (2006) Synaptic mechanisms underlying auditory processing. Curr Opin Neurobiol 16: 371-376.

Sah P, Davies P (2000) Calcium-activated potassium currents in mammalian neurons. Clin Exp Pharmacol Physiol 27: 657-663.

Stackman RW, Hammond RS, Linardatos E, Gerlach A, Maylie J, Adelman JP, Tzounopoulos T (2002) Small conductance Ca2+-activated K+ channels modulate synaptic plasticity and memory encoding. J Neurosci 22: 10163-10171.

Turner RW, Lemon N, Doiron B, Rashid AJ, Morales E, Longtin A, Maler L, Dunn RJ (2002) Oscillatory burst discharge generated through conditional backpropagation of dendritic spikes. J Physiol Paris 96: 517-530.

Turner RW, Maler L, Deerinck T, Levinson SR, Ellisman MH (1994) TTX-sensitive dendritic sodium channels underlie oscillatory discharge in a vertebrate sensory neuron. J Neurosci 14: 6453-6471.

Zakon H, Oestreich J, Tallarovic S, Triefenbach F (2002) EOD modulations of brown ghost

electric fish: JARs, chirps, rises, and dips. J Physiol Paris 96: 451-458.

# **APPENDIX**

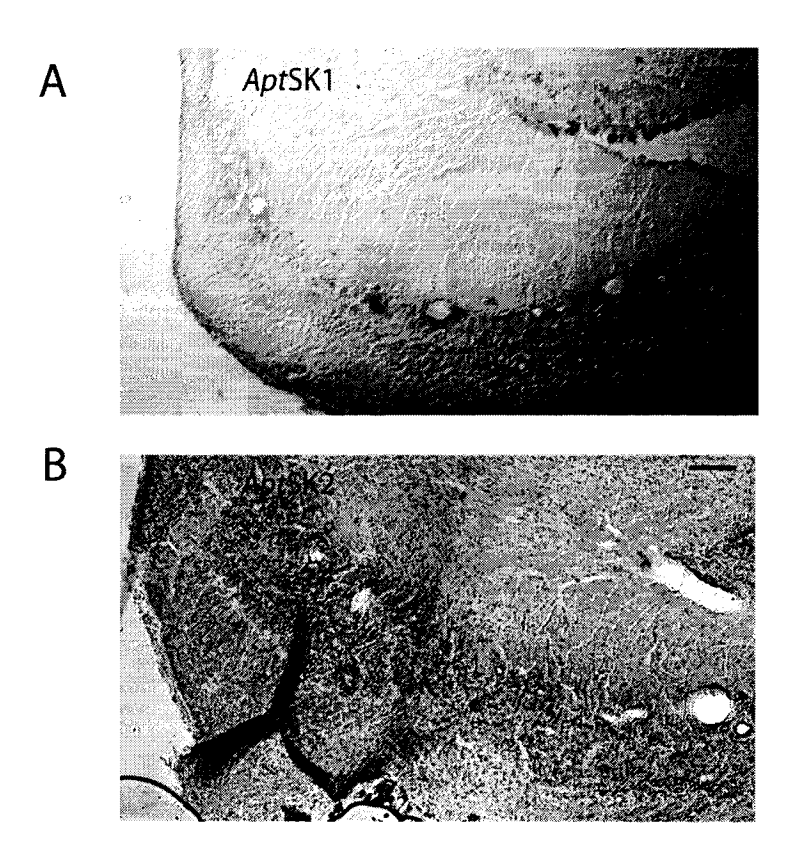
This appendix is comprised of 3 figures that supplement the manuscripts comprising the 3 chapters of this thesis. The importance of these 3 figures is as follows:

**Figure 1** is the control experiment for the *in situ* hybridization studies performed in chapters 1 and 2, showing non-specific light staining for the sense probe. The staining pattern seen for the anti-sense probes can then be considered specific for the channel sequences and is not an artifact of the experimental procedure or non-specific staining.

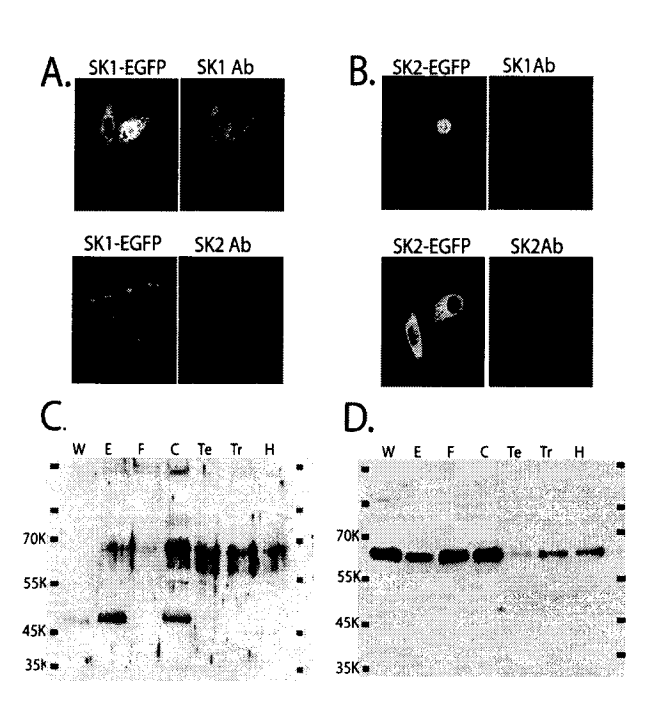
Figure 2 characterizes the AptSK1 and 2 antibodies. The CHO cell experiments show that the two antibodies are specific for their particular AptSK channel, making it unlikely that the immunohistochemistry in chapter 2 is due to binding to another AptSK channel. The western blot analysis reveals two distinct staining patterns for the AptSK1 and 2 antibodies. First, the expression levels of the AptSK1 protein in tissue extracted from the entire brain revealed a much lower expression level then that seen for the AptSK2 channel, which was robustly expressed. Secondly, the antibody to AptSK1 produced 3 bands at 67.4, 57.6 and 47.9 KDa, while the AptSK2 antibody produced a single band of approximately 63.7 KDa. This staining pattern is similar to that found in mammalian systems (Sailer et al., 2004). Two of the bands (67.4 & 47.9 KDa) correspond well to two splice isoforms that were produced during the cloning of the AptSK1 channel. The splice isoforms coincide well with splicing that has been shown in both mouse and human SK1 channels (Shmukler et al., 2001; Zhang et al., 2001). The shorter variant is spliced just before a three amino acid exon that is specific for SK1 channels (AQK). This splice site is in the 3' tail approximately 70 amino acids from the end of the S6 segment, thus likely still retaining a CaMBD. The longer variant contains the entire 3' tail including the SK1 specific AQK exon. PCR primers were been designed for the 3' UTR of both isoforms and have shown that they are both easily amplified from whole brain tissue. Interestingly when western blot analysis was performed on protein extracted from specific areas of the brain, differences in the expression of the two splice variants became apparent. The short splice variant was only apparent in the ELL and cerebellum, while

the full length version of the AptSK1 channel was found not only in the ELL and cerebellum, but also in the tectum and torus, although at apparently lower levels. The expression of the AptSK2 protein also showed a segment specific expression pattern with higher levels found in the ELL, forebrain and cerebellum and relatively low levels in the tectum, torus and hypothalamus.

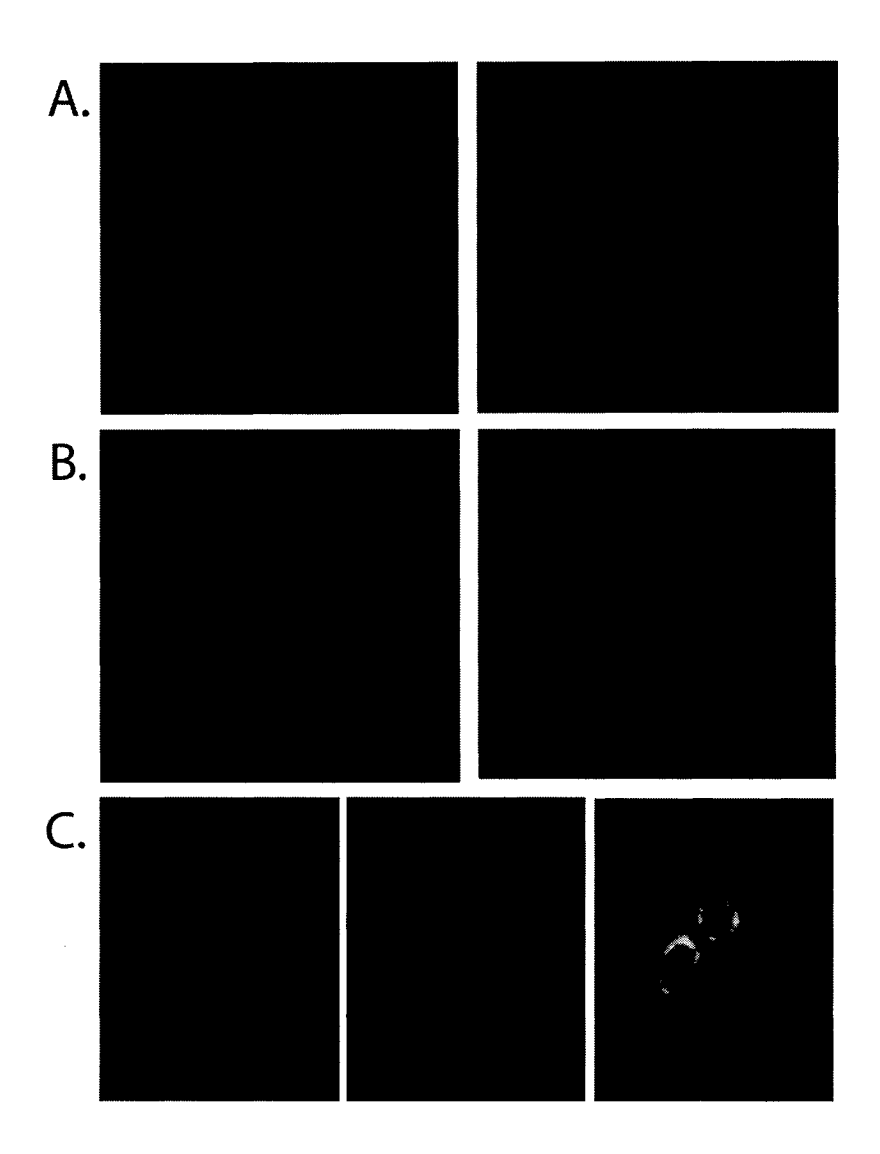
Figure 3 highlights the possible importance of the AptSK1 short splice variant (SSV). When expressed in CHO cells, the full length AptSK1 is expressed throughout the cell, however the SSV is only found very close to the nucleus, likely restricted to the golgi and ER. It has been shown that when an SK channel is truncated after the CaMBD it fails to localize to the surface (Lee et al., 2003). It would appear that similar mechanisms are at work for the AptSK1 channel. Importantly, when the SSV is co-expressed with the full-length version it appears that the surface expression of the full-length channel is also restricted. This raises a number of interesting questions regarding the SSV. What is its functional role in the cells in which it is expressed? Could its expression levels be controlled in order to regulate the surface expression of the full-length AptSK1? Also, why is it important that the SSV is expressed at high levels in only the ELL and cerebellum? Answering these questions will require a substantial amount of work but may provide insights into the regulation of SK channel expression, which I have shown in this thesis to be of great importance for controlling neuronal firing properties and response patterns.



**Supplemental Fig 1.** Sense controls for *in situ* hybridization. Sense controls for (A) the AptSK1 probe and (B) the AptSK2 probe both showed homogeneous non-specific staining across the maps of the ELL. Scalebars 100  $\mu$ M



**Supplemental Fig 2.** Evaluation of *Apt*SK1 and 2 antibodies. **A.** CHO cells transfected with *Apt*SK1-EGFP cDNA showing positive staining with the *Apt*SK1 antibody, while the *Apt*SK2 antibody resulted in no measurable staining. **B.** CHO cells transfected with *Apt*SK2-EGFP cDNA revealing positive staining with the *Apt*SK2 antibody, while the *Apt*SK1 antibody did not result in staining. **C** +**D.** Western-blot analysis of *Apt*SK antibodies. Protein was isolated from the whole brain (W), the ELL (E), forbrain (F), cerebellum (C), tectum (Te), torus (Tr) or hypothalamus (H). 10 μg of protein was loaded onto each column. **C.** Light staining was seen for the *Apt*SK1 antibody for protein isolated from the whole brain, indicating an overall low percentage of *Apt*SK1 protein. The highest levels of *Apt*SK1 protein were found in the ELL and cerebellum where 3 bands at 67.4, 57.6 and 47.9 KDa were found, indicating 3 separate splice variants. Similar SK1 splice patterns have previously been found in mammalian systems. Interestingly the shortest splice variant was expressed at undetectable levels in the other brain areas. **D.** The western-blot using the *Apt*SK2 antibody showed a single band of approximately 63.7 KDa. High expression levels were seen in whole brain tissue.



**Supplemental Fig 3.** The short splice variant (SSV) of the *Apt*SK1 channel is not expressed on the cell surface. **A.** A CHO cell transfected with the full length *Apt*SK1 channel cDNA tagged with GFP. Low exposure was used to show protein expression and high exposure was used to reveal the boundary of the cell membrane. The images reveal that the *Apt*SK1 protein is present throughout the cell. **B.** Low and high exposure images of the *Apt*SK1-SSV-GFP channel shows isolation of the protein to areas presumed to be intracellular, likely the golgi apparatus or endoplasmic reticulum. **C.** Co-expression of the *Apt*SK1 full-length cDNA with the *Apt*SK1-SSV appears to reveal that the presence of the SSV prevents surface expression of the *Apt*SK1 full-length channel.

# REFERENCES

Lee WS, Ngo-Anh TJ, Bruening-Wright A, Maylie J, Adelman JP (2003) Small conductance Ca2+-activated K+ channels and calmodulin: cell surface expression and gating. J Biol Chem 278: 25940-25946.

Sailer CA, Kaufmann WA, Marksteiner J, Knaus HG (2004) Comparative immunohistochemical distribution of three small-conductance Ca2+activated potassium channel subunits, SK1, SK2, and SK3 in mouse brain. Mol Cell Neurosci 26: 458-469.

Shmukler BE, Bond CT, Wilhelm S, Bruening-Wright A, Maylie J, Adelman JP, Alper SL (2001) Structure and complex transcription pattern of the mouse SK1 K(Ca) channel gene, KCNN1. Biochim Biophys Acta 1518: 36-46.

Zhang BM, Kohli V, Adachi R, Lopez JA, Udden MM, Sullivan R (2001) Calmodulin binding to the C-terminus of the small-conductance Ca2+-activated K+ channel hSK1 is affected by alternative splicing. Biochemistry 40: 3189-3195.